

TABLE OF CONTENTS

SECTION	PAGE
CHAPTER 6.....	6.1-1
CRITICALITY EVALUATION	6.1-1
6.1 Discussion and Results	6.1-1
6.2 Spent Fuel Loading.....	6.2-1
6.3 Model Specification	6.3-1
6.3.1 Description of Computational Model.....	6.3-1
6.3.2 Cask Regional Densities	6.3-2
6.4 Criticality Calculation.....	6.4-1
6.4.1 Computational or Experimental Method.....	6.4-1
6.4.2 Fuel Loading or Other Contents Loading Optimization.....	6.4-5
6.4.3 Criticality Results	6.4-13
6.5 Critical Benchmark Experiments	6.5-1
6.5.1 Benchmark Experiments and Applicability.....	6.5-1
6.5.2 Results of the Benchmark Calculations.....	6.5-2
6.5.3 Modeling Bias.....	6.5-2
6.6 Supplemental Data.....	6.6-1
6.6.1 Sample Input File, Most Reactive Lattice Evaluation	6.6-1
6.6.2 Variable Enrichment Patterns, Uniform Enrichment Validation.....	6.6-3
6.6.3 Sample Input Files, Uniform Enrichment Model Validation	6.6-9
6.6.4 Sample Input Files, Most Reactive Intact Assembly Configuration, Scoping Model.....	6.6-13
6.6.5 Sample Input Files, TN-68 Final Criticality Evaluation.....	6.6-17
6.7 References.....	6.7-1

TABLE OF CONTENTS

List of Tables

Table 6.1-1	Maximum Initial Enrichment for both Intact and Damaged Fuel Assemblies
Table 6.1-2	Summary of Limiting Criticality Evaluations for the TN-68 Cask
Table 6.2-1	Fuel Characteristics for Criticality
Table 6.3-2	TN-68 Fixed Poison Loading Requirements
Table 6.3-3	Description of the KENO Model Units
Table 6.3-4	Comparison of KENO Models
Table 6.3-5	Material Property Data
Table 6.4-1	Results, Most Reactive Lattice Evaluation
Table 6.4-2	Results, Uniform Enrichment Model Validation
Table 6.4-3	TN-68 Most Reactive Intact Configuration – Scoping Results
Table 6.4-4	TN-68 Intact Assembly Criticality Analysis - Final Results
Table 6.4-5	Results of the Single Ended Rod Shear Scoping Studies
Table 6.4-6	Results of the Double Ended Rod Shear Scoping Studies
Table 6.4-7	TN-68 Damaged Assembly Criticality Analysis - Final Results
Table 6.5-1	Benchmark Results
Table 6.5-2	USL-1 Results
Table 6.5-3	USL Determination for Criticality Analysis

TABLE OF CONTENTS

List of Figures

- Figure 6.3-1 Basket Views and Dimensions
- Figure 6.3-2 Basket Model Compartment Wall (View G)
- Figure 6.3-3 Basket Model Compartment Wall (View F)
- Figure 6.3-4 Basket Model Compartment with Fuel Assembly (View G)
- Figure 6.3-5 Basket Model Compartment with Fuel Assembly (View F)
- Figure 6.3-6 KENO Plot of the Center of the TN-68 Basket with Fuel Assemblies
- Figure 6.3-7 Radial Cross Section of the TN-68 Basket with Fuel Position Numbers
- Figure 6.3-8 North East Quadrant of the TN68 Basket with Fuel Assemblies
- Figure 6.3-9 Radial Cross Section of the TN-68 Basket with Fuel Assemblies
- Figure 6.4-1 TN-68 Model Cross Section, Most Reactive Lattice Evaluation
- Figure 6.4-2 TN-68 Model Cross Section, Uniform Enrichment Validation, Case 3Var
- Figure 6.4-3 Vanished Lattice Model
- Figure 6.4-4 KENO Plot of Units 247 and 248 With Channel - Single Shear Rows
- Figure 6.4-5 KENO Plot of Units 257 and 258 Without Channel - Single Shear Rows
- Figure 6.4-6 KENO Plot of the Single Sheared Rods with 12.18" Axial Shift
- Figure 6.4-7 KENO Plot of Units 247 and 248 With Channel - Double Shear Columns
- Figure 6.4-8 KENO Plot of Units 257 and 258 Without Channel - Double Shear Rows
- Figure 6.4-9 KENO Plot of the Double Sheared Rods with 12.18" Axial Shift
- Figure 6.4-10 KENO Plot of the Design Basis Double Shear Damaged Assembly Model
- Figure 6.5-1 Benchmarks – Trend Evaluation for Separation Distance

CHAPTER 6

CRITICALITY EVALUATION

6.1 Discussion and Results

Criticality control in the TN-68 is performed by the basket structural components, which maintain the relative position of the spent fuel assemblies under normal and accident conditions as demonstrated in Chapter 3, and by the neutron absorbing plates between the basket compartments.

The TN-68 contents are limited to the designs listed in Chapter 2 that includes both intact and damaged fuel assemblies. The maximum lattice-average enrichment of U235 varies with the basket type, determined by the B10 areal density in the fixed neutron absorber. The B10 areal density in the criticality analysis varies from 27 to 63 mg B10/cm², each level of areal density corresponding to a different basket type and an associated fuel enrichment limit. In the case of intact fuel, the limit is based on the lattice-average enrichment. In the case of damaged fuel, it is based on the maximum pellet enrichment.

Fuel assemblies with or without channels are acceptable. Any fuel channel thickness from 0.065 to 0.120 inch is acceptable on any of the fuel designs. Criticality control does not require special loading patterns or special rotational orientation of the fuel assemblies. The TN-68 may be loaded with pool water at maximum density, i.e., at 4 °C.

The criticality evaluation is divided into several sections:

- a) Determination of the most reactive lattice (Section 6.4.2.1). All of the design basis fuels are evaluated with uniform enrichment to determine the most reactive geometry. The effect of water in the fuel pins and of fuel channels is also evaluated.
- b) Uniform enrichment model validation (Section 6.4.2.2). The results using fuel lattice models with pin-by-pin enrichment variation are compared with results obtained using uniform enrichment models. Vanished lattices are also compared with the uniform enrichment models. If the uniform enrichment model underpredicts k_{eff} , the modeling bias will be determined and the Upper Subcritical Limit will be reduced by that amount.
- c) TN-68 criticality evaluation (Sections 6.4.2.3 through 6.4.2.6). The uniform enrichment model of the most reactive fuel lattice is used for this evaluation. The TN-68 cask is evaluated for the following conditions, which bound normal conditions and the off-normal and accident events listed in Chapter 11:
 - varied water density, both inside the cask and external to the cask,
 - varied fuel compartment inside dimension and pitch between compartments,
 - off-center placement of fuel in the compartments, and
 - postulated failures for damaged fuel payloads.

Non-uniform flooding of the basket is not evaluated because all the spaces in the basket are interconnected, and therefore this is not a credible condition.

The various effects are evaluated individually, and the minimum compartment dimension case is combined with the worst of the remaining cases. These cases demonstrate compliance with the requirement of 10CFR72.124 that "before a criticality accident is possible, at least two unlikely, independent, and concurrent or sequential changes have occurred in the conditions essential to nuclear criticality safety."

The evaluation demonstrates that the TN-68 cask meets the requirement $k_{\text{eff}} + 2\sigma \leq \text{Upper Subcritical Limit}$ for all these conditions, using the neutron poison plate materials specified in Chapter 9.

- d) Benchmarking (Section 6.5). An upper subcritical limit (USL) is determined by subtracting from unity an administrative margin of 0.05, the bias determined from benchmark calculations and any modeling bias.

All calculations assume fresh fuel composition and ignore burnable poisons. The minimum value of the Upper Subcritical Limit (USL) was determined to be 0.9423. The maximum allowed initial enrichment of the intact fuel assembly as a function of fixed poison loading is determined and is listed in Table 6.1-1. The maximum allowed initial enrichment of the damaged fuel assemblies as a function of fixed poison loading is determined and is also shown in Table 6.1-1. The results of the limiting criticality analyses are summarized in Table 6.1-2. The maximum k_{eff} for the normal fuel geometry is 0.9405 ($k_{\text{eff}}+2\sigma$) and is based on the 10x10 lattice design. The maximum k_{eff} for the damaged fuel geometry with 8 damaged assemblies and 60 intact assemblies is 0.9407 ($k_{\text{eff}}+2\sigma$).

6.2 Spent Fuel Loading

The allowable contents are listed in Chapter 2. Fuel characteristics used in the criticality calculations are listed in Table 6.2-1.

Where fuel pins have variable axial enrichment, the average is calculated for each axial zone (lattice), and the lattice with the highest average enrichment is used to characterize the entire bundle for criticality purposes. The average enrichment is defined as the simple arithmetic average of pin enrichments:

$$E_{avg} = \sum_{i=1,n} E_i / n$$

Where E_i is the enrichment of pin i , and n is the number of fuel pins in the lattice. There is no averaging of the axial enrichment variation in this evaluation; “bundle average” enrichments, which are an average enrichment over the entire fuel bundle, including natural uranium blankets, are not used to qualify fuel for storage in the TN-68.

To maintain subcriticality, the maximum lattice-average enrichment of the fuel bundle must be less than or equal to the limits determined by the criticality analysis. These limits are shown in Table 6.1-1.

Fuel bundles with cladding damaged greater than a pinhole or hairline crack may be stored in the TN-68 only in the eight perimeter fuel compartments. Fuel bundles from which fuel pins are missing are not allowable contents unless the missing pin is replaced.

6.3 Model Specification

The following subsections describe the physical models and materials of the TN-68 cask used for input to the CSAS25 module of SCALE-4.4 [1] to perform the criticality evaluation. The reactivity of the cask under storage and transfer conditions is bounded by performing the analysis with a cask fully flooded with pool water.

6.3.1 Description of Calculational Model

The TN-68 cask is explicitly modeled using the appropriate geometry options in KENO V.a of the CSAS25 module in SCALE-4.4. A KENO model (called the calculational KENO model) is developed in this calculation to determine the initial enrichment for intact and damaged fuel assemblies as a function of fixed poison loading.

The basket design modeled in the calculation is based on the TN-68 basket detailed in Chapter 1 with a section length of 12.18" (10.43" basket section + 1.75" steel plate). The key basket and cask dimensions utilized in the calculation are shown in Table 6.3-1. The fixed poison modeled in the calculation is modeled as aluminum and boron which is adequate to represent the borated aluminum alloy or boron carbide/aluminum composites. The fixed poison loading requirements are shown in Table 6.3-2.

The basic calculational KENO model is a 12.18-inch axial section and full-radial cross section of the TN-68 cask with periodic boundary conditions at the axial boundaries (top and bottom) and reflective boundary conditions at the radial boundaries (sides). This axial section essentially models one building block of the egg crate basket structure. Periodic boundary conditions ensure that the resulting KENO model is essentially infinite in the axial direction. The model does not explicitly include the solid neutron shield (neutron shielding resin in aluminum boxes); however the infinite array of casks without the neutron shield does contain water between the casks. This basic building block of the TN-68 basket is shown in Figure 6.3-1.

The fuel assemblies within the basket are modeled explicitly.

Each fuel assembly is surrounded by a the fuel compartment, and these are separated by 0.30 inch neutron absorber/ heat transfer plates. These plates are modeled as paired plates of aluminum and neutron absorber material. The thickness of the poison plate is chosen such that the amount of boron in the alloy is close to or slightly higher than the practical limit (about 4.5 wt % boron). The thermal expansion and egg-crate slot gaps are modeled with internal moderator. KENO model plots in 2D for the various views of the basket compartment are shown in Figure 6.3-2 through 6.3-9.

There are a total of 18 poison plates in the TN-68 basket. These plates are located at the eastern and southern faces of the fuel assembly. Thus, all the interior 60 fuel assemblies are surrounded by poison plates on all the four faces and the outer 8 fuel assemblies do not have poison plates on the radially outward looking face. In the KENO model, however, all the 24 peripheral fuel assemblies are modeled without the poison plates (in the model, the poison plates are replaced by aluminum plates) at their radially outward looking faces. The fuel assembly and poison plate

positions (and the aluminum plate positions) in the KENO model of the basket is shown in Figure 6.3-7.

The perimeter rail structure provides the cylindrical cross section for the basket to be effectively seated inside the TN-68 cask. The rail material is aluminum and SS304 and provides for a heat conduction path from the basket to the cask shell. These rails (triangular cross section) are not modeled explicitly in the KENO model. Instead, they are modeled as a solid aluminum interface between the basket and the cask inner shell with cylindrical water holes at appropriate locations. This modeling of the rails is conservative as reduction in the water and increase in the aluminum at the periphery of the basket tends to reduce the parasitic capture (and absorption) of neutrons in this region.

The description above refers to the model used for the final evaluation, Section 6.4.3. The models used for the most reactive fuel evaluation, the uniform enrichment validation, and the most reactive geometry determination (scoping KENO models) are somewhat different. The differences are described in the respective calculation descriptions, Section 6.4.2.1, 6.4.2.2, and 6.4.2.3.

This calculational KENO model is benchmarked with the scoping KENO model utilized in Section 6.4.2.3. The scoping KENO model is utilized to determine the most reactive configuration for intact fuel assemblies. The results of the benchmark calculation for the two KENO models are shown in Table 6.3-4. The results of the benchmark calculations indicate that their differences are statistically insignificant. The validated, calculational model is, therefore, utilized to determine the maximum allowable initial enrichment as a function of the fixed poison loading.

This KENO model is modified to model the various damaged fuel configurations like single shear, double shear, and axial fuel shifting. These models are analyzed to determine the most reactive damaged fuel configuration. The second model is based on the most reactive configuration identified above. This model is used to determine the maximum allowable initial enrichment for damaged fuel assemblies as a function of the fixed poison loading.

6.3.2 Cask Regional Densities

The Oak Ridge National Laboratory (ORNL) SCALE code package [1] contains a standard material data library for common elements, compounds, and mixtures. All the materials used for the TN-68 criticality analysis are available in this data library.

Table 6.3-5 provides a complete list of all the relevant materials used for the criticality evaluation. The B10 areal density is provided as used in these calculations; the minimum specified in Chapter 9 is greater.

6.4 Criticality Calculation

This section describes the analysis methodology utilized for the criticality analysis. The analyses are performed with the CSAS25 module of the SCALE 4.4 code system with the SCALE 44-group ENDF/B-V cross section library. A series of calculations are performed to determine the relative reactivity of the various fuel assembly designs evaluated and to determine the most reactive configuration. The most reactive intact fuel design, for a given enrichment, as demonstrated by the analyses, is the GE 10x10 fuel assembly with the 0.120" channel. The most reactive credible configuration is an infinite array of flooded casks, each containing 68 fuel assemblies, with minimum fuel compartment ID, minimum basket structure thickness and minimum assembly-to-assembly pitch.

A series of calculations are also performed to determine the relative reactivity of the various damaged fuel configurations. The most reactive damaged fuel configuration occurs due to a postulated double-ended shear with the 0.120" channel. This configuration is independent of the fuel assembly class since the most reactive intact fuel design is utilized in the scoping evaluations. The most reactive credible configuration analyzed in this calculation is an infinite array of flooded casks, each containing a maximum of 8 damaged fuel assemblies (and 60 intact fuel assemblies) with minimum fuel compartment ID, minimum basket structure thickness and minimum assembly-to-assembly pitch.

As mentioned in Section 6.1, the TN-68 is evaluated to determine the maximum initial enrichment of the fuel assemblies (both damaged and intact) as a function of fixed poison loading.

6.4.1 Calculational or Experimental Method

6.4.1.1 Computer Codes

The most reactive lattice and uniform enrichment validation model calculations are performed using the CSAS25 sequence from the SCALE4.3 code system [2] with the SCALE 27-group ENDF/B-IV cross section library. Within this sequence, resonance correction based on the fuel pin cell description is performed by NITAWL using the Nordheim Integral method, and k_{eff} is determined by the KENOva code using the Monte Carlo technique. A sufficiently large number of neutron histories are run so that the standard deviation is below 0.0020 for these calculations.

Criticality analyses were performed using KENO-Va and the 44 neutron group library based on ENDF-B Version 5 cross-section data that are part of the SCALE 4.4 code package [1]. Validation and benchmarking of these codes is discussed in Section 6.5.

SCALE 4.4 [1] is an extensive computer package which has many applications including cross section processing, criticality studies, and heat transfer analyses among others. The package is comprised of many functional modules. For the purpose of criticality analysis, only four functional modules are used and one control module. These modules are CSAS25, which includes the three dimensional criticality code KENO-Va and the preprocessing codes BONAMI-S, NITAWL-II and XSDRNPM-S.

KENO-Va, in conjunction with a suitable working library of nuclear cross section data, is used to calculate the multiplication factor, k_{eff} , of systems of fissile material. It can also compute lifetime and generation time, energy dependent leakages, energy and region-dependent absorptions, fissions, fluxes, and fission densities. KENO-Va utilizes a three-dimensional Monte-Carlo computation scheme. KENO-Va is capable of modeling complex geometries including facilities for handling arrays, arrays of arrays, and holes.

SCALE 4.4 is set up so that any number of cross-section libraries may be used with the preprocessing functional and control modules. For the purpose of this analysis, only the 44-group ENDF/B Version 5 library is used.

The preprocessing codes used for this analysis are the functional modules BONAMI-S, NITAWL-II and XSDRNPM-S. They are consolidated into the control module CSAS25. BONAMI-S has the function of performing Bondarenko calculations for resonance self-shielding. The cross sections and Bondarenko factor data are pulled from an AMPX master library. The output is placed into a master library as well. Dancoff approximations allow for different fuel lattice cell geometries. The main function of NITAWL-II is to change the format of the master cross-section libraries to one which the criticality code (KENO-Va) can access. It also provides the Nordheim Integral Treatment for resonance self-shielding. XSDRNPM-S provides cell-weighted cross sections based on the specified unit cell.

The criticality analysis, using the above computer codes, is performed in compliance with the 10CFR 72 requirements. Specifically, all cases are analyzed assuming that the basket is fully flooded with internal moderator (pure water), the neutron shield of the cask is replaced with fresh water and the cask is flooded with fresh water. Finally, KENO V.a calculates the k_{eff} of the system that is modeled. A sufficiently large number of neutron histories are run so that the standard deviation is below 0.0010 for all calculations.

6.4.1.2 Bases and Assumptions

The analytical results reported in Appendix 3A demonstrate that the cask confinement boundary and the basket structure do not experience any significant distortion under hypothetical accident conditions. Therefore, for both normal and hypothetical accident conditions the cask geometry is identical except for the neutron shield and skin. As discussed above, the neutron shield and skin are conservatively replaced with water.

The TN-68 cask is modeled with KENO V.a using the available geometry input. This option allows a model to be constructed that uses regular geometric shapes to define the material boundaries. The following conservative assumptions are also incorporated into the criticality calculations:

- (1) Unirradiated fuel – no credit taken for fissile depletion due to burnup or fission product poisoning.
- (2) Water density at optimum moderator density.
- (3) The fuel pins are modeled assuming a lattice average uniform enrichment everywhere in the lattice. Natural uranium blankets, gadolinia, Integral Fuel Burnable Absorber (IFBA), erbia or any other burnable absorber rods and axial or radial enrichment zones are modeled as fully enriched Uranium.
- (4) All fuel rods are assumed to be filled with 100% pure water in the fuel/cladding gap to account for the possibility of water being entrained in the fuel pin and because it has a slight positive effect on reactivity.
- (5) The fuel pellet stack was conservatively modeled at 96.5% of theoretical density with no allowance for dishing or chamfer.
- (6) It is assumed for all cases that the solid neutron shield and stainless steel skin of the cask are replaced by external moderator.
- (7) Only a 12.18-inch section of the basket with fuel assemblies is explicitly modeled with periodic boundary conditions at the axial boundaries, therefore the model is effectively infinitely long.
- (8) The basic model is the fully loaded basket within the TN-68 cask in fully flooded condition inside the spent fuel pool.
- (9) Though the fixed poison utilized in the KENO model is based on Borated Aluminum, the design of the KENO model ensures that this model is applicable to any of the neutron absorbers specified in Chapter 9 and that there would be no significant differences due to change in poison type for a given fixed poison loading.
- (10) All steel materials are modeled as SS304. The small differences in the composition of the various stainless steels have no effect on results of the calculation.

- (11) All zirconium based materials in the fuel are modeled as Zircaloy-4. The small differences in the composition of the various clad / tube / channel materials have no effect on the results of the calculation.
- (12) No calculations are performed that model the uncovering of poison in the active fuel region of the basket. Even though the size of the cavity in the TN-68 is larger than the size of the basket, accidents involving a relative shift of the basket and the fuel assemblies at the bottom are not considered credible when the basket is flooded with pool water and the cask is in the vertical position and the hold down ring present. Therefore, all calculations are carried out with the active fuel region fully surrounded by fixed poison in the basket.

The following are the additional assumptions that are relevant to the damaged fuel assembly calculations:

- (1) The cask confinement boundary and canister basket structure do not experience any significant distortion under hypothetical accident conditions.
- (2) The worst case gross damage resulting from a cask-drop accident is assumed to be either a single-ended or double-ended rod shear with flooding in pool water. A maximum of 12 inches of fuel may be uncovered by the poison plates due to shifting of the sheared rods.
- (3) The single-ended fuel rod shear cases assume that fuel rods that form one assembly face shear in one place and are displaced to new locations. The fuel pellets are assumed to remain in the fuel rods.
- (4) The double-ended fuel rod shear cases assume that the fuel rods that form one assembly face shear in two places and the intact fuel rod pieces are separated from the parent fuel rods.
- (5) No other damaged assembly mechanisms are postulated.

6.4.1.3 Determination of k_{eff}

The Monte Carlo calculations performed with CSAS25 (KENO V.a) use a flat neutron starting distribution. The total number of histories traced for each calculation is approximately 800,000. This number of histories is sufficient to achieve source convergence and produce standard deviations of less than 0.10% in k_{eff} . The maximum k_{eff} for the calculation is determined with the following formula:

$$k_{\text{eff}} = k_{\text{KENO}} + 2\sigma_{\text{KENO}}.$$

6.4.2 Fuel Loading or Other Contents Loading Optimization

The criticality analysis is performed for the TN-68 cask loaded with 68 intact or 60 intact and 8 damaged fuel assemblies. The following sub-sections describe the various analyses performed with the intact and damaged fuel assemblies.

6.4.2.1 Determination Of The Most Reactive Fuel Lattice

All lattices listed in Table 6.2-1 are evaluated with a lattice average enrichment of 3.7% in all pins. The lattices are analyzed with and without water in the fuel pellet-cladding annulus, and with and without fuel channels. All lattices are analyzed with the minimum and maximum fuel channel thicknesses, 0.065 and 0.120 inch thick, and one intermediate thickness. The lattices are centered in the fuel compartments.

The cask model for this evaluation differs from the TN-68 design in the following ways:

- the boron 10 content in the poison plates is lower,
- the egg-crate (vertical) slots run the full height of the poison plate,
- the fuel, basket, and cask body are infinite length (periodic reflection on "z" faces of model),
- the basket rails are a homogenized 50/50 volume % mixture of water and aluminum, and
- the stainless steel bars between compartments are modeled as carbon steel.

In all other respects, the model is the same as that described in Section 6.3.1 except that poison plates are included in the basket periphery. The sole purpose of this model is to determine the *relative* reactivity of different lattices in a configuration similar to the TN-68. The model is shown in Figure 6.4-1.

A typical input file is included in Section 6.6.1. The results of these calculations are listed in Table 6.4-1. The most reactive fuel lattice evaluated for the TN-68 is the GE generation 12 lattice, 10x10 array, with water in the fuel rods and with the 0.065 inch thick fuel channel.

6.4.2.2 Uniform Enrichment Model Validation

Except for the earliest fuels, BWR fuel lattices do not actually have the same enrichment fuel in each fuel pin. It is necessary to validate the use of fuel lattice models in which all fuel pins have the same enrichment, because the most reactive fuel evaluation and the TN-68 criticality use this model. To do this, k_{eff} 's of variable pin-enrichment lattice models and of equivalent uniform enrichment lattice models are calculated and compared. The variable enrichment pin models are all normalized so that the lattice average enrichment is 3.7%. The pin enrichment patterns and the normalized equivalents are shown in Section 6.6.2. In all those patterns, the control blade corner is in the upper right, and the highest enrichment corner is in the lower left; they are oriented this way in the quarter-basket model so that the highest enrichment zones face the cask longitudinal axis. The equivalent average enrichment for the uniform enrichment model is defined in Section 6.2.

The cask model for this evaluation differs from the TN-68 design in the following ways:

- the boron 10 content in the poison plates is lower,
- the egg-crate (vertical) slots run the full height of the poison plate,
- the fuel, basket, and cask body are infinite length (periodic reflection on "z" faces of model),
- the basket rails are a homogenized 50/50 volume % mixture of water and aluminum,
- the stainless steel bars between compartments are modeled as carbon steel, and
- the cask is modeled with a square cross section and 64 fuel assemblies. This is a significant difference from the actual cask, but again, the sole purpose of this model is to determine the *relative* reactivity of different fuel models in a configuration similar to the TN-68. The square cross section was used to simplify modeling the case where the highest enrichment zones of the variable pin enrichment fuel lattices are all rotated toward the cask longitudinal (z) axis. This is done by modeling a quarter of the cask cross section, and then using mirror reflection along the x and y axes. This orientation is more reactive than either random or uniform rotational orientation of the lattices. The model is shown in Figure 6.4-2.

The results of the calculation are listed in Table 6.4-2. The case designations may be correlated to the pin enrichment patterns by referring to Section 6.6.2. The last six cases in the table are vanished lattice cases corresponding to the six cases immediately before them. These are the lattices above the partial length fuel rods; the partial length rod has vanished, and is replaced by water, as shown in Figure 6.4-3. Because of the improved moderation, the vanished lattice can be more reactive than the complete lattice. Typical input files for the varied enrichment model of both the full and vanished lattices are included in Section 6.6.3.

Examination of the difference between k_{eff} calculated with the uniform enrichment model and k_{eff} calculated with the varied enrichment model indicates that the uniform enrichment model has an average positive (conservative) bias of $0.0032 \pm 0.0037 \Delta k_{\text{eff}}$. This clearly demonstrates that the uniform enrichment model can be used conservatively to model the BWR fuel lattices.

6.4.2.3 Determination of the Most Reactive Configuration

The fuel loading configuration of the cask affects the reactivity of the package. Several series of analyses determined the most reactive configuration for the cask. For this analysis, the most reactive fuel type is used to determine the most reactive configuration. The TN68 cask is modeled with the GE 10x10 assembly (uniform lattice average enrichment) over a 12.18-inch axial section with periodic axial boundary conditions and reflective radial boundary conditions. This represents an infinite array in the x-y direction of casks that are infinite in length which is conservative for criticality analysis.

The next set of analyses determines the effect of geometry and material tolerances for the TN-68 cask. Calculations were carried out with off-centered fuel positioning, variation in the rail material composition and fuel compartment inside dimension.

The following are the conditions evaluated for these scoping calculations.

- Baseline: Fuel centered in compartments, 100% water density utilizing the TN-68 scoping model.
- The inside dimension of the compartment is increased to 6.05 inches. All compartments move correspondingly further apart. This case verifies that the minimum compartment size is the most reactive dimensional configuration. By moving the compartments closer together, it reduces the neutron leakage, and by reducing the thickness of the water layer between the lattice and the compartment wall, it reduces the effectiveness of the neutron poison plates between the compartments.
- Variation of water density throughout: The water density in the fuel and the entire basket is varied from 1 to 100%, including water at the maximum density of 1.000 g/cm^3 , which occurs at $4 \text{ }^\circ\text{C}$. The water reflector remains at full density for all cases.
- Fuel lattices off-center in the compartments: Several channel thicknesses and a lattice with no channel are investigated. All lattices are shifted toward the longitudinal axis of the basket until the fuel channel or the outer pin cells of the lattice contact two compartment walls. This is not a credible configuration, but is intended to bound all cases of off-center fuel.

The results of these calculations are shown in Table 6.4-3. These results indicate that the most reactive configuration is due to off-center or “inward” positioning of the fuel where the fuel assemblies are moved closer to the center of the basket and the fuel compartment is modeled at the minimum width. All other variations are not expected to result in any significant change in the reactivity of the TN-68 cask. A sample input file at minimum compartment width is given in Section 6.6.4.

6.4.2.4 Determination of Maximum Initial Enrichment for Intact Assemblies

The most reactive configuration determined based on parametric studies is with the rail structure represented with aluminum and cylindrical holes of internal moderator, fuel compartment at minimum width and nominal thickness and the fuel assemblies positioned in the “inward” position. The most reactive fuel assembly is the GE 10x10 fuel assembly with a uniform lattice average enrichment and 0.120” thick channel. The following analysis uses this configuration to determine the maximum allowable initial enrichment as a function of poison plate loading. Only the fixed poison loading is changed for each model. In addition, the internal and external moderator density is varied to determine the peak reactivity for the specific configuration. The calculational KENO model described in Section 6.3 was utilized in the criticality calculations. This KENO model was benchmarked with the scoping KENO model utilized in Section 6.4.2.3 to ensure that the differences are statistically insignificant. The results of the benchmark calculation (discussed in Section 6.3.1) for the KENO models shown in Table 6.3-4 confirms this.

The canister / cask model for this evaluation differs from the actual design in the following ways:

- the neutron shield and outer shell of the cask are conservatively replaced with water between the casks, and
- the worst case geometry and material conditions, as determined in the previous sections, are modeled.

Eight different fixed poison loadings are analyzed in the criticality calculations as described in Section 6.3. The maximum analyzed initial enrichment is 4.70 wt % U235. Reconstituted fuel assemblies, where the fuel pins are replaced by non-fuel pins are also considered intact fuel assemblies provided they displace the same amount of moderator.

The results for the GE 10x10 lattice with 0.120 inch channels are shown in Table 6.4-4.

6.4.2.5 Determination of the Most Reactive Damaged Fuel Configuration

The TN68 basket is also authorized to load up to 8 damaged assemblies at the peripheral locations. These locations are 247, 248, 257, 258, 267, 268, 277 and 278. The most reactive damaged assembly model is determined in this section. This was completed by utilizing a limiting intact fuel configuration from the previous section. Based on the results shown in Table 6.4-4, the configuration chosen was based on a 0.200" thick, 54 mg B10/cm² poison plate (Type F Basket) with an initial enrichment of 4.50 wt % U235.

The structural analysis of Appendix 6A demonstrates that undamaged fuel remains intact under accident accelerations. Appendix 6B demonstrates that damaged fuel remains intact for normal and off-normal accelerations. Damaged fuel is assumed to sustain some further damage under accident accelerations. In order to bound the credible criticality effect of any resulting fuel reconfiguration, the damage resulting from a cask drop accident is modeled as both a single-ended and a double-ended shearing of a single row of fuel rods with moderator intrusion.

This damage is evaluated by a series of models constructed to evaluate the effects of radial movement of fuel rod pieces (the result of "single-ended" breaks), and axial movement (the result of "double-ended" breaks). Loose fuel pellets or shards may become dislodged if a rod becomes severed, but this will not result in a more reactive state than the cases described below because the fuel assembly is under-moderated by design. The models used to study these reconfigurations are described below.

The single-ended fuel rod shear cases assume that a fuel rod shears in one place and is displaced to a new location. The fuel pellets are assumed to remain in the fuel rod. This case will be evaluated by displacing one row of rods from the base fuel assembly matrix at small increments towards the side of the fuel compartment. The base fuel assembly matrix will be at nominal pitch and positioned in the "inward" position within the TN-68 cask to maximize the separation distance between the fuel array and the sheared row of fuel rods. The GE 10x10 fuel assembly is analyzed for the single-ended shear configuration.

The double-ended fuel rod shear cases assume that the fuel rod shears in two places and the intact fuel rod piece is separated from the parent fuel rod. Three resulting conditions are exhibited by the occurrence of a double-ended rod shear. These are, the fuel rod piece can remain in place, it can be displaced in the same plane, or it can be displaced to a different plane. The “remain in place” situation results in no deviation from the base fuel assembly matrix, and is therefore considered trivial and will not be evaluated separately. The fuel rod piece displaced in the same plane is equivalent to the single-ended rod shear case discussed above and will not be reevaluated in these cases. The fuel rod piece displaced in a different plane results in two possibilities: an added rod or a removed rod. As in the single-ended shear cases, the base fuel assembly matrix will be positioned in the “inward” position of the TN-68 cask to allow room for a row of displaced fuel rods. The nominal rod pitch is used for the base fuel matrix just as in the single-ended shear rod cases. The GE 10x10 fuel assembly is analyzed for the double-ended shear configuration.

In order to determine the effect of an axial shift in the sheared rods beyond the poison during transfer, bounding calculations that consider a 12.18" axial shift of these sheared rods (both single and double shear) are performed. The nominal rod pitch is used for these cases and the GE 10x10 fuel assembly is analyzed for this configuration.

The following is a breakdown of runs made in this analysis:

- Single-ended shear study (With axial shifting of a row of rods by 12.18").
- Double-ended shear study (With axial shifting of a row of rods by 12.18").

With the selection of the most reactive damaged fuel assembly geometry, the next set of analyses determined the maximum k_{eff} for various damaged fuel assembly loading configurations in the TN-68. The most reactive damaged fuel assembly geometry for the two damaged fuel mechanisms will be used to determine the maximum enrichment as a function of fixed poison loading for loading 8 damaged fuel assemblies in the basket. In other words, cases are analyzed for all the configurations described in this Section.

Single Ended Rod Shear Study

The first set of analyses performed is for the single-ended rod shear. The Single-ended rod shear study depicts the fuel assembly with its last row of rods separated from the rest of the assembly. The displacement of the sheared row of rods varies radially (both X and Y direction) from fuel assembly up to a maximum that is governed by the fuel assembly width and the fuel compartment size.

To model this in KENO, the base case was slightly modified. First, for the intact fuel lattice, the fuel assemblies are modeled as either a 10X9 array (array 5) or a 9X10 array (array 6) depending on the direction of shear. Unit 101 is a 10X1 array (array 3) and represents the sheared row of rods. Unit 102 is a 1X10 array (array 4) and represents the sheared column of rods. Units 104, 105, 106 and 107 represent the damaged fuel assembly in the compartment. The fuel assembly is represented by two arrays, array 5 or 6, depending on the direction of sheared rod movement and a corresponding array based on Unit 100 or 101. The eight peripheral locations are represented by eight new units with the same numbers (247, 248, 257, 258, 267, 268, 277 and 278) as the fuel assembly positions.

The displaced row of rod array is then shifted (separation distance is "D") away from the fuel assembly either in the X-direction or Y-direction. The amount of fuel remains the same, i.e. no new fuel is added to the system. Nominal rod pitch for all of the fuel assembly classes is used for the base fuel assembly. To study the reactivity of effect of separation distances greater than 0.450 cm, the fuel channel is assumed to be absent. The study is repeated for varying separation distances at full internal moderator density. The sheared model is utilized at zero separation distance to model the base case to determine if the two modeling approaches produce significantly different results. Figure 6.4-4 shows a sheared row of rods (units 247 and 248) with channel with radial rod movement. Figure 6.4-5 shows a sheared row of rods (units 257 and 258) without channel with circumferential rod movement. The results of this evaluation are shown in Table 6.4-5. The results indicate that the two modeling approaches produce very similar results at zero shear distance. The results also indicate that the system exhibits no major trends as a function of shear distance or the direction of shear. However, the cases with the highest k_{eff} will be analyzed for the 12.18" axial shift of sheared fuel rods.

A description of the modifications made to the KENO model(s) to implement the axial rod movement is as follows. The axial movement of a single sheared row of rods is modeled in KENO by introducing an additional row of rods at the top of the basket without removing an equal amount of fuel from the bottom of the basket. This approach is conservative. The base case for the single shear is modified first by including UNIT 11 and UNIT 12 as two axial segments of 12.18" each. UNIT 11 is the same as old UNIT 10 except that it is not the GLOBAL unit. UNIT 12 is the 12.18" axial segment that consists of just the sheared rods. UNIT 301 models all the interior cells without fuel (all locations except those that contain the damaged rods). UNITS 304, 305, 306 and 307 model the sheared rods within the fuel compartment without poison. UNITS 341 through 345 are similar to UNITS 241 through 245 except that they contain empty locations. Finally, UNITS 347, 348, 357, 358, 367, 368, 377 and 378 model the peripheral locations. UNIT 10 is the global unit that is an array of UNITS 11 and 12 (11 segments of UNIT 11 and 1 segment of UNIT 12). Periodic boundary conditions are

applied to the axial boundary making the model, essentially infinite axially. A KENO plot of this model, Figure 6.4-6, shows the sheared rods in the basket section above the zone of the neutron absorber plates.

The reference case shown in Table 6.4-5 is similar to the shift case described above except that the UNIT 12 contains no fuel rods. This case is analyzed to determine the reactivity effect of sheared rods since the base case always results in a higher k_{eff} than the 12.18" shift case. It is expected that there would be statistically insignificant differences between the 12.18" shift case and the reference cases. The results on Table 6.4-5 show that, for all of the three cases analyzed, the reference case had a higher k_{eff} than the shift case. These results indicate that the analyzed configuration with single shear is more conservative than the shift (axial rod movement) cases. The chosen single shear configuration is indicated in Table 6.4-5.

Double Ended Rod Shear Study

The Double Ended Rod Shear study is based on a shearing of a single row (or column) of rods radially and a subsequent axial shear of rods followed by axial rod movement such that portions of the fuel assembly have an extra row or column of rods. This scenario is modeled conservatively assuming that the entire fuel assembly contains an extra row (or column) of rods (10% additional uranium in the system). The base case for the KENO model is the single shear case with no channel and circumferential rod movement. First, the UNITS 104, 105, 106 and 107 are modified to include an additional row (or column) of rods so that the damaged locations are represented by fuel assemblies containing a 11x10 or a 10x11 array of rods. All the other UNITS remain the same. The variation in sheared distance (D) between the two rod arrays is analyzed for trends as a function of separation distance. Due to the presence of an extra row (or column) of rods, all the double shear cases are analyzed with no channel. Figure 6.4-7 shows a double sheared column of rods (units 247 and 248) without channel with circumferential rod movement. Figure 6.4-8 shows a double sheared row of rods (units 257 and 258) without channel with circumferential rod movement.

The 12.18" axial movement (shift) of sheared rods is implemented for double shear along similar lines as described for single shear in the previous section. A KENO plot of this model showing the sheared rods beyond poison is shown in Figure 6.4-9. Further, the reference case to determine the reactivity effect of the sheared rods alone is also analyzed for the worst double shear case. An additional case that depicts a more realistic double shear case is also analyzed. In this case, the UNIT 12 is modeled with intact fuel assemblies. The GLOBAL UNIT is an array of 12 segments containing 6 segments of UNIT 11 and 6 segments of UNIT 12. This case represents a fuel assembly represented by equal axial segments of a 10x10 and an 11x10 array of rods. This case is shown in Table 6.4-6 as the "classic" double shear case. Note that the "classic" double shear is based on a fuel assembly represented by equal segments of a 9x10 and an 11x10 array of rods. This case (10x10 and an 11x10 array of rods) is a conservative representation of the "classic" double shear case. The results of the double shear studies are shown in Table 6.4-6. The results indicate that there is a small but a positive change (increase) in reactivity with increase in separation distance of the sheared rods. The axial rod movement case results show that the difference with the reference case is statistically insignificant. A comparison of the double shear results (worst case k_{eff}) with the conservative "classic" double

shear case indicates that the implementation of double shear mechanism in this analysis is conservative and bounds all the rod movement cases. The chosen double shear configuration is indicated in Table 6.4-6.

6.4.2.6 Determination of Maximum Initial Enrichment for Damaged Assemblies

The most reactive damaged assembly configuration determined from the various damaged assembly studies is based on both the double-ended shear and single-ended shear models described in the previous section. The following analysis uses these configurations to determine the maximum allowable initial enrichment as a function of poison plate loading for the TN-68 cask. The analysis is carried out with the TN-68 containing 8 damaged assemblies and 60 design basis intact fuel assemblies. Only the damaged mechanism and the fixed poison loading is varied for each model. In addition, the internal moderator and external moderator density is varied to determine the peak reactivity for the specific configuration.

The cask model for this evaluation differs from the actual design in the following ways:

- the neutron shield and the skin of the cask are conservatively replaced with water between the casks, and
- the worst case geometry and material conditions as determined in Section 6.4.2.3 and the worst case damaged assembly configuration as determined in Section 6.4.2.5 are modeled.

Seven different fixed poison loadings (except 27 mg B10/cm² poison loading) are analyzed in the criticality calculations as described in Section 6.3. A comparison of the intact fuel assembly results for 27.0 mg B10/cm² poison loading and 31.5 mg B10/cm² poison loading (Type 0 and Type A) indicates that the Type A results are conservative. Due to the relatively large difference in reactivity between the two types, the conclusions based on the difference in initial enrichments of intact and damaged assemblies for the Type A basket can be conservatively applied to the Type 0 basket. Therefore, the damaged assembly calculations for Type 0 basket are not performed. The maximum analyzed initial enrichment is 4.70 wt % U235. A KENO plot of the design basis double shear model is shown in Figure 6.4-10. The results for the damaged fuel assembly analysis for the TN-68 cask are shown in Table 6.4-7. Note that there is no special basket type designation for the poison loading of 27.0 mg B10/cm². The Type 0 designation for this basket is for illustration purposes only and is restricted to this chapter.

6.4.3 Criticality Results

This section presents the results of the analyses used to demonstrate the acceptability of storing qualified fuel in the TN-68 cask under normal, off-normal, and accident conditions for fuel loading, handling, and storage.

Table 6.1-2 lists the bounding results for intact and damaged fuel assemblies for all conditions of storage. The highest calculated k_{eff} , including 2σ uncertainty for the intact assemblies, is 0.9405 for the GE 10x10 fuel assembly with an initial enrichment of 3.95 wt % U235 and a poison loading of 31.5 mg B10/cm² (Type A Basket). The maximum allowable initial enrichment as a function of fixed poison loading is given in Table 6.1-1. The input file for the cases with the highest calculated reactivity for intact assemblies is included in the Section 6.6.5

The highest calculated k_{eff} , including 2σ uncertainty for the damaged assembly calculations, is 0.9407 and it occurs for the GE 10x10 damaged fuel assembly (double shear) with an initial enrichment of 3.95 wt % U235 and a poison loading of 31.5 mg B10/cm² (Type A Basket). Based on the results for the Type A calculations, it can be inferred that the maximum initial enrichment of the damaged fuel assemblies in the Type 0 basket is the same as that of the intact assemblies. The maximum allowable initial enrichment as a function of fixed poison loading for the 8 damaged assemblies is given in Table 6.1-1. The input file for the case with the highest calculated reactivity for damaged assemblies is also included in Section 6.6.5

An Upper Subcritical Limit (USL) provides a high degree of confidence that a given system is subcritical if a criticality calculation based on the system yields a k_{eff} below the USL.

The criterion for subcriticality is that

$$k_{\text{KENO}} + 2\sigma_{\text{KENO}} \leq \text{USL},$$

Where USL is the upper subcritical limit established by an analysis of benchmark criticality experiments. In Section 6.5, the minimum USL over the parameter range is determined to be 0.9423. From Table 6.1-2, for the most reactive case,

$$k_{\text{KENO}} + 2\sigma_{\text{KENO}} = 0.9387 + 2(0.0010) = 0.9407 \leq 0.9423.$$

This indicates that the fuel will remain subcritical. Conclusions regarding specific aspects of the methods used or the analyses presented can be drawn from the quantitative results presented in the associated tables.

6.5 Critical Benchmark Experiments

The criticality safety analysis of the TN-68 cask uses the CSAS25 module of the SCALE system of codes. The CSAS25 control module allows simplified data input to the functional modules BONAMI-S, NITAWL-S, and KENO V.a. These modules process the required cross-section data and calculate the k_{eff} of the system. BONAMI-S performs resonance self-shielding calculations for nuclides that have Bondarenko data associated with their cross sections. NITAWL-S applies a Nordheim resonance self-shielding correction to nuclides having resonance parameters. Finally, KENO V.a calculates the effective neutron multiplication (k_{eff}) of a 3-D system.

The analysis presented herein uses the fresh fuel assumption for criticality analysis. The analysis employs the 44-group ENDF/B-V cross-section library because it has a small bias, as determined by 83 benchmark calculations. The Upper Subcritical Limit (USL-1) was determined using the results of these 83 benchmark calculations.

The benchmark problems used in this verification are representative of the benchmarks of commercial light water reactor (LWR) fuels with the following characteristics:

- A. water moderation
- B. boron neutron absorbers
- C. unirradiated light water reactor type fuel (no fission products or “burnup credit”)
- D. close reflection
- E. near room temperature (vs. reactor operating temperature)
- F. Uranium oxide fuels.

Criticality codes are verified by comparing benchmark calculations to actual critical benchmark experiments. The difference between the calculated reactivity and the experimental reactivity is referred to as ‘calculational’ bias. This bias may be a function of system parameters such as fuel lattice separation, fuel enrichment, neutron absorber properties, reflector properties, or fuel/moderator volume ratio; or, there may be no specific correlation with system parameters. These experiments are discussed in detail in reference [5].

6.5.1 Benchmark Experiments and Applicability

The critical experiments and input files are taken from NUREG/CR-6361 [6]. The input files are obtained from ORNL, and modified to change the cross section library to the SCALE 44 group library that is used in all the TN-68 criticality evaluations. Experiments which feature simple arrays, separator plates, steel reflector walls, water holes, and borated poison plates are selected. Experiments with features that are not characteristic of the TN-68 storage cask are not used. Such features include soluble boron, poisons other than boron, poison rods, reflector walls other than steel, and flux traps. The 83 critical experiments chosen and their descriptive characteristics are listed in Table 6.5-1.

An upper subcritical limit (USL) is determined using Method 1, "confidence band with administrative margin", described in Section 4.1.1 of NUREG/CR-6361. The USLSTATS program also described therein is used to perform the statistical analysis. The administrative margin will be 0.05, and the confidence level $1-\gamma_1$ will be 0.95. It is assumed that the actual value of k_{eff} in all the experiments is exactly 1.

The characteristics water/fuel volume, hydrogen to fissile atom ratio (H/X), fuel pin pitch, and enrichment are listed in Tables 2.1 and 3.5 of NUREG/CR-6361. A comparison of the range of these characteristics in the experiments, and the corresponding values for the TN-68 and its contents verifies that the TN-68 falls within the range covered by the critical experiments.

6.5.2 Results of the Benchmark Calculations

The quantitative characteristics of the critical experiments and results of the benchmark calculations are listed in Table 6.5-1.

Six subsets of the results are analyzed to determine if there is a trend in the bias (calculated $k_{\text{eff}} - 1$) as a function of an experimental variable and in all subsets, the data test normal. A least mean squares linear regression is performed to fit the data of k_{eff} as a function of each independent variable, and the Pearson correlation coefficient r is determined. A coefficient of zero indicates no correlation, and a coefficient of $|1|$ indicates exact correlation. The results are listed in Table 6.5-3. The values of the correlation coefficient, as well as a visual examination of the data plots, indicate that there is very little correlation between the bias and any of the experimental variables, and therefore, no discernable trend. The best correlation between bias and an experimental variable occurs for the fuel assembly separation distance. The data and the linear regression results for the ratio of water volume to fuel volume in the pin cell are plotted in Figure 6.5-1.

The modeling techniques and the applicable parameters for the actual criticality evaluations fall within the range of those addressed by the benchmarks in Table 6.5-2. The results from the comparisons of physical parameters of each of the fuel assembly types to the applicable USL value are presented in Table 6.5-2. The minimum value of the USL from all the data sets is 0.9423, which occurs for the fuel assembly separation distance, as shown in Table 6.5-3.

6.5.3 Modeling Bias

There is no modeling bias due to the cask model as discussed in Section 6.3.1. The modeling bias due to the use of a uniform pin enrichment model of the lattice is 0.0032, as discussed in Section 6.4.2.2. This value for the bias indicates that the uniform pin enrichment model results in a higher k_{eff} than the non-uniform model. Therefore, for fuel assemblies with non-uniform pin enrichments, the criticality evaluation with a uniform enrichment model produces conservative results. This bias, 0.0032 in Δk_{eff} units, is treated as an additional conservatism in the criticality analysis.

6.6 Supplemental Data

6.6.1 Sample Input File, Most Reactive Lattice Evaluation

```
=CSAS25
TN68 case 12wc, G12 fuel, wet annulus, 0.065 channel
27GROUPNDF4 LATTICECELL
UO2      1 0.965 293. 92235 3.7 92238 96.3 END
ZIRCALLOY 2 1.0 END
H2O      3 1.0 END
SS304    4 1.0 END
CARBONSTEEL 5 1.0 END
AL       6 DEN=2.668 END
B-10    6 DEN=0.025 END
H2O      7 1.0 END
H2O      8 0.5 END
AL       8 0.5 END
END COMP
SQUAREPITCH 1.2954 0.8763 1 3 1.0262 2 0.8941 7 END
TN68
READ PARAM RUN=yes PLT=yes TME=5000 GEN=203 NPG=1000 END PARAM
READ GEOM
UNIT 1 com='fuel rod'
CYLINDER 1 1 0.4382 2P15.456
CYLINDER 7 1 0.4470 2P15.456
CYLINDER 2 1 0.5131 2P15.456
CUBOID 3 1 4P 0.6477 2P15.456
UNIT 2 com='water rod'
CUBOID 3 1 4P 0.6477 2P15.456
UNIT 3 com='fuel compartment'
ARRAY 1 -6.4770 -6.4770 -15.456
CUBOID 7 1 4P6.703 2P15.456
CUBOID 2 1 4P6.868 2P15.456
CUBOID 7 1 4P7.62 2P15.456
CUBOID 4 1 4P8.095 2P15.456
CUBOID 6 1 4P8.491 2P15.456
HOLE 7 0 8.293 15.4559
HOLE 7 0 -8.293 15.4559
HOLE 8 8.293 0 -15.4559
HOLE 8 -8.293 0 -15.4559
HOLE 9 8.293 0 15.4559
HOLE 9 -8.293 0 15.4559
HOLE 10 7.4549 8.293 -2.3755
HOLE 10 -7.4549 8.293 -2.3755
HOLE 10 7.4549 -8.293 -2.3755
HOLE 10 -7.4549 -8.293 -2.3755
HOLE 11 8.293 7.4549 2.0695
HOLE 11 -8.293 7.4549 2.0695
HOLE 11 8.293 -7.4549 2.0695
HOLE 11 -8.293 -7.4549 2.0695
UNIT 4
ARRAY 3 -16.982 -8.491 -15.456
UNIT 5
ARRAY 4 -8.491 -16.982 -15.456
UNIT 6
ARRAY 5 -50.946 -8.491 -15.456
UNIT 7 com='stainless spacer and horizontal gap'
CUBOID 5 1 2P8.491 2P0.19799 0 -4.445
CUBOID 7 1 2P8.491 2P0.19799 0 -4.75
UNIT 8 com='stainless spacer'
CUBOID 5 1 2P0.19799 2P8.491 4.445 0
UNIT 9 com='horizontal gap'
CUBOID 7 1 2P0.19799 2P8.0949 0 -0.305
UNIT 10 com='vertical egg crate gap'
CUBOID 7 1 2P0.64 2P0.19799 2P13.08
UNIT 11 com='vertical egg crate gap'
CUBOID 7 1 2P0.19799 2P0.64 2P13.08
GLOBAL UNIT 12
```



```
ARRAY 2 -67.928 -50.946 -15.456
CYLINDER 8 1 88.26 2P15.4561
HOLE 6 0 59.4371 0
HOLE 6 0 -59.4371 0
HOLE 4 0 76.4192 0
HOLE 4 0 -76.4192 0
HOLE 5 76.4191 0 0
HOLE 5 -76.4191 0 0
CYLINDER 5 1 107.31 2P15.4561
CYLINDER 7 1 137.31 2P15.4561
CUBOID 0 1 4P137.31 2P15.4561
END GEOM
READ ARRAY
ARA=1 NUX=10 NUY=10 FILL F1 A34 2.2 A44 2.2 A56 2.2 A66 2.2 END FILL
ARA=2 NUX=8 NUY=6 FILL F3 END FILL
ARA=3 NUX=2 FILL F3 END FILL
ARA=4 NUY=2 FILL F3 END FILL
ARA=5 NUX=6 FILL F3 END FILL
END ARRAY
READ BNDS ZFC=PER END BNDS
READ PLOT
TTL='CLOSE UP top'
XUL=-1 YUL=18. ZUL=10.86 XLR=18. YLR=-1 ZLR=10.86
UAX=1 VDN=-1
NAX=1000 LPI=10.0 END
SCR=YES
END PLOT
END DATA
END
```

6.6.2 Variable Enrichment Patterns, Uniform Enrichment Validation
(from reference [3], [4])

GE 7x7, fuel model 3

Case: 3var

location	Qty	enrichment	normalized
1	30	2.930	4.331
11	12	1.940	2.868
10	6	1.690	2.498
9	1	1.330	1.966
	Total	average	average
	49	2.508	3.7

10	11	11	11	10	10	9
11	1	1	1	1	11	10
1	1	1	1	1	1	10
1	1	1	1	1	1	11
1	1	1	1	1	1	11
11	1	1	1	1	1	11
11	11	1	1	1	11	10

GE, 8x8, fuel model 4

Case: 4var1

location	Qty	enrichment	normalized
11	1	1.450	1.960
10	4	1.870	2.528
9	14	2.220	3.001
1	44	3.010	4.069
	Total	average	average
	63	2.737	3.7

10	9	9	9	9	9	10	11
9	1	1	1	1	1	9	10
1	1	1	1	1	1	1	9
1	1	1	1	1	1	1	9
1	1	1	w	1	1	1	9
1	1	1	1	1	1	1	9
1	1	1	1	1	1	1	9
9	1	1	1	1	1	9	10

Case: 4var2

location	Qty	enrichment	normalized
11	1	1.450	2.046
10	4	1.870	2.639
9	14	2.140	3.020
1	44	2.870	4.050
	Total	average	average
	63	2.622	3.7

Note: w= water rod

GE, 8x8, fuel model 5

Case: 5var1

location	Qty	enrichment	normalized
11	1	1.450	1.963
10	4	1.870	2.532
9	14	2.220	3.006
1	43	3.010	4.075
	Total	average	average
	62	2.733	3.7

10	9	9	9	9	9	10	11
9	1	1	1	1	1	9	10
1	1	1	1	1	1	1	9
1	1	1	w	1	1	1	9
1	1	1	1	w	1	1	9
1	1	1	1	1	1	1	9
1	1	1	1	1	1	1	9
9	1	1	1	1	1	9	10

Case: 5var2

location	Qty	enrichment	normalized
1	16	3.950	4.822
9	14	3.300	4.029
10	11	3.000	3.663
11	12	2.400	2.930
12	6	2.000	2.442
13	2	1.700	2.075
14	1	1.300	1.587
	Total	average	average
	62	3.031	3.7

12	11	11	11	12	12	13	14
11	9	10	9	10	11	11	13
9	10	1	1	9	10	11	12
9	1	1	w	1	9	10	12
9	1	1	1	w	1	9	11
9	10	1	1	1	1	10	11
10	1	10	1	1	10	9	11
11	10	9	9	9	9	11	12

Case: 5var3

location	Qty	enrichment	normalized
1	18	3.950	4.581
9	7	3.800	4.407
10	6	3.300	3.827
11	12	2.800	3.247
12	8	2.400	2.783
13	4	2.000	2.320
14	1	1.500	1.740
15	6	3.000	3.479
	total	average	average
	62	3.190	3.7

13	12	11	11	11	12	13	14
12	10	9	15	10	11	12	13
11	15	1	1	1	9	11	12
9	1	1	w	1	1	10	11
9	1	1	1	w	1	15	11
10	15	1	1	1	1	9	11
11	1	15	1	1	15	10	12
12	11	10	9	9	11	12	13

GE 8x8 with 4 water rods, fuel model 84

Case: 84var1

location	qty	enrichment	normalized
1	26	3.950	4.313
9	4	3.600	3.931
10	8	3.400	3.713
11	4	3.200	3.494
12	5	3.000	3.276
13	4	2.800	3.058
14	1	2.600	2.839
15	4	2.400	2.621
16	1	2.200	2.402
17	2	2.000	2.184
18	1	1.600	1.747
	total	average	average
	60	3.388	3.7

15	13	12	12	13	15	17	18
11	10	10	9	10	11	14	17
1	9	1	1	1	12	11	15
1	1	1	W	w	1	10	13
1	1	1	w	W	1	9	12
1	1	1	1	1	1	10	12
10	1	1	1	1	9	10	13
16	10	1	1	1	1	11	15

Case: 84var2

location	qty	enrichment	normalized
1	29	3.950	4.283
9	2	3.800	4.120
10	2	3.600	3.903
11	6	3.400	3.686
12	8	3.000	3.253
13	5	2.800	3.036
14	2	2.600	2.819
15	3	2.200	2.385
16	2	1.800	1.952
17	1	1.600	1.735
	total	average	average
	60	3.413	3.7

16	14	12	12	13	13	15	17
12	10	11	9	11	12	13	15
1	1	1	1	1	1	12	13
1	1	1	W	w	1	11	13
1	1	1	w	W	1	9	12
1	1	1	1	1	1	11	12
11	1	1	1	1	1	10	14
15	11	1	1	1	1	12	16

GE 8x8 with 1 large water rod, fuel model 9

Case: 9var1

location	qty	enrichment	normalized
9	1	1.800	1.815
10	2	2.800	2.824
11	5	3.000	3.025
12	7	3.400	3.429
13	2	3.600	3.630
14	2	2.400	2.420
1	41	3.950	3.983
	total	average	average
	60	3.669	3.7

14	11	12	13	12	11	10	9
12	1	1	1	1	1	11	10
1	1	1	1	1	1	1	11
1	1	1	w	w	1	1	12
1	1	1	w	w	1	1	13
1	1	1	1	1	1	1	12
1	1	1	1	1	1	1	11
12	1	1	1	1	1	12	14

Case: 9var2

location	qty	enrichment	normalized
9	1	1.600	1.650
10	2	2.200	2.269
11	4	2.600	2.682
12	2	3.200	3.300
13	7	3.400	3.507
14	2	3.000	3.094
15	1	2.400	2.475
16	4	3.600	3.713
1	35	3.950	4.074
17	2	3.800	3.919
	total	average	average
	60	3.588	3.7

11	14	13	13	12	11	10	9
13	1	1	1	16	16	15	10
1	1	1	1	1	1	16	11
1	1	1	w	w	1	16	12
1	1	1	w	w	1	1	13
1	1	1	1	1	1	1	13
17	1	1	1	1	1	1	14
13	17	1	1	1	1	13	11

Case: 9var3

location	qty	enrichment	normalized
9	1	1.600	1.696
10	2	2.600	2.756
11	2	3.200	3.393
12	16	3.400	3.605
13	4	3.000	3.181
14	5	2.400	2.544
1	28	3.950	4.188
15	2	3.600	3.817
	total	average	average
	60	3.490	3.7

14	13	12	12	12	11	10	9
12	1	13	1	1	14	12	10
1	12	1	1	1	1	14	11
1	1	15	w	w	1	1	12
1	12	1	w	w	1	1	12
1	1	1	1	15	1	13	12
12	12	1	12	1	12	1	13
14	12	1	1	1	1	12	14

GE 9x9 with two large water rods, model 11

Case: 11var1

location	qty	enrichment	normalized
9	1	1.800	1.690
10	5	2.200	2.065
11	7	3.000	2.816
12	8	3.600	3.380
13	4	3.200	3.004
14	19	3.950	3.708
1	23	4.800	4.506
15	7	4.400	4.131
	total	average	average
	74	3.941	3.7

10	11	12	12	12	12	11	10	9
13	14	14	14	1	14	13	11	10
15	1	14	14	15	15	14	13	11
1	14	1	w	w	15	15	14	12
1	1	1	w	w	w	15	1	12
1	14	1	1	w	w	14	14	12
14	1	1	1	1	1	14	14	12
11	1	1	14	1	14	1	14	11
10	11	14	1	1	1	15	13	10

Case: 11var2

location	qty	enrichment	normalized
9	1	1.600	1.651
10	2	2.400	2.476
11	2	2.200	2.270
12	8	3.200	3.302
13	2	3.000	3.096
14	2	3.800	3.921
15	2	2.600	2.683
16	4	2.800	2.889
17	4	3.600	3.715
18	2	3.400	3.508
1	45	3.950	4.076
	total	average	average
	74	3.586	3.7

15	12	12	14	13	12	11	10	9
18	1	17	1	1	17	16	16	10
1	1	1	12	1	1	1	16	11
1	1	1	w	w	1	1	17	12
1	1	1	w	w	w	1	1	13
1	1	1	1	w	w	12	1	14
1	1	1	1	1	1	1	17	12
1	1	1	1	1	1	1	1	12
16	1	1	1	1	1	1	18	15

Case: 11var3

location	qty	enrichment	normalized
9	1	1.600	1.734
10	4	2.200	2.384
11	8	2.600	2.817
12	4	3.200	3.467
13	8	3.000	3.250
14	4	3.400	3.684
15	19	3.600	3.901
1	26	3.950	4.280
	total	average	average
	74	3.415	3.7

11	13	13	13	12	11	10	10	9
15	15	13	15	15	14	11	11	10
1	15	15	12	1	15	15	11	10
1	15	1	w	w	1	15	14	11
1	1	1	w	w	w	1	15	12
1	15	1	1	w	w	12	15	13
1	1	1	1	1	1	15	13	13
14	1	1	15	1	15	15	15	13
11	14	1	1	1	1	1	15	11

GE 9x9 with two large water rods, model 11

Case: 13var1

location	qty	enrichment	normalized
9	1	1.600	1.408
10	4	2.400	2.112
11	2	3.200	2.816
12	12	3.950	3.476
13	4	2.800	2.464
14	4	3.600	3.168
1	29	4.900	4.313
15	14	4.400	3.872
16	4	4.200	3.696
	total	average	average
	74	4.204	3.7

10	13	12	12	12	12	11	10	9
14	12	15	16	1	16	14	13	10
15	1	15	1	15	1	15	14	11
1	15	1	w	w	1	1	16	12
1	1	1	w	w	w	15	1	12
1	15	1	15	w	w	1	16	12
1	1	1	1	1	1	15	15	12
12	1	1	15	1	15	1	12	13
13	12	1	1	1	1	15	14	10

Case: 13var2

location	qty	enrichment	normalized
9	1	2.000	1.736
10	7	2.800	2.430
11	3	3.200	2.777
12	11	3.950	3.428
13	4	3.600	3.125
1	32	4.900	4.253
14	12	4.400	3.819
15	4	4.200	3.645
	total	average	average
	74	4.263	3.7

10	10	12	12	12	12	11	10	9
13	14	14	15	1	15	13	10	10
14	1	14	1	14	1	12	13	11
1	14	1	w	w	1	1	15	12
1	1	1	w	w	w	14	1	12
1	1	1	1	w	w	1	15	12
1	1	1	1	1	1	14	14	12
12	1	1	1	1	14	1	14	10
11	12	1	1	1	1	14	13	10

Case: 13var3

location	qty	enrichment	normalized
9	1	2.000	1.724
10	2	2.800	2.414
11	6	3.200	2.759
12	17	3.950	3.406
13	2	2.400	2.069
1	36	4.900	4.225
14	8	4.400	3.794
15	2	3.600	3.104
	total	average	average
	74	4.291	3.7

13	11	12	12	12	12	11	10	9
15	1	14	12	1	12	12	11	10
14	1	12	1	1	1	12	12	11
1	14	1	w	w	1	1	12	12
1	1	1	w	w	w	1	1	12
1	1	1	1	w	w	1	12	12
1	1	1	1	1	1	12	14	12
14	1	1	1	1	14	1	1	11
11	14	1	1	1	1	14	15	13

6.6.3 Sample Input Files, Uniform Enrichment Model Validation

A. Varied Enrichment, Complete Lattice

```
=CSAS25
TN68 case 11var2, G11 fuel, wet annulus, 0.100 channel, varied enrichment
27GROUPPDF4 LATTICECELL
UO2 1 0.965 293. 92235 4.076 92238 95.924 END
ZIRCALLOY 2 1.0 END
H2O 3 1.0 END
SS304 4 1.0 END
CARBONSTEEL 5 1.0 END
AL 6 DEN=2.668 END
B-10 6 DEN=0.025 END
H2O 7 1.0 END
H2O 8 0.5 END
AL 8 0.5 END
UO2 9 0.965 293. 92235 1.651 92238 98.349 END
UO2 10 0.965 293. 92235 2.476 92238 97.524 END
UO2 11 0.965 293. 92235 2.270 92238 97.730 END
UO2 12 0.965 293. 92235 3.302 92238 96.698 END
UO2 13 0.965 293. 92235 3.096 92238 96.904 END
UO2 14 0.965 293. 92235 3.921 92238 96.079 END
UO2 15 0.965 293. 92235 2.683 92238 97.317 END
UO2 16 0.965 293. 92235 2.889 92238 97.111 END
UO2 17 0.965 293. 92235 3.715 92238 96.285 END
UO2 18 0.965 293. 92235 3.508 92238 96.492 END
END COMP
SQUAREPITCH 1.4376 0.9550 1 3 1.1176 2 0.9754 7 END
MORE DATA res=9 cylinder 0.4775 dan(9)=0.24577753
res=10 cylinder 0.4775 dan(10)=0.24577753
res=11 cylinder 0.4775 dan(11)=0.24577753
res=12 cylinder 0.4775 dan(12)=0.24577753
res=13 cylinder 0.4775 dan(13)=0.24577753
res=14 cylinder 0.4775 dan(14)=0.24577753
res=15 cylinder 0.4775 dan(15)=0.24577753
res=16 cylinder 0.4775 dan(16)=0.24577753
res=17 cylinder 0.4775 dan(17)=0.24577753
res=18 cylinder 0.4775 dan(18)=0.24577753 END MORE DATA
TN68
READ PARAM RUN=yes PLT=yes TME=5000 GEN=203 NPG=1000 END PARAM
READ GEOM
UNIT 1 com='fuel rod'
CYLINDER 1 1 0.4775 2P15.456
CYLINDER 7 1 0.4877 2P15.456
CYLINDER 2 1 0.5588 2P15.456
CUBOID 3 1 4P 0.7188 2P15.456
UNIT 2 com='water rod'
CUBOID 3 1 4P 0.7188 2P15.456
UNIT 3 com='fuel compartment'
ARRAY 1 -6.4692 -6.4692 -15.456
CUBOID 7 1 4P6.703 2P15.456
CUBOID 2 1 4P6.957 2P15.456
CUBOID 7 1 4P7.62 2P15.456
CUBOID 4 1 4P8.095 2P15.456
CUBOID 6 1 4P8.491 2P15.456
HOLE 4 0 8.293 15.4559
HOLE 4 0 -8.293 15.4559
HOLE 5 8.293 0 -15.4559
HOLE 5 -8.293 0 -15.4559
HOLE 6 8.293 0 15.4559
HOLE 6 -8.293 0 15.4559
HOLE 7 7.4549 8.293 -2.3755
HOLE 7 -7.4549 8.293 -2.3755
HOLE 7 7.4549 -8.293 -2.3755
HOLE 7 -7.4549 -8.293 -2.3755
HOLE 8 8.293 7.4549 2.0695
HOLE 8 -8.293 7.4549 2.0695
```



```

HOLE 8 8.293 -7.4549 2.0695
HOLE 8 -8.293 -7.4549 2.0695
UNIT 4 com='stainless spacer and horizontal gap'
CUBOID 5 1 2P8.491 2P0.19799 0 -4.445
CUBOID 7 1 2P8.491 2P0.19799 0 -4.75
UNIT 5 com='stainless spacer'
CUBOID 5 1 2P0.19799 2P8.491 4.445 0
UNIT 6 com='horizontal gap'
CUBOID 7 1 2P0.19799 2P8.0949 0 -0.305
UNIT 7 com='vertical egg crate gap'
CUBOID 7 1 2P0.64 2P0.19799 2P13.08
UNIT 8 com='vertical egg crate gap'
CUBOID 7 1 2P0.19799 2P0.64 2P13.08
UNIT 9 com='fuel rod'
CYLINDER 9 1 0.4775 2P15.456
CYLINDER 7 1 0.4877 2P15.456
CYLINDER 2 1 0.5588 2P15.456
CUBOID 3 1 4P 0.7188 2P15.456
UNIT 10 com='fuel rod'
CYLINDER 10 1 0.4775 2P15.456
CYLINDER 7 1 0.4877 2P15.456
CYLINDER 2 1 0.5588 2P15.456
CUBOID 3 1 4P 0.7188 2P15.456
UNIT 11 com='fuel rod'
CYLINDER 11 1 0.4775 2P15.456
CYLINDER 7 1 0.4877 2P15.456
CYLINDER 2 1 0.5588 2P15.456
CUBOID 3 1 4P 0.7188 2P15.456
UNIT 12 com='fuel rod'
CYLINDER 12 1 0.4775 2P15.456
CYLINDER 7 1 0.4877 2P15.456
CYLINDER 2 1 0.5588 2P15.456
CUBOID 3 1 4P 0.7188 2P15.456
UNIT 13 com='fuel rod'
CYLINDER 13 1 0.4775 2P15.456
CYLINDER 7 1 0.4877 2P15.456
CYLINDER 2 1 0.5588 2P15.456
CUBOID 3 1 4P 0.7188 2P15.456
UNIT 14 com='fuel rod'
CYLINDER 14 1 0.4775 2P15.456
CYLINDER 7 1 0.4877 2P15.456
CYLINDER 2 1 0.5588 2P15.456
CUBOID 3 1 4P 0.7188 2P15.456
UNIT 15 com='fuel rod'
CYLINDER 15 1 0.4775 2P15.456
CYLINDER 7 1 0.4877 2P15.456
CYLINDER 2 1 0.5588 2P15.456
CUBOID 3 1 4P 0.7188 2P15.456
UNIT 16 com='fuel rod'
CYLINDER 16 1 0.4775 2P15.456
CYLINDER 7 1 0.4877 2P15.456
CYLINDER 2 1 0.5588 2P15.456
CUBOID 3 1 4P 0.7188 2P15.456
UNIT 17 com='fuel rod'
CYLINDER 17 1 0.4775 2P15.456
CYLINDER 7 1 0.4877 2P15.456
CYLINDER 2 1 0.5588 2P15.456
CUBOID 3 1 4P 0.7188 2P15.456
UNIT 18 com='fuel rod'
CYLINDER 18 1 0.4775 2P15.456
CYLINDER 7 1 0.4877 2P15.456
CYLINDER 2 1 0.5588 2P15.456
CUBOID 3 1 4P 0.7188 2P15.456
GLOBAL UNIT 19
ARRAY 2 0 0 -15.456
CUBOID 8 1 73 0 73 0 2P15.456
CUBOID 5 1 92 0 92 0 2P15.456
CUBOID 7 1 122 0 122 0 2P15.456
END GEOM
READ ARRAY

```

```

ARA=1 NUX=9 NUY=9 FILL 16 6R1 18 15
8R1 12 7R1 17 12 4R1 2 2 12 1 14
3R1 3R2 1 1 13 3R1 2 2 1 1 17 12
3R1 12 3R1 16 11 18 1 17 1 1 17 16 16 10
15 12 12 14 13 12 11 10 9 END FILL
ARA=2 NUX=4 NUY=4 FILL F3 END FILL
END ARRAY
READ BNDS ZFC=PER -XY=MIR END BNDS
READ PLOT
TTL='CLOSE UP'
XUL=-1 YUL=20. ZUL=0 XLR=20. YLR=-1 ZLR=0
UAX=1 VDN=-1
NAX=1000 LPI=10.0 END
SCR=YES
END PLOT
END DATA
END

```

B. Varied Enrichment, Vanished Lattice

```

=CSAS25
TN68 case 11van2, G11 fuel, wet annulus, 0.100 channel, vanish lattice
27GROUPNDF4 LATTICECELL
UO2 1 0.965 293. 92235 4.076 92238 95.924 END
ZIRCALLOY 2 1.0 END
H2O 3 1.0 END
SS304 4 1.0 END
CARBONSTEEL 5 1.0 END
AL 6 DEN=2.668 END
B-10 6 DEN=0.025 END
H2O 7 1.0 END
H2O 8 0.5 END
AL 8 0.5 END
UO2 9 0.965 293. 92235 1.651 92238 98.349 END
UO2 10 0.965 293. 92235 2.476 92238 97.524 END
UO2 11 0.965 293. 92235 2.270 92238 97.730 END
UO2 12 0.965 293. 92235 3.302 92238 96.698 END
UO2 13 0.965 293. 92235 3.096 92238 96.904 END
UO2 14 0.965 293. 92235 3.921 92238 96.079 END
UO2 15 0.965 293. 92235 2.683 92238 97.317 END
UO2 16 0.965 293. 92235 2.889 92238 97.111 END
UO2 17 0.965 293. 92235 3.715 92238 96.285 END
UO2 18 0.965 293. 92235 3.508 92238 96.492 END
END COMP
SQUAREPITCH 1.4376 0.9550 1 3 1.1176 2 0.9754 7 END
MORE DATA res=9 cylinder 0.4775 dan(9)=0.24577753
res=10 cylinder 0.4775 dan(10)=0.24577753
res=11 cylinder 0.4775 dan(11)=0.24577753
res=12 cylinder 0.4775 dan(12)=0.24577753
res=13 cylinder 0.4775 dan(13)=0.24577753
res=14 cylinder 0.4775 dan(14)=0.24577753
res=15 cylinder 0.4775 dan(15)=0.24577753
res=16 cylinder 0.4775 dan(16)=0.24577753
res=17 cylinder 0.4775 dan(17)=0.24577753
res=18 cylinder 0.4775 dan(18)=0.24577753 END MORE DATA
TN68
READ PARAM RUN=yes PLT=no TME=5000 GEN=203 NPG=1000 END PARAM
READ GEOM
UNIT 1 com='fuel rod'
CYLINDER 1 1 0.4775 2P15.456
CYLINDER 7 1 0.4877 2P15.456
CYLINDER 2 1 0.5588 2P15.456
CUBOID 3 1 4P 0.7188 2P15.456
UNIT 2 com='water rod'
CUBOID 3 1 4P 0.7188 2P15.456
UNIT 3 com='fuel compartment'
ARRAY 1 -6.4692 -6.4692 -15.456
CUBOID 7 1 4P6.703 2P15.456
CUBOID 2 1 4P6.957 2P15.456

```

CUBOID 7 1 4P7.62 2P15.456
 CUBOID 4 1 4P8.095 2P15.456
 CUBOID 6 1 4P8.491 2P15.456
 HOLE 4 0 8.293 15.4559
 HOLE 4 0 -8.293 15.4559
 HOLE 5 8.293 0 -15.4559
 HOLE 5 -8.293 0 -15.4559
 HOLE 6 8.293 0 15.4559
 HOLE 6 -8.293 0 15.4559
 HOLE 7 7.4549 8.293 -2.3755
 HOLE 7 -7.4549 8.293 -2.3755
 HOLE 7 7.4549 -8.293 -2.3755
 HOLE 7 -7.4549 -8.293 -2.3755
 HOLE 8 8.293 7.4549 2.0695
 HOLE 8 -8.293 7.4549 2.0695
 HOLE 8 8.293 -7.4549 2.0695
 HOLE 8 -8.293 -7.4549 2.0695
 UNIT 4 com='stainless spacer and horizontal gap'
 CUBOID 5 1 2P8.491 2P0.19799 0 -4.445
 CUBOID 7 1 2P8.491 2P0.19799 0 -4.75
 UNIT 5 com='stainless spacer'
 CUBOID 5 1 2P0.19799 2P8.491 4.445 0
 UNIT 6 com='horizontal gap'
 CUBOID 7 1 2P0.19799 2P8.0949 0 -0.305
 UNIT 7 com='vertical egg crate gap'
 CUBOID 7 1 2P0.64 2P0.19799 2P13.08
 UNIT 8 com='vertical egg crate gap'
 CUBOID 7 1 2P0.19799 2P0.64 2P13.08
 UNIT 9 com='fuel rod'
 CYLINDER 9 1 0.4775 2P15.456
 CYLINDER 7 1 0.4877 2P15.456
 CYLINDER 2 1 0.5588 2P15.456
 CUBOID 3 1 4P 0.7188 2P15.456
 UNIT 10 com='fuel rod'
 CYLINDER 10 1 0.4775 2P15.456
 CYLINDER 7 1 0.4877 2P15.456
 CYLINDER 2 1 0.5588 2P15.456
 CUBOID 3 1 4P 0.7188 2P15.456
 UNIT 11 com='fuel rod'
 CYLINDER 11 1 0.4775 2P15.456
 CYLINDER 7 1 0.4877 2P15.456
 CYLINDER 2 1 0.5588 2P15.456
 CUBOID 3 1 4P 0.7188 2P15.456
 UNIT 12 com='fuel rod'
 CYLINDER 12 1 0.4775 2P15.456
 CYLINDER 7 1 0.4877 2P15.456
 CYLINDER 2 1 0.5588 2P15.456
 CUBOID 3 1 4P 0.7188 2P15.456
 UNIT 13 com='fuel rod'
 CYLINDER 13 1 0.4775 2P15.456
 CYLINDER 7 1 0.4877 2P15.456
 CYLINDER 2 1 0.5588 2P15.456
 CUBOID 3 1 4P 0.7188 2P15.456
 UNIT 14 com='fuel rod'
 CYLINDER 14 1 0.4775 2P15.456
 CYLINDER 7 1 0.4877 2P15.456
 CYLINDER 2 1 0.5588 2P15.456
 CUBOID 3 1 4P 0.7188 2P15.456
 UNIT 15 com='fuel rod'
 CYLINDER 15 1 0.4775 2P15.456
 CYLINDER 7 1 0.4877 2P15.456
 CYLINDER 2 1 0.5588 2P15.456
 CUBOID 3 1 4P 0.7188 2P15.456
 UNIT 16 com='fuel rod'
 CYLINDER 16 1 0.4775 2P15.456
 CYLINDER 7 1 0.4877 2P15.456
 CYLINDER 2 1 0.5588 2P15.456
 CUBOID 3 1 4P 0.7188 2P15.456
 UNIT 17 com='fuel rod'
 CYLINDER 17 1 0.4775 2P15.456

```

CYLINDER 7 1 0.4877 2P15.456
CYLINDER 2 1 0.5588 2P15.456
CUBOID 3 1 4P 0.7188 2P15.456
UNIT 18 com='fuel rod'
CYLINDER 18 1 0.4775 2P15.456
CYLINDER 7 1 0.4877 2P15.456
CYLINDER 2 1 0.5588 2P15.456
CUBOID 3 1 4P 0.7188 2P15.456
GLOBAL UNIT 19
ARRAY 2 0 0 -15.456
CUBOID 8 1 73 0 73 0 2P15.456
CUBOID 5 1 92 0 92 0 2P15.456
CUBOID 7 1 122 0 122 0 2P15.456
END GEOM
READ ARRAY
ARA=1 NUX=9 NUZ=9 FILL 16 6R1 18 15
1 2 1 1 2 1 1 2 12 7R1 17 12 4R1 2 2 12 1 14
1 2 1 3R2 1 2 13 3R1 2 2 1 1 17 12
3R1 12 3R1 16 11 18 2 17 1 2 17 16 2 10
15 12 12 14 13 12 11 10 9 END FILL
ARA=2 NUX=4 NUZ=4 FILL F3 END FILL
END ARRAY
READ BNDS ZFC=PER -XY=MIR END BNDS
READ PLOT
TTL='CLOSE UP'
XUL=-1 YUL=20. ZUL=0 XLR=20. YLR=-1 ZLR=0
UAX=1 VDN=-1
NAX=1000 LPI=10.0 END
SCR=YES
END PLOT
END DATA
END

```

6.6.4 Sample Input Files, Most Reactive Intact Assembly Configuration, Scoping Model

10x10 fuel, 5.97 inch compartment, borated aluminum absorber

```

=csas25
TN68 case dbljprdy597, G12 fuel, 5.97 inch comp, 0.120 channel, off-ctr fuel
27GROUPNDF4 LATTICECELL
UO2 1 0.965 293. 92235 3.7 92238 96.3 END
ZIRCALLOY 2 1.0 END
H2O 3 1.0 END
SS304 4 1.0 END
CARBONSTEEL 5 1.0 END
AL 6 DEN=2.659 END
B-10 6 DEN=0.034 END
H2O 7 1.0 END
AL 8 1.0 END
UO2 9 0.965 293. 92235 5 92238 95 END
END COMP
SQUAREPITCH 1.2954 0.8763 1 3 1.0262 2 0.8941 7 END
MORE DATA res=9 cylinder 0.43815 dan(9)=2.8563458E-01 END MORE DATA
TN68
READ PARAM RUN=yes PLT=no TME=5000 GEN=403 NPG=2000 END PARAM
READ GEOM
UNIT 1 com='fuel rod'
CYLINDER 1 1 0.4382 2P15.456
CYLINDER 7 1 0.4470 2P15.456
CYLINDER 2 1 0.5131 2P15.456
CUBOID 3 1 4P 0.6477 2P15.456
UNIT 2 com='water rod'
CUBOID 3 1 4P 0.6477 2P15.456
UNIT 3 com='fuel compartment upper left quadrant'
ARRAY 1 -5.9028 -7.0512 -15.456
CUBOID 7 1 7.2772 -6.1288 6.1288 -7.2772 2P15.456

```

CUBOID 2 1 7.582 -6.4336 6.4336 -7.582 2P15.456
 CUBOID 7 1 4P7.582 2P15.456
 CUBOID 4 1 4P8.057 2P15.456
 CUBOID 6 1 4P8.453 2P15.456
 HOLE 7 0 8.255 15.4559
 HOLE 7 0 -8.255 15.4559
 HOLE 8 8.255 0 -15.4559
 HOLE 8 -8.255 0 -15.4559
 HOLE 9 8.255 0 15.4559
 HOLE 9 -8.255 0 15.4559
 HOLE 10 7.4169 8.255 5.14
 HOLE 10 -7.4169 8.255 5.14
 HOLE 10 7.4169 -8.255 5.14
 HOLE 10 -7.4169 -8.255 5.14
 HOLE 11 8.255 7.4169 -5.445
 HOLE 11 -8.255 7.4169 -5.445
 HOLE 11 8.255 -7.4169 -5.445
 HOLE 11 -8.255 -7.4169 -5.445
 HOLE 12 7.4169 8.255 -13.155
 HOLE 12 -7.4169 8.255 -13.155
 HOLE 12 7.4169 -8.255 -13.155
 HOLE 12 -7.4169 -8.255 -13.155
 HOLE 13 8.255 7.4169 12.85
 HOLE 13 -8.255 7.4169 12.85
 HOLE 13 8.255 -7.4169 12.85
 HOLE 13 -8.255 -7.4169 12.85
 UNIT 4
 ARRAY 3 -16.906 -8.453 -15.456
 UNIT 5
 ARRAY 4 -8.453 -16.906 -15.456
 UNIT 6
 ARRAY 5 -50.718 -8.453 -15.456
 UNIT 7 com='stainless spacer and horizontal gap'
 CUBOID 5 1 2P8.453 2P0.19799 0 -4.445
 CUBOID 7 1 2P8.453 2P0.19799 0 -4.75
 UNIT 8 com='stainless spacer'
 CUBOID 5 1 2P0.19799 2P8.453 4.445 0
 UNIT 9 com='horizontal gap'
 CUBOID 7 1 2P0.19799 2P8.0569 0 -0.305
 UNIT 10 com='vertical egg crate gap'
 CUBOID 7 1 2P0.64 2P0.19799 2P5.565
 UNIT 11 com='vertical egg crate gap'
 CUBOID 7 1 2P0.19799 2P0.64 2P5.565
 UNIT 12 com='vertical egg crate gap'
 CUBOID 7 1 2P0.64 2P0.19799 2P2.3
 UNIT 13 com='vertical egg crate gap'
 CUBOID 7 1 2P0.19799 2P0.64 2P2.3
 UNIT 14 com='basket rail hole'
 CYLINDER 7 1 5.5 2P15.4561
 UNIT 15 com='basket rail hole'
 CYLINDER 7 1 4.4 2P15.4561
 UNIT 16 com='basket rail hole'
 CYLINDER 7 1 3.0 2P15.4561
 UNIT 17 com='fuel compartment upper right quadrant'
 ARRAY 1 -7.0512 -7.0512 -15.456
 CUBOID 7 1 6.1288 -7.2772 6.1288 -7.2772 2P15.456
 CUBOID 2 1 6.4336 -7.582 6.4336 -7.582 2P15.456
 CUBOID 7 1 4P7.582 2P15.456
 CUBOID 4 1 4P8.057 2P15.456
 CUBOID 6 1 4P8.453 2P15.456
 HOLE 7 0 8.255 15.4559
 HOLE 7 0 -8.255 15.4559
 HOLE 8 8.255 0 -15.4559
 HOLE 8 -8.255 0 -15.4559
 HOLE 9 8.255 0 15.4559
 HOLE 9 -8.255 0 15.4559
 HOLE 10 7.4169 8.255 5.14
 HOLE 10 -7.4169 8.255 5.14
 HOLE 10 7.4169 -8.255 5.14
 HOLE 10 -7.4169 -8.255 5.14

HOLE 11 8.255 7.4169 -5.445
HOLE 11 -8.255 7.4169 -5.445
HOLE 11 8.255 -7.4169 -5.445
HOLE 11 -8.255 -7.4169 -5.445
HOLE 12 7.4169 8.255 -13.155
HOLE 12 -7.4169 8.255 -13.155
HOLE 12 7.4169 -8.255 -13.155
HOLE 12 -7.4169 -8.255 -13.155
HOLE 13 8.255 7.4169 12.85
HOLE 13 -8.255 7.4169 12.85
HOLE 13 8.255 -7.4169 12.85
HOLE 13 -8.255 -7.4169 12.85
UNIT 18 com='fuel compartment lower right quadrant'
ARRAY 1 -7.0512 -5.9028 -15.456
CUBOID 7 1 6.1288 -7.2772 7.2772 -6.1288 2P15.456
CUBOID 2 1 6.4336 -7.582 7.582 -6.4336 2P15.456
CUBOID 7 1 4P7.582 2P15.456
CUBOID 4 1 4P8.057 2P15.456
CUBOID 6 1 4P8.453 2P15.456
HOLE 7 0 8.255 15.4559
HOLE 7 0 -8.255 15.4559
HOLE 8 8.255 0 -15.4559
HOLE 8 -8.255 0 -15.4559
HOLE 9 8.255 0 15.4559
HOLE 9 -8.255 0 15.4559
HOLE 10 7.4169 8.255 5.14
HOLE 10 -7.4169 8.255 5.14
HOLE 10 7.4169 -8.255 5.14
HOLE 10 -7.4169 -8.255 5.14
HOLE 11 8.255 7.4169 -5.445
HOLE 11 -8.255 7.4169 -5.445
HOLE 11 8.255 -7.4169 -5.445
HOLE 11 -8.255 -7.4169 -5.445
HOLE 12 7.4169 8.255 -13.155
HOLE 12 -7.4169 8.255 -13.155
HOLE 12 7.4169 -8.255 -13.155
HOLE 12 -7.4169 -8.255 -13.155
HOLE 13 8.255 7.4169 12.85
HOLE 13 -8.255 7.4169 12.85
HOLE 13 8.255 -7.4169 12.85
HOLE 13 -8.255 -7.4169 12.85
UNIT 19 com='fuel compartment lower left quadrant'
ARRAY 1 -5.9028 -5.9028 -15.456
CUBOID 7 1 7.2772 -6.1288 7.2772 -6.1288 2P15.456
CUBOID 2 1 7.582 -6.4336 7.582 -6.4336 2P15.456
CUBOID 7 1 4P7.582 2P15.456
CUBOID 4 1 4P8.057 2P15.456
CUBOID 6 1 4P8.453 2P15.456
HOLE 7 0 8.255 15.4559
HOLE 7 0 -8.255 15.4559
HOLE 8 8.255 0 -15.4559
HOLE 8 -8.255 0 -15.4559
HOLE 9 8.255 0 15.4559
HOLE 9 -8.255 0 15.4559
HOLE 10 7.4169 8.255 5.14
HOLE 10 -7.4169 8.255 5.14
HOLE 10 7.4169 -8.255 5.14
HOLE 10 -7.4169 -8.255 5.14
HOLE 11 8.255 7.4169 -5.445
HOLE 11 -8.255 7.4169 -5.445
HOLE 11 8.255 -7.4169 -5.445
HOLE 11 -8.255 -7.4169 -5.445
HOLE 12 7.4169 8.255 -13.155
HOLE 12 -7.4169 8.255 -13.155
HOLE 12 7.4169 -8.255 -13.155
HOLE 12 -7.4169 -8.255 -13.155
HOLE 13 8.255 7.4169 12.85
HOLE 13 -8.255 7.4169 12.85
HOLE 13 8.255 -7.4169 12.85
HOLE 13 -8.255 -7.4169 12.85

UNIT 20
 ARRAY 6 -16.906 -8.453 -15.456
 UNIT 21
 ARRAY 7 -8.453 -16.906 -15.456
 UNIT 22
 ARRAY 8 -50.718 -8.453 -15.456
 UNIT 23 com='fuel rod, 5%'
 CYLINDER 9 1 0.4382 2P15.456
 CYLINDER 7 1 0.4470 2P15.456
 CYLINDER 2 1 0.5131 2P15.456
 CUBOID 3 1 4P 0.6477 2P15.456
 UNIT 24 com='fuel compartment lower left, 5%'
 ARRAY 9 -5.9028 -5.9028 -15.456
 CUBOID 7 1 7.2772 -6.1288 7.2772 -6.1288 2P15.456
 CUBOID 2 1 7.582 -6.4336 7.582 -6.4336 2P15.456
 CUBOID 7 1 4P7.582 2P15.456
 CUBOID 4 1 4P8.057 2P15.456
 CUBOID 6 1 4P8.453 2P15.456
 HOLE 7 0 8.255 15.4559
 HOLE 7 0 -8.255 15.4559
 HOLE 8 8.255 0 -15.4559
 HOLE 8 -8.255 0 -15.4559
 HOLE 9 8.255 0 15.4559
 HOLE 9 -8.255 0 15.4559
 HOLE 10 7.4169 8.255 5.14
 HOLE 10 -7.4169 8.255 5.14
 HOLE 10 7.4169 -8.255 5.14
 HOLE 10 -7.4169 -8.255 5.14
 HOLE 11 8.255 7.4169 -5.445
 HOLE 11 -8.255 7.4169 -5.445
 HOLE 11 8.255 -7.4169 -5.445
 HOLE 11 -8.255 -7.4169 -5.445
 HOLE 12 7.4169 8.255 -13.155
 HOLE 12 -7.4169 8.255 -13.155
 HOLE 12 7.4169 -8.255 -13.155
 HOLE 12 -7.4169 -8.255 -13.155
 HOLE 13 8.255 7.4169 12.85
 HOLE 13 -8.255 7.4169 12.85
 HOLE 13 8.255 -7.4169 12.85
 HOLE 13 -8.255 -7.4169 12.85
 GLOBAL UNIT 25
 ARRAY 2 -67.624 -50.718 -15.456
 CYLINDER 8 1 87.96 2P15.4561
 HOLE 6 0 59.1711 0
 HOLE 22 0 -59.1711 0
 HOLE 4 0 76.0772 0
 HOLE 20 0 -76.0772 0
 HOLE 5 76.0771 0 0
 HOLE 21 -76.0771 0 0
 HOLE 14 25.0 75.5 0
 HOLE 14 75.5 25.0 0
 HOLE 15 57.4 57.4 0
 HOLE 16 72.8 40.0 0
 HOLE 16 40.0 72.8 0
 HOLE 14 -25.0 75.5 0
 HOLE 14 -75.5 25.0 0
 HOLE 15 -57.4 57.4 0
 HOLE 16 -72.8 40.0 0
 HOLE 16 -40.0 72.8 0
 HOLE 14 25.0 -75.5 0
 HOLE 14 75.5 -25.0 0
 HOLE 15 57.4 -57.4 0
 HOLE 16 72.8 -40.0 0
 HOLE 16 40.0 -72.8 0
 HOLE 14 -25.0 -75.5 0
 HOLE 14 -75.5 -25.0 0
 HOLE 15 -57.4 -57.4 0
 HOLE 16 -72.8 -40.0 0
 HOLE 16 -40.0 -72.8 0
 CYLINDER 7 1 88.26 2P15.4561

```

CYLINDER 5 1 107.31 2P15.4561
CYLINDER 7 1 137.31 2P15.4561
CUBOID 0 1 4P137.31 2P15.4561
END GEOM
READ ARRAY
ARA=1 NUX=10 NUY=10 FILL F1 A34 2 2 A44 2 2 A56 2 2 A66 2 2 END FILL
ARA=2 NUX=8 NUY=6 FILL 4R19 4R18 2Q8 4R3 4R17 2Q8 A20 24 END FILL
ARA=3 NUX=2 FILL 3 17 END FILL
ARA=4 NUY=2 FILL 18 17 END FILL
ARA=5 NUX=6 FILL 3R3 3R17 END FILL
ARA=6 NUX=2 FILL 19 18 END FILL
ARA=7 NUY=2 FILL 19 3 END FILL
ARA=8 NUX=6 FILL 3R19 3R18 END FILL
ARA=9 NUX=10 NUY=10 FILL F23 A34 2 2 A44 2 2 A56 2 2 A66 2 2 END FILL
END ARRAY
READ BNDS ZFC=PER END BNDS
END DATA
END

```

6.6.5 Sample Input Files, TN-68 Final Criticality Evaluation

This section provides representative input files for the CSAS25 computer models for the final criticality calculations. These input files are provided as part of a separate proprietary compact disc. A listing and a brief description of the input files utilized as part of the criticality analysis is given below:

File Name	Description
dbinact.inp	Design basis, worst case intact – calculational model
dbdamaged.inp	Design basis, worst case damaged – calculational model

6.7 References

1. "SCALE, A Modular Code System for Performing Standardized Computer Analyses for Licensing Evaluation", NUREG/CR-0200, Rev. 6 (ORNL/NUREG/CSD-2/R6), Vol. I-III, September 1998.
2. SCALE-4.3, Modular Code System for Performing Standardized Computer Analyses for Licensing Evaluation for Workstations and Personal Computers, CCC-545, ORNL, March 1997.
3. ORNL/TM-10902, Physical Characteristics of GE BWR Fuel Assemblies, 1989.
4. GE Proprietary Data
 - a. Initial Core Fuel Design Summary for Peach Bottom Atomic Power Station Unit 3, NEDC-10816, March 1973
 - b. Peach Bottom 2 Reload 1 Nuclear Design Report, NEDE 21051, September 1975
 - c. Peach Bottom 3 Reload 2 Nuclear Design Report, NEDE 21759, December 1977
 - d. Peach Bottom 2 Reload 3 Nuclear Design Report, NEDE 23896, July 1978
 - e. Fuel Bundle Design Report GE8B-P8DQB321-11GZ-80M-4WR-150-T
 - f. Fuel Bundle Design Report GE8B-P8DQB319-9GZ-80M-4WR-150-T
 - g. Fuel Bundle Design Report GE9B-P8DWB310-11GZ-80M-150-T
 - h. Fuel Bundle Design Report GE9B-P8DWB324-10GZ-80M-150-T
 - i. Fuel Bundle Design Report GE9B-P8DWB320-10GZ-80M-150-T
 - j. Fuel Bundle Design Report GE9B-P8DWB324-10GZ1-80M-150-T
 - k. Fuel Bundle Design Report GE9B-P8DWB328-11GZ-80M-150-T
 - l. Fuel Bundle Design Report GE11-P9HUB307-5G5.0/4G4.0-100M-146-T-LTA
 - m. Fuel Bundle Design Report GE11-P9HUB334-10GZ1-100M-146-T
 - n. Fuel Bundle Design Report GE11-P9HUB367-11GZ-100M-146-T
 - o. Fuel Bundle Design Report GE11-P9HUB387-12GZ3-100T-146-T
 - p. Fuel Bundle Design Report GE11-P9HUB405-13GZ1-100T-146-T
 - q. Fuel Bundle Design Report GE13-P9DTB400-13GZ-100T-146-T
 - r. Fuel Bundle Design Report GE13-P9DTB397-13GZ-100T-146-T
 - s. Fuel Bundle Design Report GE13-P9DTB392-15GZ-100T-146-T
 - t. Fuel Bundle Design Report GE13-P9DTB39-13GZ-100T-146-T
 - u. Fuel Bundle Design Report 8DRB284-7G4.0-100M-150
 - v. Fuel Bundle Design Report 8DRB285-4G2.0-100M-150
 - w. Fuel Bundle Design Report 8DRB299-7G4.0-100M-150
 - x. Fuel Bundle Design Report P8DRB299-3G5.0/4G4.0-100M-150
5. Power Authority of the State of New York, Inquiry No. Q-02-1961 (RFQ for FitzPatrick Dry Spent Fuel Storage System)
6. NUREG/CR-6361, Criticality Benchmark Guide for Light-Water-Reactor Fuel in Transportation and Storage Packages, 1997

Table 6.1-1
Maximum Initial Enrichment for both Intact and Damaged Fuel Assemblies

Basket Type ⁽¹⁾	B10 Areal Density (mg B10/cm ²) ⁽²⁾	Intact Assembly Lattice Average Enrichment (wt % U235)	Damaged Assembly Peak Pellet Enrichment (wt % U235)
-	27.0	3.70	3.70
A	31.5	3.95	3.95
B	36.0	4.05	4.05
C	40.5	4.15	4.15
D	45.0	4.30	4.30
E	49.5	4.40	4.40
F	54.0	4.50	4.50
G	63.0	4.70	4.70

- (1) Basket Types are classified according to the fixed poison loading. No designation is provided for the basket with a poison plate loading of 27.0 mg B10/cm²
- (2) The areal density listed here is that used in the criticality calculations; the minimum specified in Chapter 9 is greater

Table 6.1-2
Summary of Limiting Criticality Evaluations for the TN-68 Cask

Description ⁽¹⁾	K _{keno}	σ _{keno}	K _{eff}
Intact Assemblies, GE 10x10 Lattice, 3.95 wt % U235 Poison plate - 0.120" thick, 31.5 mg B10/cm²,			
Dry Case, Normal Condition for Storage	0.4365	0.0004	0.4373
100% IMD, 50% EMD, Hypothetical Accident	0.9387	0.0009	0.9405
Damaged Assemblies, GE 10x10 Lattice, 3.95 wt % U235 Poison plate - 0.120" thick, 31.5 mg B10/cm²			
Dry Case for Damaged	0.4382	0.0003	0.4388
100% IMD, 0.01% EMD, Hypothetical Accident	0.9387	0.0010	0.9407

- (1) IMD = Internal Moderator Density, EMD = External Moderator Density

Table 6.2-1
Fuel Characteristics for Criticality
(from references[3], [4] and [5])

GE fuel generation	model	array	rod pitch	fuel rods	rod od	clad thick	pellet dia	water rods	water rod od	water rod id
2A	2a	7x7	0.738	49	0.570	0.036	0.488	0	x	x
2, 2B	2	7x7	0.738	49	0.563	0.032	0.487	0	x	x
3, 3A, 3B	3	7x7	0.738	49	0.563	0.037	0.477	0	x	x
4, 4A, 4B	4	8x8	0.640	63	0.493	0.034	0.416	1	0.493	0.425
5	5	8x8	0.640	62	0.483	0.032	0.410	2	0.591	0.531
6, 6B	5	8x8	0.640	62	0.483	0.032	0.410	2	0.591	0.531
7, 7B	5	8x8	0.640	62	0.483	0.032	0.410	2	0.591	0.531
8, 8B - 2w	82	8x8	0.640	62	0.483	0.032	0.411	2	0.591	0.531
8, 8B - 4w	84	8x8	0.640	60	0.483	0.032	0.411	4	0.591	0.531
This fuel has 2 large water rods and 2 small water rods									0.483	0.431
9, 9B	9	8x8	0.640	60	0.483	0.032	0.411	1	1.34	1.26
10	9	8x8	0.640	60	0.483	0.032	0.411	1	1.34	1.26
11	11	9x9	0.566	74	0.440	0.028	0.376	2	0.98	0.92
13	11	9x9	0.566	74	0.440	0.028	0.376	2	0.98	0.92
12	12	10x10	0.510	92	0.404	0.026	0.345	2	0.98	0.92

Notes:

1. All dimensions in inches
2. All fuel channels 5.278 inches inside, and from 0.065 to 0.120 inch thick.
3. All fuels are evaluated with 96.5% theoretical density and 3.7 wt % U235 average enrichment.
4. The fuel rod pitch is for C and D lattice designs. The S lattice has a smaller pitch, which is less reactive as shown in Table 6.4-4.
5. The fuel designs designated by GE as 6, 6B, 7, and 7B are sometimes referred to as "P" (pressurized) and "B" (barrier).

Table 6.3-1
TN-68 - Basket and Cask Dimensions

Parameter	Actual inches	Model inches (cm)
Compartment Inside (Nominal)	6.00	5.97 (15.1638)
Compartment Inside (Maximum)	6.05	
Compartment Inside (Minimum)	5.97	
Compartment wall (Nominal)	0.1874	0.187 (0.4749)
Compartment wall (Maximum)	0.2014	
Compartment wall (Minimum)	0.1734	
Stainless steel strip height	1.75	1.75 (4.445)
Stainless steel strip thickness	0.3125	0.300 (0.762)
Poison/Al plates height	10.4	10.25 (26.035)
Poison/Al plates thickness	0.300 – 0.310	0.300 (0.762)
horizontal (thermal expansion) gap	0.03 – 0.09	0.180 (0.457)
vertical (egg-crate) slot width	1.25	1.37 (3.479)
vertical (egg-crate) slot height	1.81 + 4.38	1.81 + 4.38 (4.6 + 11.13)
Cavity inside radius	34.75	34.75 (88.26)
Cask wall thickness	7.50	7.50 (19.05)

Table 6.3-2
TN-68 Fixed Poison Loading Requirements

Basket Type	Minimum Plate Thickness (inches / cm)	Model ⁽¹⁾ B10 Loading (mg/cm ²)	Model ⁽²⁾ Boron wt % in Alloy
0 ⁽³⁾	0.100 / 0.254	27.0	4.385
A	0.120 / 0.304	31.5	4.275
B	0.135 / 0.342	36.0	4.343
C	0.150 / 0.381	40.5	4.385
D	0.167 / 0.424	45.0	4.378
E	0.187 / 0.475	49.5	4.299
F	0.200 / 0.508	54.0	4.385
G	0.240 / 0.609	63.0	4.268

(1) The fixed poison (Borated Aluminum) loading utilized in the KENO model

(2) Based on a B10 enrichment of 90%

(3) Type 0 basket designation is just for illustration purposes

Table 6.3-3
Description of the KENO Model Units

Geometry Units	Description
1	Fuel Pin Cell
2	Water Pin (for 10x10 Fuel)
3	Fuel Assembly in the Channel (Array 1)
5	Additional Fuel Pin Cell
6	Extra Fuel Assembly in the Channel (Array 2)
21 - 28	Basket Cells with Poison along the West Face of F/A
31 - 38	Basket Cells with / without Poison along the North Face of F/A
41 - 48	Basket Cells with / without Poison along the East Face of F/A
51 - 58	Basket Cells with Poison along the South Face of F/A
25,35,45,55	Arrays that define the West, North, East and South Faces of the Basket Cell without fuel
61 - 68	Basket Cells without Poison along the West Face of F/A
71 - 78	Basket Cells without Poison along the North Face of F/A
81 - 88	Basket Cells without Poison along the East Face of F/A
91 - 98	Basket Cells without Poison along the South Face of F/A
65,75,85,95	Arrays that define the West, North, East and South Faces of the Basket Cell without fuel and poison
201	Basket Cell with Fuel Assembly Positions 201, 202, 203, 207, 208, 209, 213, 214, 215, 243, 253 representing the South West Interior Positions
202	Basket Cell with Fuel Assembly Positions 219, 220, 221, 225, 226, 227, 231, 232, 233, 254, 263 representing the South East Positions
203	Basket Cell with Fuel Assembly Positions 222, 223, 224, 228, 229, 230, 234, 235, 236, 264, 274 representing the North West Positions
204	Basket Cell with Fuel Assembly Positions 204, 205, 206, 210, 211, 212, 216, 217, 218, 244, 273 representing the North East Positions
205	Basket Cell with Fuel Assembly Positions 241, 247, 251, 257 representing South West Facing Corner Positions
206	Basket Cell with Fuel Assembly Positions 256, 258, 261, 267 representing North West Facing Corner Positions
207	Basket Cell with Fuel Assembly Positions 266, 268, 276, 278 representing the North East Facing Corner Positions
208	Basket Cell with Fuel Assembly Positions 246, 248, 271, 277 representing South East Facing Corner Positions

Table 6.3-3
Description of the KENO Model Units
(continued)

Geometry Units	Description
211 - 218	Same as 201 - 208 containing extra fuel for additional options
221	Basket Cell with Fuel Assembly Position # 252
222	Basket Cell with Fuel Assembly Position # 255
223	Basket Cell with Fuel Assembly Position # 262
224	Basket Cell with Fuel Assembly Position # 265
225	Basket Cell with Fuel Assembly Position # 275
226	Basket Cell with Fuel Assembly Position # 272
227	Basket Cell with Fuel Assembly Position # 245
228	Basket Cell with Fuel Assembly Position # 242
241	A (6X1) Array of Peripheral Basket Cells at the West Face
242	A (1X6) Array of Peripheral Basket Cells at the North Face
243	A (6X1) Array of Peripheral Basket Cells at the East Face
244	A (1X6) Array of Peripheral Basket Cells at the South Face
245	A (6X6) Array of Basket Cells defining the inner 36 locations
14, 15, 16	Cells representing the Aluminum cylinders to be used as rail material
10	Global Unit

Table 6.3-4
Comparison of KENO Models

Description	K_{keno}	σ_{keno}	K_{eff}
Scoping Model discussed in Section 6.3	0.9305	0.0009	0.9323
KENO Model utilized in this analysis	0.9302	0.0009	0.9320

Table 6.3-5
Material Property Data

Material	ID	Density g/cm ³	Element	Weight %	Atom Density (atoms/b-cm)
UO ₂ (Enrichment - 3.95 wt%)	1	10.576	U235	3.482	9.4355E-04
			U238	84.670	2.2654E-02
			O	11.848	4.7195E-02
Zircaloy-4	2	6.56	Zr	98.23	4.2541E-02
			Sn	1.45	4.8254E-04
			Fe	0.21	1.4856E-04
			Cr	0.10	7.5978E-05
			Hf	0.01	2.2133E-06
Water (Pellet Clad Gap)	3	0.998	H	11.1	6.6769E-02
			O	88.9	3.3385E-02
Stainless Steel (SS304)	4	7.94	C	0.080	3.1877E-04
			Si	1.000	1.7025E-03
			P	0.045	6.9468E-05
			Cr	19.000	1.7473E-02
			Mn	2.000	1.7407E-03
			Fe	68.375	5.8545E-02
			Ni	9.500	7.7402E-03
Internal Moderator (Water)	5	0.998	H	11.1	6.6769E-02
			O	88.9	3.3385E-02
UO ₂ (Extra Fuel) (Enrichment - 4.70 wt%)	6	10.686	U235	4.143	1.1227E-03
			U238	84.007	2.2477E-02
			O	11.850	4.7199E-02
Aluminum	8	2.70	Al	100.0	6.0307E-02
Type A Borated Aluminum Poison Plate (31.50 mg B10/cm ²)	9	2.693	B10	3.848	6.2317E-03
			B11	0.428	6.2974E-04
			Al	97.725	5.7536E-02
External Moderator (Water)	10	0.998	H	11.1	6.6769E-02
			O	88.9	3.3385E-02
Type D Borated Aluminum Poison Plate (45.0 mg B10/cm ²)	9	2.693	B10	3.940	6.3818E-03
			B11	0.438	6.4492E-04
			Al	95.622	5.7474E-02
Type G Borated Aluminum Poison Plate (63.0 mg B10/cm ²)	9	2.693	B10	3.841	6.2215E-03
			B11	0.427	6.2871E-04
			Al	95.732	5.7540E-02

Table 6.4-1
Results, Most Reactive Lattice Evaluation

array	GE fuel generation	water in rods	channel	k _{eff}	σ
7x7	2a	no	none	0.9087	0.0017
		yes	none	0.9135	0.0015
		yes	0.065	0.9190	0.0016
		yes	0.080	0.9213	0.0017
		yes	0.120	0.9213	0.0017
7x7	2, 2b	no	none	0.9136	0.0016
		yes	none	0.9199	0.0015
		yes	0.065	0.9207	0.0016
		yes	0.080	0.9219	0.0016
		yes	0.120	0.9229	0.0015
7x7	3, 3A, 3B	no	none	0.9093	0.0018
		yes	none	0.9190	0.0016
		yes	0.065	0.9150	0.0017
		yes	0.080	0.9167	0.0016
		yes	0.120	0.9208	0.0016
8x8	4, 4a, 4b	no	none	0.9032	0.0017
		yes	none	0.9104	0.0016
		yes	0.065	0.9114	0.0015
		yes	0.100	0.9156	0.0015
		yes	0.120	0.9141	0.0015
8x8	5, 6, 6B, 7, 7B	no	none	0.9131	0.0016
		yes	none	0.9152	0.0018
		yes	0.065	0.9190	0.0015
		yes	0.100	0.9180	0.0016
		yes	0.120	0.9200	0.0016
8x8	8, 8b, 2 water rods	no	none	0.9156	0.0016
		yes	none	0.9137	0.0016
		yes	0.065	0.9183	0.0017
		yes	0.100	0.9226	0.0017
		yes	0.120	0.9199	0.0016
8x8	8, 8b, 4 water rods	no	none	0.9145	0.0016
		yes	none	0.9145	0.0015
		yes	0.065	0.9171	0.0016
		yes	0.100	0.9197	0.0016
		yes	0.120	0.9218	0.0016

Table 6.4-1
Results, Most Reactive Lattice Evaluation
(Continued)

array	GE fuel generation	water in rods	channel	k_{eff}	σ
8x8	9, 9b, 10	no	none	0.9149	0.0017
		yes	none	0.9159	0.0015
		yes	0.065	0.9212	0.0017
		yes	0.100	0.9220	0.0015
		yes	0.120	0.9235	0.0016
9x9	11, 13	no	none	0.9114	0.0017
		yes	none	0.9175	0.0017
		yes	0.065	0.9204	0.0015
		yes	0.100	0.9212	0.0016
		yes	0.120	0.9223	0.0016
10x10	12	no	none	0.9183	0.0014
		yes	none	0.9226	0.0016
		yes	0.065	0.9270	0.0015
		yes	0.100	0.9250	0.0015
		yes	0.120	0.9268	0.0016

Table 6.4-2
Results, Uniform Enrichment Model Validation

Uniform 3.7% enrichment			Varied enrichment			
Case	k_{eff}	σ	Case	k_{eff}	σ	Δk_{eff}
7x7 GE3, 0.080 channel	0.9107	0.0017	3var	0.9054	0.0017	0.0053
8x8 GE4, 0.100 channel	0.9152	0.0018	4var1	0.9094	0.0016	0.0058
			4var2	0.9073	0.0016	0.0079
8x8 GE5, 0.100 channel	0.923	0.0016	5var1	0.9122	0.0016	0.0108
			5var2	0.9148	0.0016	0.0082
			5var3	0.9115	0.0017	0.0115
8x8 GE8, 0.100 channel 4 water rods	0.9179	0.0016	84var1	0.9171	0.0016	0.0008
			84var2	0.9149	0.0013	0.0030
8x8 GE9, 0.100 channel	0.9206	0.0015	9var1	0.9189	0.0016	0.0017
			9var2	0.9214	0.0017	-0.0008
			9var3	0.9201	0.0015	0.0005
9x9 GE11, 0.100 channel	0.922	0.0016	11var1	0.9174	0.0016	0.0046
			11var2	0.9196	0.0016	0.0024
			11var3	0.9218	0.0016	0.0002
			13var1	0.9180	0.0016	0.0040
			13var2	0.9208	0.0016	0.0012
			13var3	0.9198	0.0015	0.0022
			11van1 ⁽¹⁾	0.9184	0.0015	0.0036
			11van2	0.9211	0.0015	0.0009
			11van3	0.9252	0.0017	-0.0032
			13van1	0.9218	0.0016	0.0002
			13van2	0.9209	0.0015	0.0011
			13van3	0.9204	0.0016	0.0016
				average Δk_{eff}⁽²⁾		0.0032
				std deviation		0.0037

Note:

1. The last six cases are vanished lattices. They are the same as the six immediately preceding cases, except that the partial length fuel rods have vanished and are replaced by water.

Table 6.4-3
 TN-68 Most Reactive Intact Configuration – Scoping Results

10x10 GE12

Case description	k_{eff}	σ	$k_{eff}+2\sigma$
centered 10x10 fuel, 0.065 channel, 6.05 inch cell	0.9109	0.0015	0.9139
baseline: centered 10x10 fuel, 0.065 channel, 6 inch cell	0.9151	0.0016	0.9183
Investigation of individual effects, centered fuel, 6 inch cells:			
water density 0.01 g/cm ³	0.4004	0.0006	0.4016
water density 0.25	0.5901	0.0012	0.5925
water density 0.50	0.7521	0.0014	0.7549
water density 0.75	0.8530	0.0015	0.8560
water density 0.96	0.9078	0.0015	0.9108
water density 0.98	0.9092	0.0015	0.9122
water density 1.00	0.9136	0.0016	0.9168
Investigation of offcenter fuel with 6 inch cells:			
offcenter 10x10 fuel, no channel, 6 inch cell	0.9109	0.0015	0.9139
offcenter 10x10 fuel, 0.065 channel, 6 inch cell	0.9189	0.0016	0.9221
offcenter 10x10 fuel, 0.100 channel, 6 inch cell	0.9205	0.0015	0.9235
offcenter 10x10 fuel, 0.120 channel, 6 inch cell	0.9221	0.0015	0.9251
offcenter 10x10 fuel, 0.120 channel, 6 inch cell, one 5% assy ⁽²⁾	0.9260	0.0008	0.9276
offcenter 10x10 fuel, 0.120 channel, 5.97 inch cell, one 5% assy ⁽²⁾	0.9275	0.0008	0.9291

Notes:

1. All cases are evaluated with water in the fuel pellet-cladding annulus of all pins and in the cask. Water density is 100% except where noted. The baseline and individual effects are all evaluated with a 0.065 inch thick channel.
2. Loading of 5% fuel for information only; not a design basis accident

Table 6.4-4
TN-68 Intact Assembly Criticality Analysis - Final Results

Description	K_{keno}	σ_{keno}	K_{eff}
0.100" thick, 27.0 mg B10/cm² poison, 3.70 wt % U235			
100% IMD, 100% EMD	0.9288	0.0009	0.9306
100% IMD, 0.1% EMD	0.9308	0.0010	0.9328
100% IMD, 10% EMD	0.9310	0.0009	0.9328
100% IMD, 30% EMD	0.9307	0.0009	0.9325
100% IMD, 50% EMD	0.9301	0.0008	0.9317
100% IMD, 70% EMD	0.9309	0.0009	0.9327
100% IMD, 90% EMD	0.9301	0.0009	0.9319
0.120" thick, 31.5 mg B10/cm² poison, 3.95 wt % U235			
0.1% IMD, 100% EMD	0.4365	0.0004	0.4373
10% IMD, 100% EMD	0.5132	0.0005	0.5142
30% IMD, 100% EMD	0.6607	0.0006	0.6619
50% IMD, 100% EMD	0.6607	0.0006	0.6619
70% IMD, 100% EMD	0.8559	0.0009	0.8577
90% IMD, 100% EMD	0.9148	0.0009	0.9166
100% IMD, 100% EMD	0.9369	0.0008	0.9385
100% IMD, 0.1% EMD	0.9383	0.0009	0.9401
100% IMD, 10% EMD	0.9369	0.0009	0.9387
100% IMD, 30% EMD	0.9366	0.0010	0.9386
100% IMD, 50% EMD	0.9387	0.0009	0.9405
100% IMD, 70% EMD	0.9362	0.0008	0.9378
100% IMD, 90% EMD	0.9362	0.0009	0.9380
0.135" thick, 36.0 mg B10/cm² poison, 4.05 wt % U235			
100% IMD, 100% EMD	0.9346	0.0009	0.9364
100% IMD, 0.1% EMD	0.9370	0.0010	0.9390
100% IMD, 10% EMD	0.9354	0.0010	0.9374
100% IMD, 30% EMD	0.9363	0.0008	0.9379
100% IMD, 50% EMD	0.9357	0.0009	0.9375
100% IMD, 70% EMD	0.9359	0.0009	0.9377
100% IMD, 90% EMD	0.9354	0.0008	0.9370
0.150" thick, 40.5 mg B10/cm² poison, 4.15 wt % U235			
100% IMD, 100% EMD	0.9347	0.0009	0.9365
100% IMD, 0.1% EMD	0.9357	0.0009	0.9375
100% IMD, 10% EMD	0.9353	0.0008	0.9369
100% IMD, 30% EMD	0.9342	0.0009	0.9360
100% IMD, 50% EMD	0.9348	0.0008	0.9364
100% IMD, 70% EMD	0.9350	0.0010	0.9370
100% IMD, 90% EMD	0.9367	0.0009	0.9385

Table 6.4-4
 TN-68 Intact Assembly Criticality Analysis - Final Results
 (Continued)

Description	K_{keno}	σ_{keno}	K_{eff}
0.167" thick, 45.0 mg B10/cm² poison, 4.30 wt % U235			
100% IMD, 100% EMD	0.9356	0.0008	0.9372
100% IMD, 0.1% EMD	0.9362	0.0009	0.9380
100% IMD, 10% EMD	0.9364	0.0009	0.9382
100% IMD, 30% EMD	0.9383	0.0009	0.9401
100% IMD, 50% EMD	0.9373	0.0009	0.9391
100% IMD, 70% EMD	0.9362	0.0009	0.9380
100% IMD, 90% EMD	0.9368	0.0009	0.9386
0.186" thick, 49.5 mg B10/cm² poison, 4.40 wt % U235			
100% IMD, 100% EMD	0.9355	0.0009	0.9373
100% IMD, 0.1% EMD	0.9363	0.0009	0.9381
100% IMD, 10% EMD	0.9360	0.0009	0.9378
100% IMD, 30% EMD	0.9350	0.0008	0.9366
100% IMD, 50% EMD	0.9360	0.0009	0.9378
100% IMD, 70% EMD	0.9360	0.0009	0.9378
100% IMD, 90% EMD	0.9360	0.0009	0.9378
0.200" thick, 54.0 mg B10/cm² poison, 4.50 wt % U235			
0.1% IMD, 100% EMD	0.4315	0.0003	0.4321
10% IMD, 100% EMD	0.4974	0.0004	0.4982
30% IMD, 100% EMD	0.6390	0.0008	0.6406
50% IMD, 100% EMD	0.7584	0.0008	0.7600
70% IMD, 100% EMD	0.8451	0.0008	0.8467
90% IMD, 100% EMD	0.9106	0.0010	0.9126
100% IMD, 100% EMD	0.9365	0.0008	0.9381
100% IMD, 0.1% EMD	0.9372	0.0010	0.9392
100% IMD, 10% EMD	0.9379	0.0008	0.9395
100% IMD, 30% EMD	0.9367	0.0008	0.9383
100% IMD, 50% EMD	0.9360	0.0009	0.9378
100% IMD, 70% EMD	0.9364	0.0009	0.9382
100% IMD, 90% EMD	0.9366	0.0009	0.9384
0.240" thick, 63.0 mg B10/cm² poison, 4.70 wt % U235			
100% IMD, 100% EMD	0.9353	0.0008	0.9369
100% IMD, 0.1% EMD	0.9360	0.0009	0.9378
100% IMD, 10% EMD	0.9378	0.0009	0.9396
100% IMD, 30% EMD	0.9364	0.0009	0.9382
100% IMD, 50% EMD	0.9357	0.0010	0.9377
100% IMD, 70% EMD	0.9341	0.0008	0.9357
100% IMD, 90% EMD	0.9369	0.0009	0.9387

Table 6.4-5
Results of the Single Ended Rod Shear Scoping Studies

Description	K_{keno}	σ_{keno}	K_{eff}
0.200" thick, 54.0 mg B10/cm² poison, 4.50 wt % U235, No Shear			
Base Case from Section 6.2	0.9365	0.0008	0.9381
Case based on Sheared Rods	0.9363	0.0009	0.9381
Movement of Sheared Rods Radially Inward, X-array			
D=0.225 cm, Channel	0.9371	0.0009	0.9389
D=0.450 cm, Channel	0.9356	0.0010	0.9376
D=0.225 cm, No Channel	0.9361	0.0008	0.9377
D=0.450 cm, No Channel	0.9365	0.0008	0.9381
D=0.750 cm, No Channel	0.9371	0.0008	0.9387
D=1.05 cm, No Channel	0.9374	0.0009	0.9392
D=1.50 cm, No Channel	0.9374	0.0010	0.9394
Movement of Sheared Rods Circumferentially, Y-array			
D=0.225 cm, Channel	0.9377	0.0009	0.9395
D=0.450 cm, Channel	0.9361	0.0009	0.9379
D=0.225 cm, No Channel	0.9377	0.0009	0.9395
D=0.450 cm, No Channel	0.9367	0.0009	0.9385
D=0.750 cm, No Channel	0.9348	0.0009	0.9366
D=1.05 cm, No Channel	0.9352	0.0009	0.9370
D=1.50 cm, No Channel	0.9364	0.0008	0.9380
Movement of Sheared Row of Rods, X-array, Axial movement of Rods by 12.18"			
Analyzed Case, No Shift	0.9374	0.0010	0.9394
12.18" shift	0.9332	0.0010	0.9352
Reference case	0.9341	0.0010	0.9361
Movement of Sheared Row of Rods, Y-array with Channel, Axial movement of Rods by 12.18"			
Analyzed Case, No Shift	0.9377	0.0009	0.9395
12.18" shift	0.9328	0.0010	0.9348
Reference case	0.9353	0.0010	0.9373
Movement of Sheared Row of Rods, Y-array, No Channel, Axial movement of Rods by 12.18"			
Analyzed Case, No Shift *	0.9377	0.0009	0.9395
12.18" shift	0.9336	0.0009	0.9354
Reference case	0.9340	0.0009	0.9358

* used for accident analysis

Table 6.4-6
Results of the Double Ended Rod Shear Scoping Studies

Description	K_{keno}	σ_{keno}	K_{eff}
Movement of Sheared Rods Circumferentially, Y-array			
D=0 cm	0.9351	0.0010	0.9371
D=0.300 cm	0.9361	0.0008	0.9377
D=0.467 cm (max) *	0.9368	0.0010	0.9388
Classic Double Shear (modified from case above)	0.9353	0.0009	0.9371
Movement of Sheared Row of Rods, Y-array, Axial movement of Rods by 12.18"			
12.18" shift	0.9351	0.0009	0.9369
Reference case	0.9343	0.0009	0.9361

* used for accident analysis

Table 6.4-7
TN-68 Damaged Assembly Criticality Analysis - Final Results

Description	K_{keno}	σ_{keno}	K_{eff}
0.120" thick, 31.5 mg B10/cm² poison, 3.95 wt % U235, Double Shear			
0.1% IMD, 100% EMD	0.4382	0.0003	0.4388
10% IMD, 100% EMD	0.5160	0.0004	0.5168
30% IMD, 100% EMD	0.6627	0.0006	0.6639
50% IMD, 100% EMD	0.7770	0.0008	0.7786
70% IMD, 100% EMD	0.8591	0.0008	0.8607
90% IMD, 100% EMD	0.9150	0.0009	0.9168
100% IMD, 100% EMD	0.9369	0.0008	0.9385
100% IMD, 0.1% EMD	0.9387	0.0010	0.9407
100% IMD, 10% EMD	0.9387	0.0008	0.9403
100% IMD, 30% EMD	0.9373	0.0008	0.9389
100% IMD, 50% EMD	0.9380	0.0009	0.9398
100% IMD, 70% EMD	0.9378	0.0010	0.9398
100% IMD, 90% EMD	0.9377	0.0009	0.9395
0.120" thick, 31.5 mg B10/cm² poison, 3.95 wt % U235, Single Shear			
0.1% IMD, 100% EMD	0.4365	0.0003	0.4371
10% IMD, 100% EMD	0.5139	0.0004	0.5147
30% IMD, 100% EMD	0.6595	0.0007	0.6609
50% IMD, 100% EMD	0.7744	0.0008	0.7760
70% IMD, 100% EMD	0.8561	0.0008	0.8577
90% IMD, 100% EMD	0.9154	0.0009	0.9172
100% IMD, 100% EMD	0.9362	0.0010	0.9382
100% IMD, 0.1% EMD	0.9384	0.0009	0.9402
100% IMD, 10% EMD	0.9379	0.0010	0.9399
100% IMD, 30% EMD	0.9380	0.0008	0.9396
100% IMD, 50% EMD	0.9365	0.0009	0.9383
100% IMD, 70% EMD	0.9353	0.0009	0.9371
100% IMD, 90% EMD	0.9383	0.0008	0.9399
0.135" thick, 36.0 mg B10/cm² poison, 4.05 wt % U235, Double Shear			
100% IMD, 100% EMD	0.9345	0.0008	0.9361
100% IMD, 0.1% EMD	0.9388	0.0008	0.9404
100% IMD, 10% EMD	0.9381	0.0009	0.9399
100% IMD, 30% EMD	0.9375	0.0009	0.9393
100% IMD, 50% EMD	0.9374	0.0008	0.9390
100% IMD, 70% EMD	0.9371	0.0009	0.9389
100% IMD, 90% EMD	0.9380	0.0009	0.9398

Table 6.4-7
 TN-68 Damaged Assembly Criticality Analysis - Final Results
 (Continued)

Description	K_{keno}	σ_{keno}	K_{eff}
0.135" thick, 36.0 mg B10/cm² poison, 4.05 wt % U235, Single Shear			
100% IMD, 100% EMD	0.9356	0.0008	0.9372
100% IMD, 0.1% EMD	0.9366	0.0010	0.9386
100% IMD, 10% EMD	0.9328	0.0009	0.9346
100% IMD, 30% EMD	0.9349	0.0009	0.9367
100% IMD, 50% EMD	0.9349	0.0009	0.9367
100% IMD, 70% EMD	0.9346	0.0009	0.9364
100% IMD, 90% EMD	0.9369	0.0008	0.9385
0.150" thick, 40.5 mg B10/cm² poison, 4.15 wt % U235, Double Shear			
100% IMD, 100% EMD	0.9355	0.0008	0.9371
100% IMD, 0.1% EMD	0.9364	0.0009	0.9382
100% IMD, 10% EMD	0.9373	0.0009	0.9391
100% IMD, 30% EMD	0.9364	0.0010	0.9384
100% IMD, 50% EMD	0.9357	0.0010	0.9377
100% IMD, 70% EMD	0.9353	0.0009	0.9371
100% IMD, 90% EMD	0.9344	0.0008	0.9360
0.150" thick, 40.5 mg B10/cm² poison, 4.15 wt % U235, Single Shear			
100% IMD, 100% EMD	0.9353	0.0010	0.9373
100% IMD, 0.1% EMD	0.9354	0.0008	0.9370
100% IMD, 10% EMD	0.9356	0.0009	0.9374
100% IMD, 30% EMD	0.9347	0.0008	0.9363
100% IMD, 50% EMD	0.9334	0.0008	0.9350
100% IMD, 70% EMD	0.9344	0.0009	0.9362
100% IMD, 90% EMD	0.9364	0.0010	0.9384
0.167" thick, 45.0 mg B10/cm² poison, 4.30 wt % U235, Double Shear			
100% IMD, 100% EMD	0.9369	0.0008	0.9385
100% IMD, 0.1% EMD	0.9373	0.0010	0.9393
100% IMD, 10% EMD	0.9376	0.0009	0.9394
100% IMD, 30% EMD	0.9384	0.0009	0.9402
100% IMD, 50% EMD	0.9374	0.0008	0.9390
100% IMD, 70% EMD	0.9372	0.0009	0.9390
100% IMD, 90% EMD	0.9365	0.0009	0.9383

Table 6.4-7
 TN-68 Damaged Assembly Criticality Analysis - Final Results
 (Continued)

Description	K_{keno}	σ_{keno}	K_{eff}
0.167" thick, 45.0 mg B10/cm² poison, 4.30 wt % U235, Single Shear			
100% IMD, 100% EMD	0.9351	0.0009	0.9369
100% IMD, 0.1% EMD	0.9349	0.0009	0.9367
100% IMD, 10% EMD	0.9340	0.0009	0.9358
100% IMD, 30% EMD	0.9341	0.0009	0.9359
100% IMD, 50% EMD	0.9351	0.0009	0.9369
100% IMD, 70% EMD	0.9346	0.0009	0.9364
100% IMD, 90% EMD	0.9342	0.0008	0.9358
0.187" thick, 49.5 mg B10/cm² poison, 4.40 wt % U235, Double Shear			
100% IMD, 100% EMD	0.9369	0.0009	0.9387
100% IMD, 0.1% EMD	0.9380	0.0009	0.9398
100% IMD, 10% EMD	0.9374	0.0009	0.9392
100% IMD, 30% EMD	0.9377	0.0009	0.9395
100% IMD, 50% EMD	0.9362	0.0009	0.9380
100% IMD, 70% EMD	0.9373	0.0009	0.9391
100% IMD, 90% EMD	0.9359	0.0008	0.9375
0.187" thick, 49.5 mg B10/cm² poison, 4.40 wt % U235, Single Shear			
100% IMD, 100% EMD	0.9348	0.0009	0.9366
100% IMD, 0.1% EMD	0.9351	0.0008	0.9367
100% IMD, 10% EMD	0.9360	0.0009	0.9378
100% IMD, 30% EMD	0.9335	0.0009	0.9353
100% IMD, 50% EMD	0.9361	0.0008	0.9377
100% IMD, 70% EMD	0.9343	0.0009	0.9361
100% IMD, 90% EMD	0.9349	0.0009	0.9367
0.200" thick, 54.0 mg B10/cm² poison, 4.50 wt % U235, Double Shear			
0.1% IMD, 100% EMD	0.4331	0.0003	0.4337
10% IMD, 100% EMD	0.4998	0.0004	0.5006
30% IMD, 100% EMD	0.6437	0.0007	0.6451
50% IMD, 100% EMD	0.7611	0.0007	0.7625
70% IMD, 100% EMD	0.8479	0.0008	0.8495
90% IMD, 100% EMD	0.9113	0.0010	0.9133
100% IMD, 100% EMD	0.9368	0.0010	0.9388
100% IMD, 0.1% EMD	0.9372	0.0009	0.9390
100% IMD, 10% EMD	0.9374	0.0009	0.9392
100% IMD, 30% EMD	0.9378	0.0008	0.9394
100% IMD, 50% EMD	0.9380	0.0009	0.9398
100% IMD, 70% EMD	0.9385	0.0009	0.9403
100% IMD, 90% EMD	0.9366	0.0008	0.9382

Table 6.4-7
 TN-68 Damaged Assembly Criticality Analysis - Final Results
 (Continued)

Description	K_{keno}	σ_{keno}	K_{eff}
0.200" thick, 54.0 mg B10/cm² poison, 4.50 wt % U235, Single Shear			
0.1% IMD, 100% EMD	0.4316	0.0003	0.4322
10% IMD, 100% EMD	0.4988	0.0004	0.4996
30% IMD, 100% EMD	0.6403	0.0006	0.6415
50% IMD, 100% EMD	0.7584	0.0008	0.7600
70% IMD, 100% EMD	0.8471	0.0009	0.8489
90% IMD, 100% EMD	0.9125	0.0009	0.9143
100% IMD, 100% EMD	0.9377	0.0009	0.9395
100% IMD, 0.1% EMD	0.9357	0.0008	0.9373
100% IMD, 10% EMD	0.9372	0.0010	0.9392
100% IMD, 30% EMD	0.9351	0.0010	0.9371
100% IMD, 50% EMD	0.9358	0.0008	0.9374
100% IMD, 70% EMD	0.9357	0.0010	0.9377
100% IMD, 90% EMD	0.9345	0.0009	0.9363
0.240" thick, 63.0 mg B10/cm² poison, 4.70 wt % U235, Double Shear			
100% IMD, 100% EMD	0.9375	0.0008	0.9391
100% IMD, 0.1% EMD	0.9386	0.0008	0.9402
100% IMD, 10% EMD	0.9381	0.0009	0.9399
100% IMD, 30% EMD	0.9381	0.0009	0.9399
100% IMD, 50% EMD	0.9365	0.0010	0.9385
100% IMD, 70% EMD	0.9382	0.0009	0.9400
100% IMD, 90% EMD	0.9356	0.0009	0.9374
0.240" thick, 63.0 mg B10/cm² poison, 4.70 wt % U235, Single Shear			
100% IMD, 100% EMD	0.9373	0.0010	0.9393
100% IMD, 0.1% EMD	0.9378	0.0008	0.9394
100% IMD, 10% EMD	0.9363	0.0010	0.9383
100% IMD, 30% EMD	0.9349	0.0010	0.9369
100% IMD, 50% EMD	0.9370	0.0010	0.9390
100% IMD, 70% EMD	0.9376	0.0009	0.9394
100% IMD, 90% EMD	0.9350	0.0010	0.9370

Table 6.5-1
Benchmark Results

Run ID	U235 Enrich. wt %	Pitch (cm)	H ₂ O/ Fuel volume	H/X Ratio	Assy Sep (cm)	AEG	K _{eff}	1σ
ANS33AL1	4.74	1.350	2.302	138.4	5.00	34.0214	1.0073	0.0010
ANS33AL2	4.74	1.350	2.302	138.4	2.50	34.4099	1.0115	0.0009
ANS33AL3	4.74	1.350	2.302	138.4	10.00	34.6327	1.0029	0.0009
ANS33SLG	4.74	1.350	2.302	138.4	5.00	34.4244	0.9990	0.0009
BW1484SL	2.46	1.636	1.841	216.1	6.54	35.4203	0.9944	0.0009
EPRU65	2.35	1.562	1.196	163.6		33.9138	0.9959	0.0008
EPRU75	2.35	1.905	2.408	329.4		35.8676	0.9968	0.0009
EPRU87	2.35	2.210	3.687	504.2		36.6120	1.0011	0.0009
NSE71H1	4.74	1.350	1.804	108.3		33.5260	0.9983	0.0011
NSE71H2	4.74	1.260	3.811	228.8		35.7415	0.9993	0.0010
NSE71H3	4.74	2.260	7.608	456.8		36.8848	1.0037	0.0009
NSE71SQ	4.74	1.260	1.823	110.0		33.7627	0.9978	0.0009
NSE71W1	4.74	1.260	1.823	110.0		34.0088	0.9981	0.0010
NSE71W2	4.74	1.260	1.823	110.0		34.3856	0.9995	0.0010
P2438AL	2.35	2.032	2.918	398.7	8.67	36.2934	0.9983	0.0009
P2438BA	2.35	2.032	2.918	398.7	5.05	36.2244	0.9973	0.0009
P2438SLG	2.35	2.032	2.918	398.7	8.39	36.2906	0.9985	0.0009
P2438SS	2.35	2.032	2.918	398.7	6.88	36.2690	0.9979	0.0009
P2438ZR	2.35	2.032	2.918	398.7	8.79	36.2891	0.9976	0.0009
P2615AL	4.31	2.540	3.883	256.1	10.72	35.7595	0.9967	0.0010
P2615BA	4.31	2.540	3.883	256.1	6.72	35.7276	1.0005	0.0011
P2615SS	4.31	2.540	3.883	256.1	8.58	35.7456	0.9959	0.0011
P2615ZR	4.31	2.540	3.883	256.1	10.92	35.7709	0.9980	0.0010
P2827SLG	2.35	2.032	2.918	398.7	8.31	36.3010	0.9957	0.0008
P3314AL	4.31	1.892	1.600	105.4	9.04	33.9722	0.9972	0.0010
P3314BA	4.31	1.892	1.600	105.4	2.83	33.1874	1.0000	0.0009
P3314BC	4.31	1.892	1.600	105.4	2.83	33.2334	0.9992	0.0009
P3314BF1	4.31	1.892	1.600	105.4	2.83	33.2422	1.0024	0.0009
P3314BF2	4.31	1.892	1.600	105.4	2.83	33.2121	1.0001	0.0010
P3314BS1	2.35	1.684	1.600	218.6	3.86	34.8545	0.9957	0.0010
P3314BS2	2.35	1.684	1.600	218.6	3.46	34.8324	0.9940	0.0008
P3314BS3	4.31	1.892	1.600	105.4	7.23	33.4328	0.9996	0.0009
P3314BS4	4.31	1.892	1.600	105.4	6.63	33.4152	1.0000	0.0008
P3314SLG	4.31	1.892	1.600	105.4	2.83	34.0109	0.9971	0.0010
P3314SS1	4.31	1.892	1.600	105.4	2.83	33.9613	0.9984	0.0010
P3314SS2	4.31	1.892	1.600	105.4	2.83	33.7719	1.0014	0.0009
P3314SS3	4.31	1.892	1.600	105.4	2.83	33.8956	0.9995	0.0010
P3314SS4	4.31	1.892	1.600	105.4	2.83	33.7604	0.9962	0.0009
P3314SS5	2.35	1.684	1.600	218.6	7.80	34.9476	0.9947	0.0010
P3314SS6	4.31	1.892	1.600	105.4	10.52	33.5406	1.0010	0.0008
P3314W1	4.31	1.892	1.600	105.4		34.3962	1.0009	0.0010
P3314W2	2.35	1.684	1.600	218.6		35.2153	0.9972	0.0008
P3314ZR	4.31	1.892	1.600	105.4	2.83	33.9897	0.9977	0.0010
P3602BB	4.31	1.892	1.600	105.4	8.30	33.3198	1.0031	0.0010

Table 6.5-1
Benchmark Results
(Continued)

Run ID	U235 Enrich. wt %	Pitch (cm)	H ₂ O/ Fuel volume	H/X Ratio	Assy Sep (cm)	AEG	K _{eff}	1σ
P3602BS1	2.35	1.684	1.600	218.6	4.80	34.7746	1.0034	0.0009
P3602BS2	4.31	1.892	1.600	105.4	9.83	33.3649	1.0047	0.0010
P3602N11	2.35	1.684	1.600	218.6	8.98	34.7410	1.0025	0.0008
P3602N12	2.35	1.684	1.600	218.6	9.58	34.8378	1.0048	0.0009
P3602N13	2.35	1.684	1.600	218.6	9.66	34.9334	1.0006	0.0009
P3602N14	2.35	1.684	1.600	218.6	8.54	35.0287	0.9969	0.0010
P3602N21	2.35	2.032	2.918	398.7	10.36	36.2787	0.9999	0.0009
P3602N22	2.35	2.032	2.918	398.7	11.20	36.1963	1.0014	0.0008
P3602N31	4.31	1.892	1.600	105.4	14.87	33.2015	1.0063	0.0010
P3602N32	4.31	1.892	1.600	105.4	15.74	33.3085	1.0072	0.0010
P3602N33	4.31	1.892	1.600	105.4	15.87	33.4168	1.0084	0.0010
P3602N34	4.31	1.892	1.600	105.4	15.84	33.4653	1.0028	0.0010
P3602N35	4.31	1.892	1.600	105.4	15.45	33.5169	1.0030	0.0009
P3602N36	4.31	1.892	1.600	105.4	13.82	33.5832	1.0003	0.0010
P3602N41	4.31	2.540	3.883	256.1	12.89	35.5269	1.0127	0.0010
P3602N42	4.31	2.540	3.883	256.1	14.12	35.6711	1.0068	0.0009
P3602N43	4.31	2.540	3.883	256.1	12.44	35.7505	1.0049	0.0009
P3602SS1	2.35	1.684	1.600	218.6	8.28	34.8708	1.0007	0.0009
P3602SS2	4.31	1.892	1.600	105.4	13.75	33.4133	1.0026	0.0010
P3926SL1	2.35	1.684	1.600	218.6	6.59	35.0674	0.9950	0.0009
P3926SL2	4.31	1.892	1.600	105.4	12.79	33.5810	0.9998	0.0009
P4267SL1	4.31	1.890	1.590	105.1		33.4692	0.9987	0.0011
P4267SL2	4.31	1.715	1.090	71.9		31.9346	0.9995	0.0011
P49-194	4.31	1.598	0.509	33.6		27.6263	1.0071	0.0009
P62FT231	4.31	1.891	1.600	105.0	5.67	32.9228	1.0020	0.0009
P71F14F3	4.31	1.891	1.600	105.0	5.19	32.8227	1.0009	0.0010
P71F14V3	4.31	1.891	1.600	105.0	5.19	32.8587	0.9977	0.0010
P71F14V5	4.31	1.891	1.600	105.0	5.19	32.8662	0.9980	0.0010
P71F214R	4.31	1.891	1.600	105.0	5.19	32.8669	0.9976	0.0009
PAT80L1	4.74	1.600	3.807	228.6	2.00	35.0276	1.0014	0.0009
PAT80L2	4.74	1.600	3.807	228.6	2.00	35.1079	0.9986	0.0011
PAT80SS1	4.74	1.600	3.807	228.6	2.00	35.0125	0.9998	0.0009
PAT80SS2	4.74	1.600	3.807	228.6	2.00	35.1128	0.9967	0.0010
W3269SL1	2.72	1.524	1.494	156.1		33.3862	0.9974	0.0010
W3269SL2	5.70	1.422	1.930	98.3		33.1006	1.0024	0.0010
W3269W1	2.72	1.524	1.494	156.1		33.5160	0.9972	0.0012
W3269W2	5.70	1.422	1.930	98.3		33.1786	1.0015	0.0010
W3385SL1	5.74	1.422	1.932	97.6		33.2320	1.0004	0.0009
W3385SL2	5.74	2.012	5.067	255.9		35.8876	1.0014	0.0010
Correlation	0.346	0.096	0.091	0.161	0.412	0.126	N/A	N/A

Table 6.5-2
USL-1 Results

Parameter	Range of Applicability	Formula to Determine USL
Pin Pitch (cm)	1.260 - 2.540	0.9416 + (1.1344E-03)*X (X < 1.610) 0.9434 (X ≥ 1.610)
Water to Fuel Volume Ratio	0.509 - 7.608	0.9423 + (3.0692E-04)*X (X < 1.433) 0.9427 (X ≥ 1.433)
Average Energy Group Causing Fission (AEG)	31.94 - 36.88	0.9573 - (3.9533E-04)*X (X < 34.841) 0.9435 (X ≥ 34.841)
Assembly Separation (cm)	2.000 - 15.87	0.9409 + (3.9576E-04)*X (X < 6.521) 0.9434 (X ≥ 6.521)
Hydrogen to Fissile (H/X Ratio)	33.6 - 504.2	0.9446 - (5.6445E-06)*X (X < 229.4) 0.9433 (X ≥ 229.4)
Enrichment (wt % U235)	2.350 - 5.740	0.9392 + (1.2426E-03)*X (X < 3.673) 0.9438 (X ≥ 3.673)

Table 6.5-3
USL Determination for Criticality Analysis

Parameter	Value from Limiting GE 10x10 Analysis	Bounding USL-1
Pin Pitch (cm)	1.2954	0.9431
Water to Fuel Volume Ratio	1.411	0.9427
Average Energy Group Causing Fission (AEG)	< 34.8 ⁽¹⁾	0.9435
Assembly Separation (cm)	3.46	0.9423
Hydrogen to Fissile (H/X Ratio)	106.7	0.9440
Enrichment (wt % U235)	3.7 (minimum)	0.9438

1) Examination of the results shows that the value is between 32 - 34 and hence a conservative value that produces the minimum USL was chosen

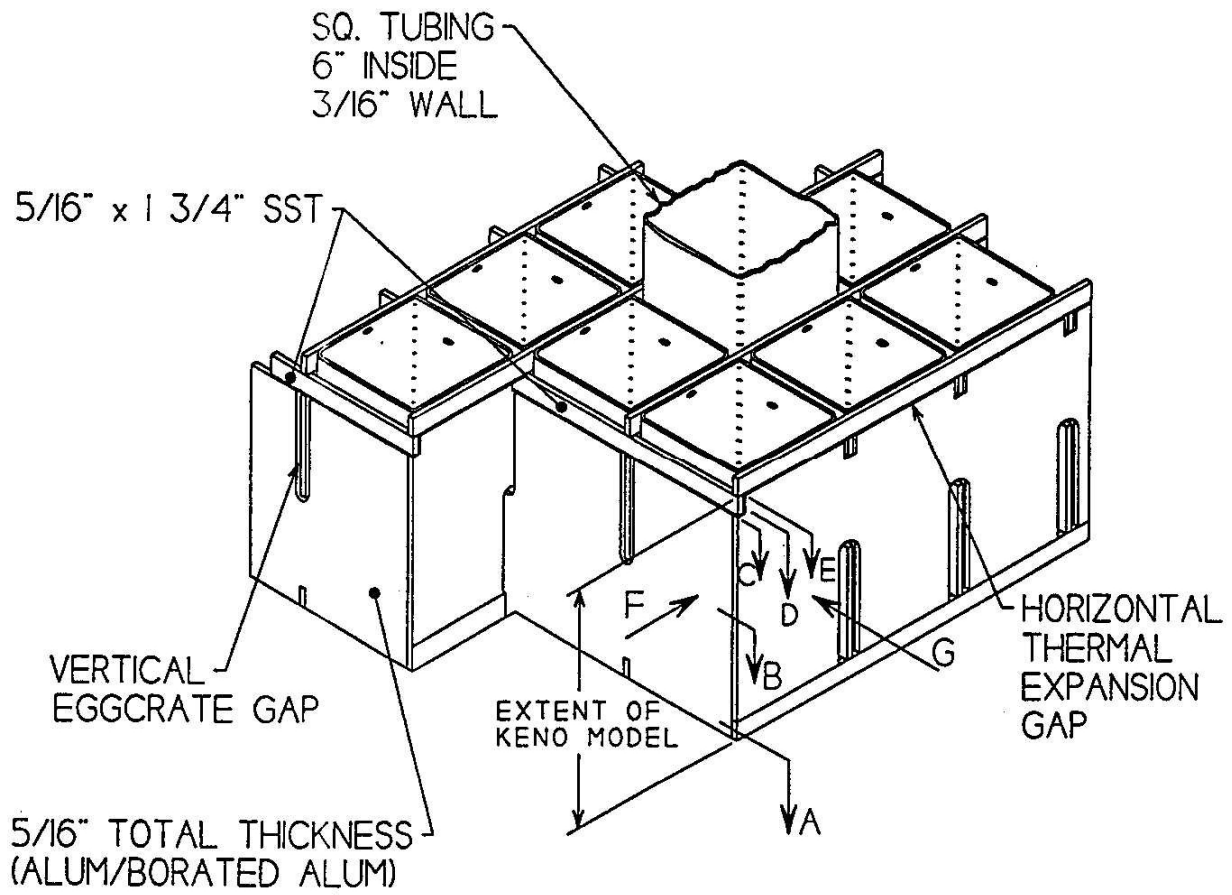


Figure 6.3-1
Basket Views and Dimensions

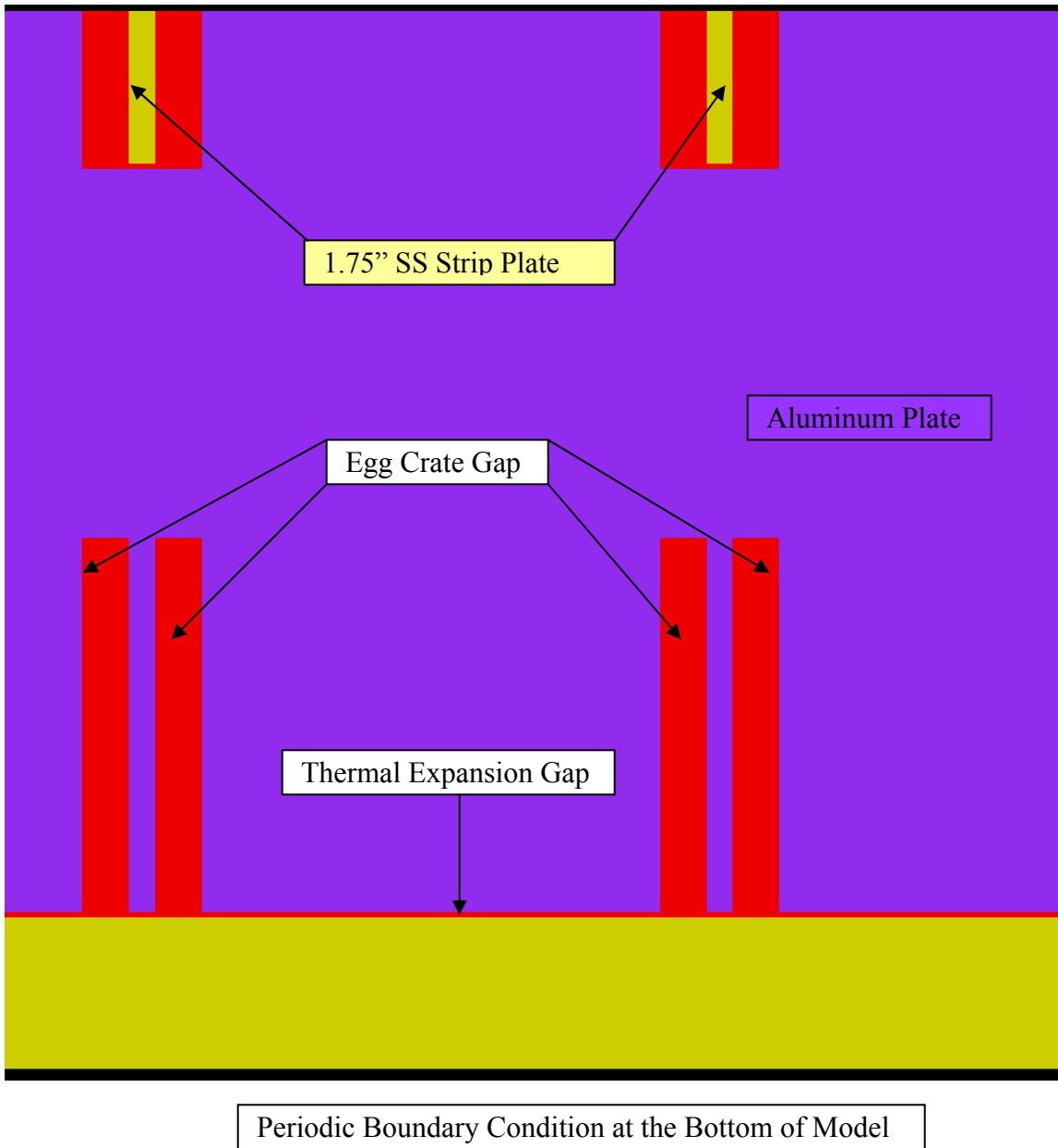


Figure 6.3-2
Basket Model Compartment Wall (View G)

Periodic Boundary Condition at the Top of Model

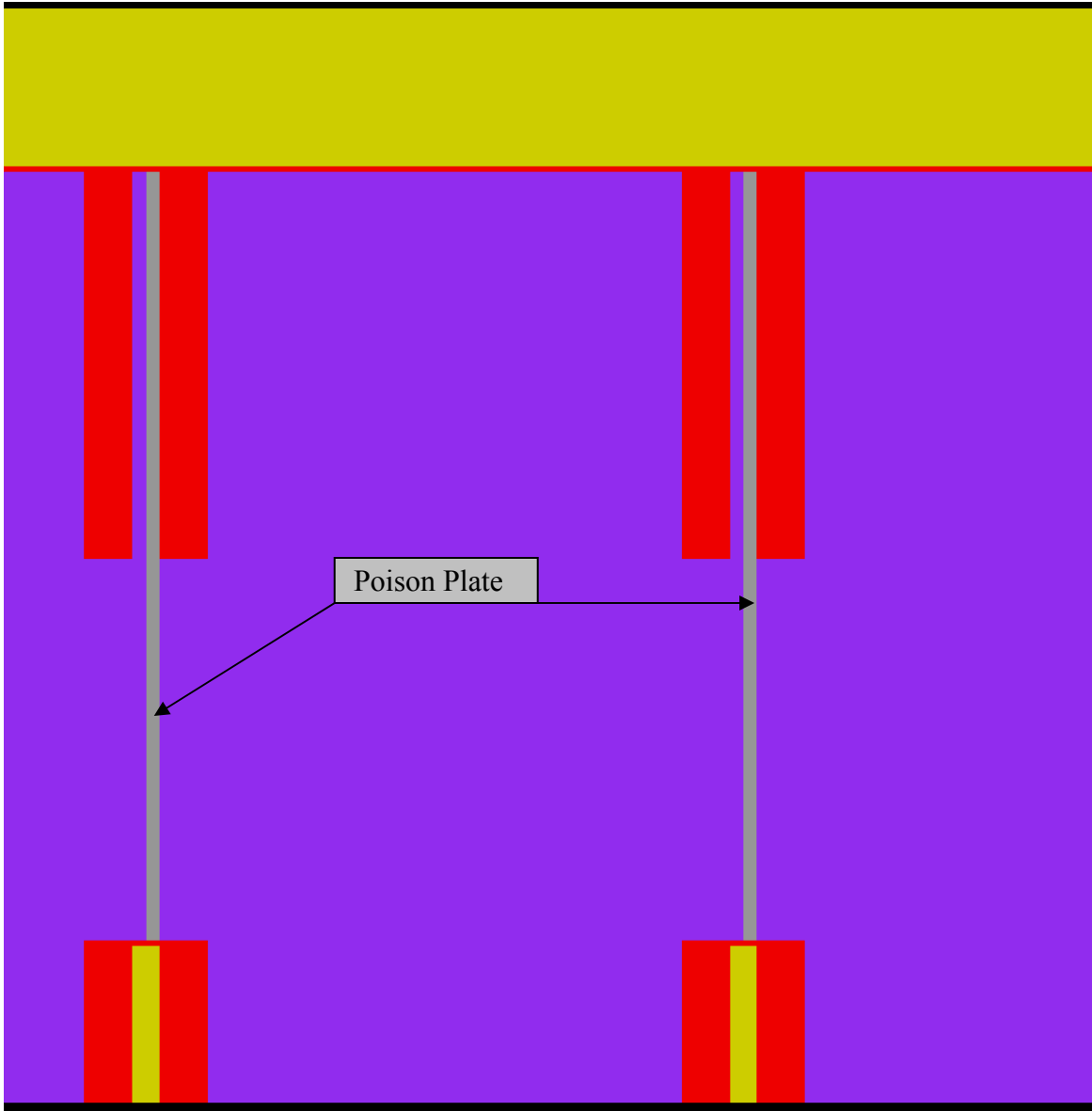


Figure 6.3-3
Basket Model Compartment Wall (View F)

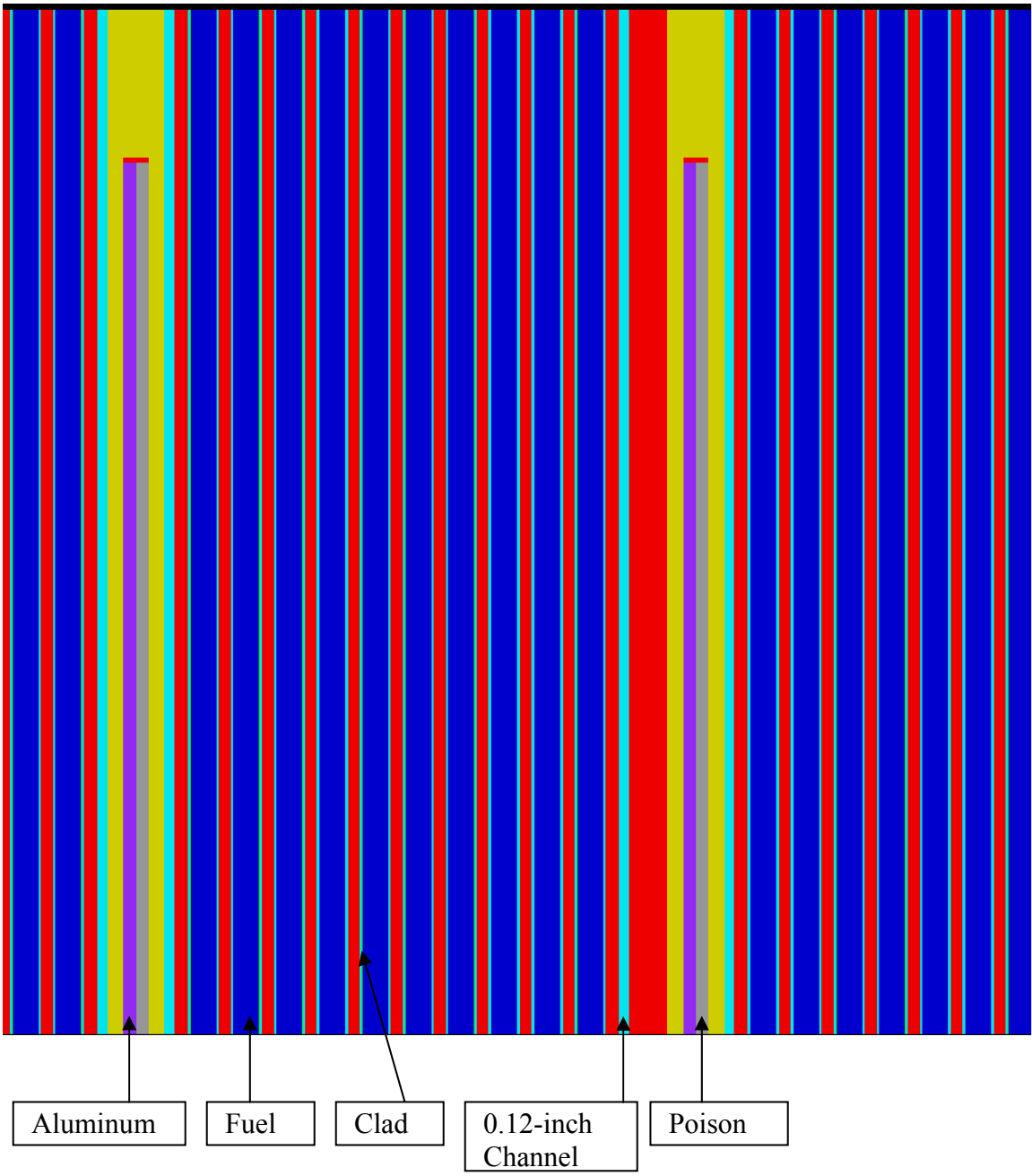


Figure 6.3-4
Basket Model Compartment with Fuel Assembly (View G)



Figure 6.3-5
Basket Model Compartment with Fuel Assembly (View F)

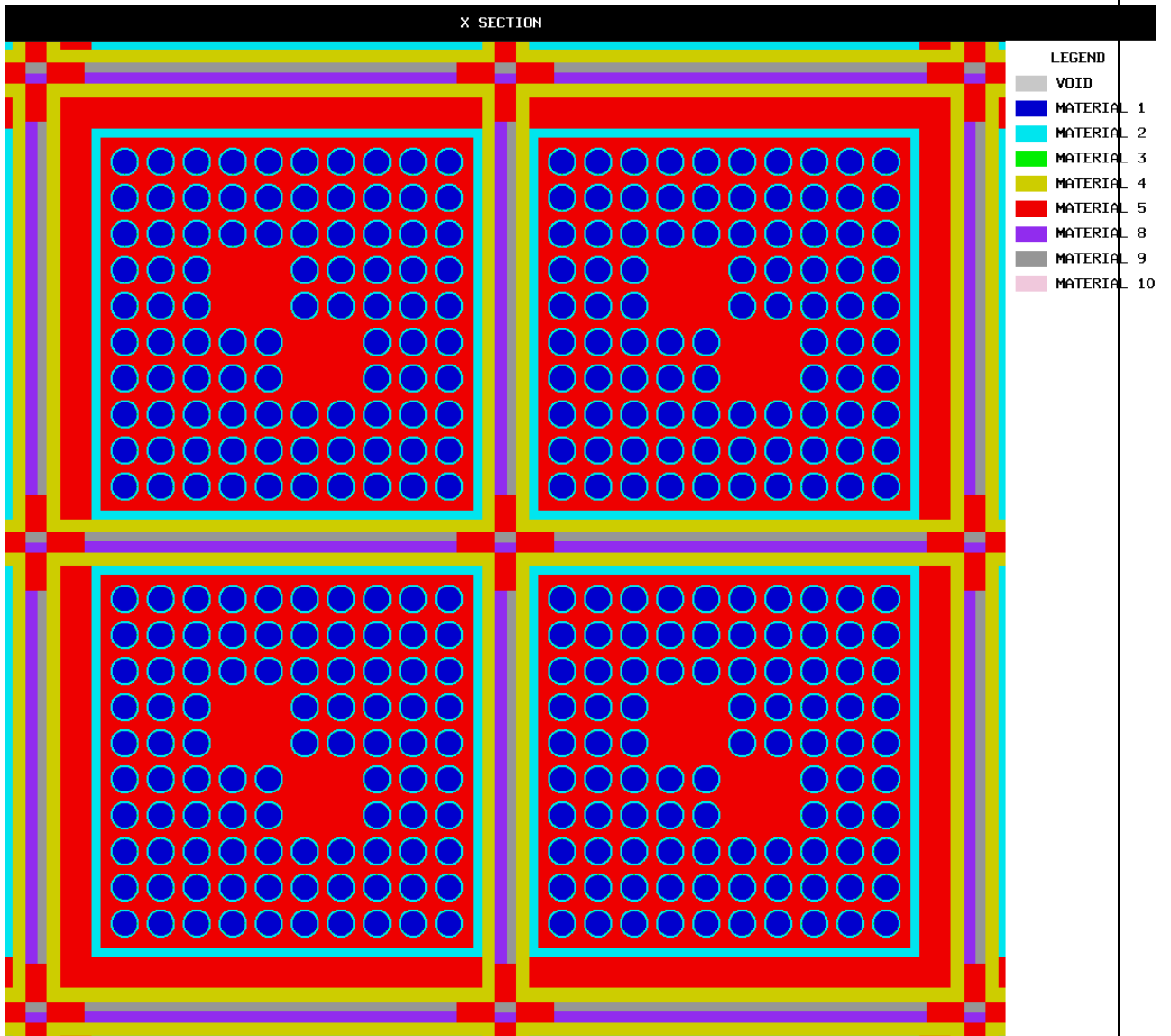


Figure 6.3-6
KENO Plot of the Center of the TN-68 Basket with Fuel Assemblies

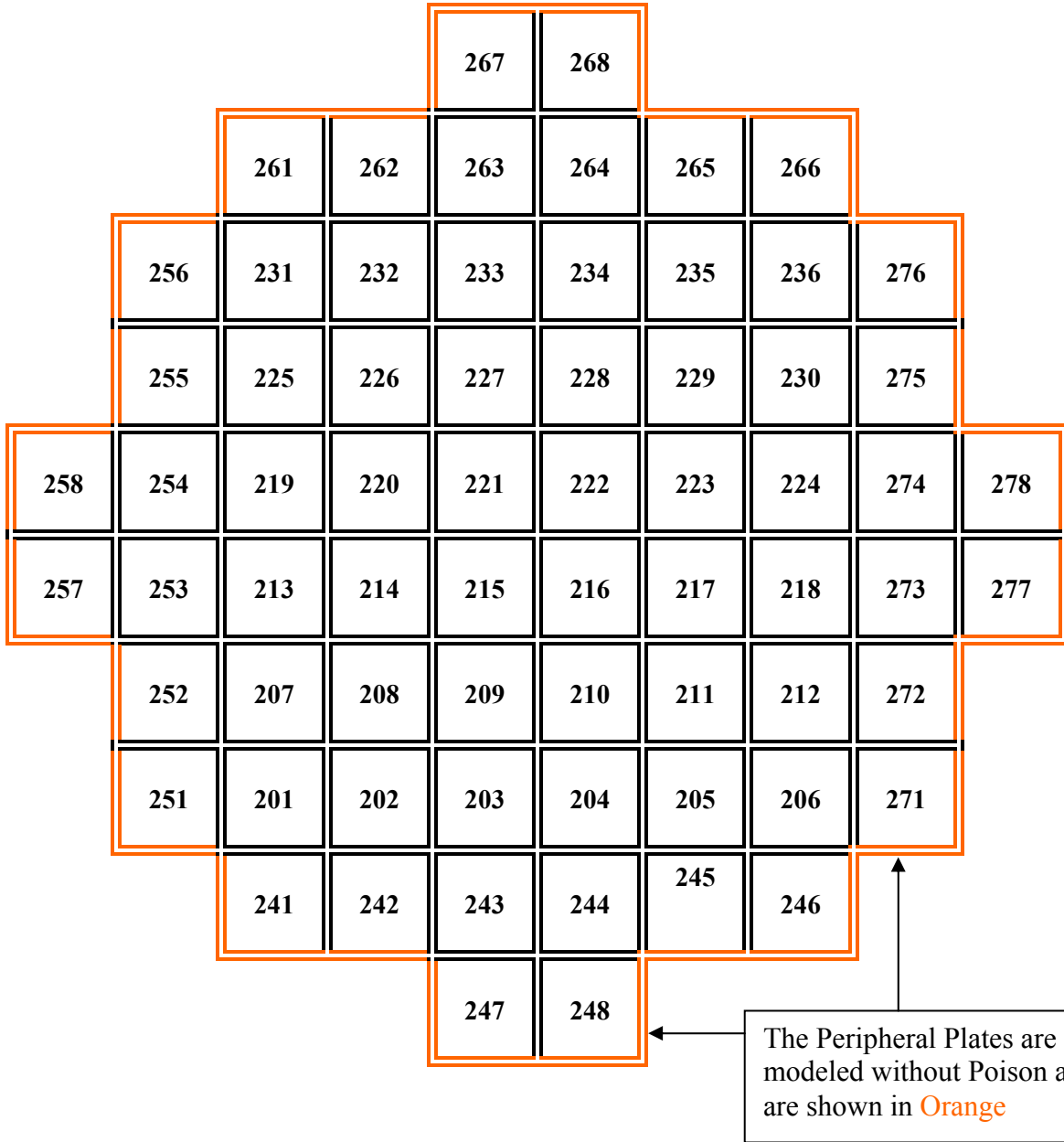


Figure 6.3-7
Radial Cross Section of the TN-68 Basket with Fuel Position Numbers

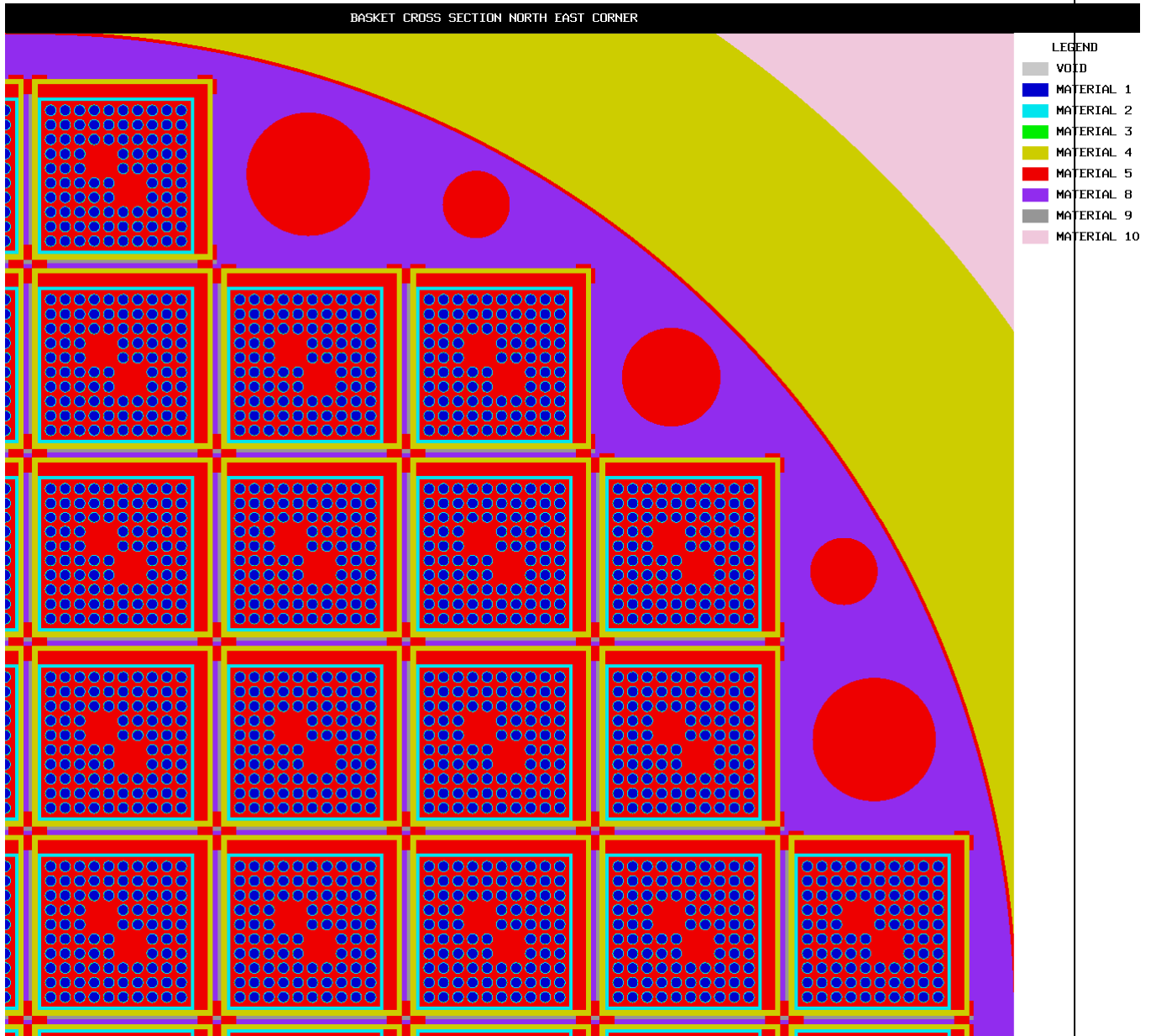


Figure 6.3-8
North East Quadrant of the TN68 Basket with Fuel Assemblies

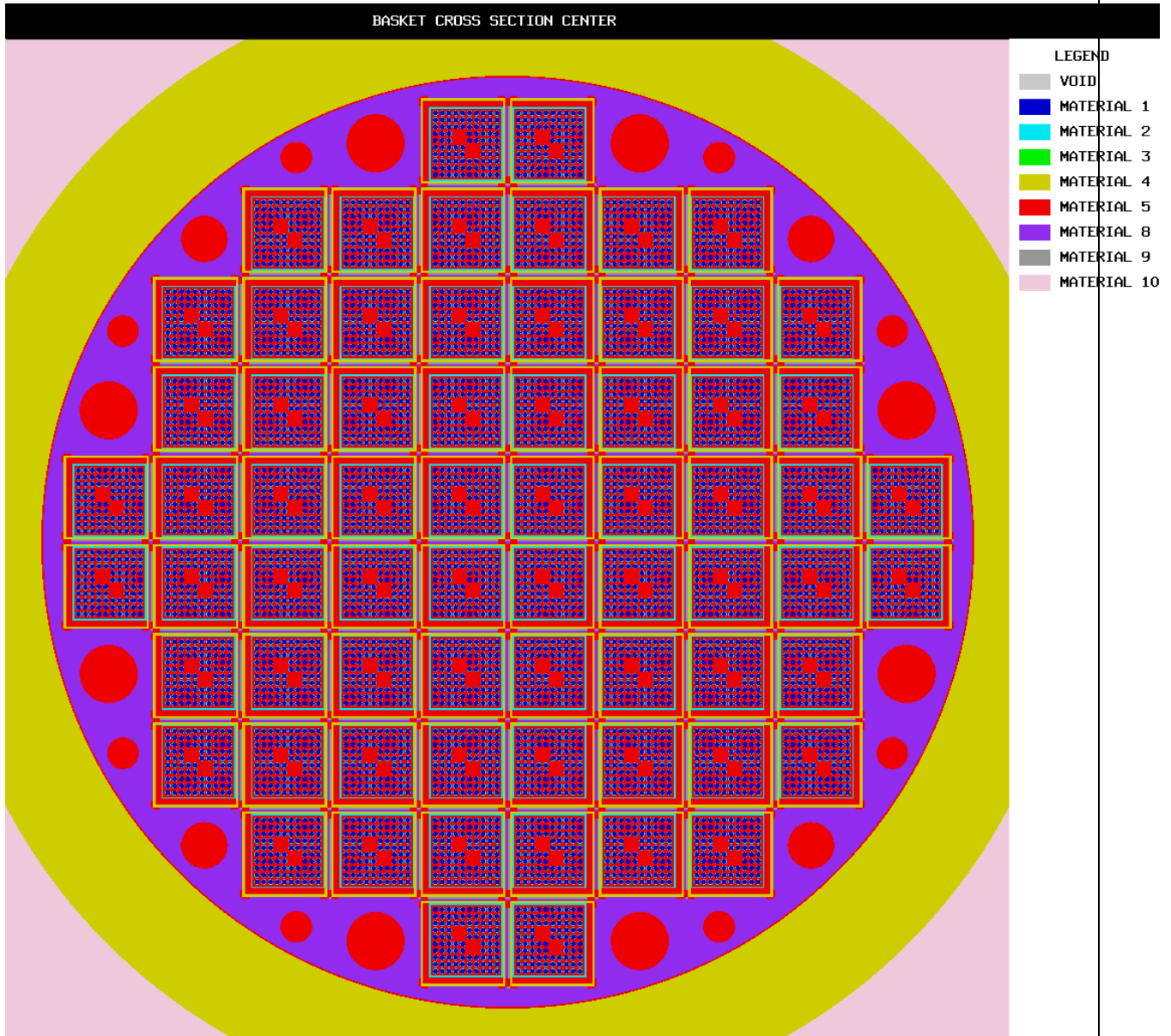


Figure 6.3-9
Radial Cross Section of the TN-68 Basket with Fuel Assemblies

Fuel assemblies centered in compartments
 Fuel compartments 6.00 inch (15.24 cm) inside
 Model is 12.17 inch (30.912 cm) high, with periodic reflection top and bottom

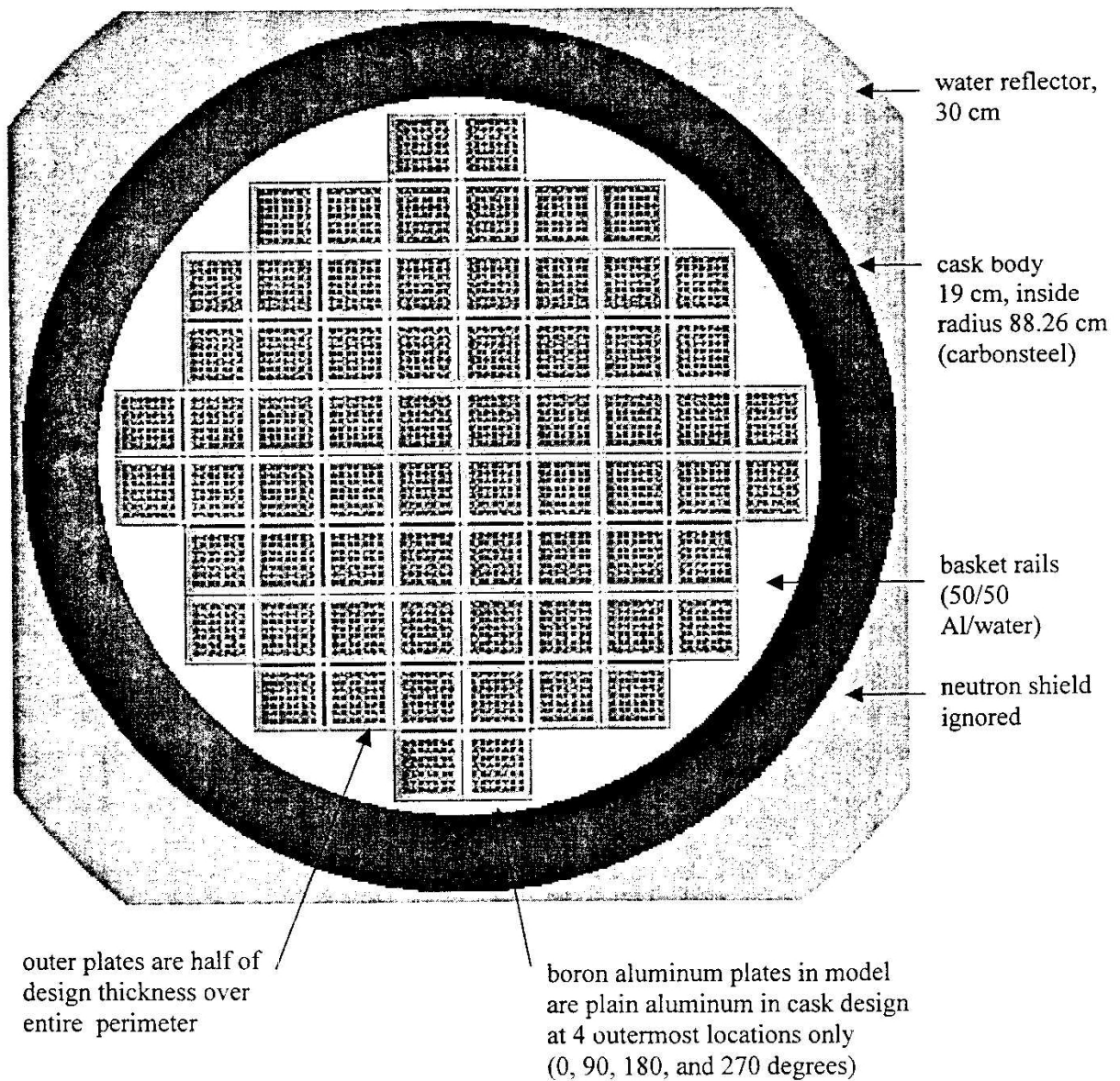
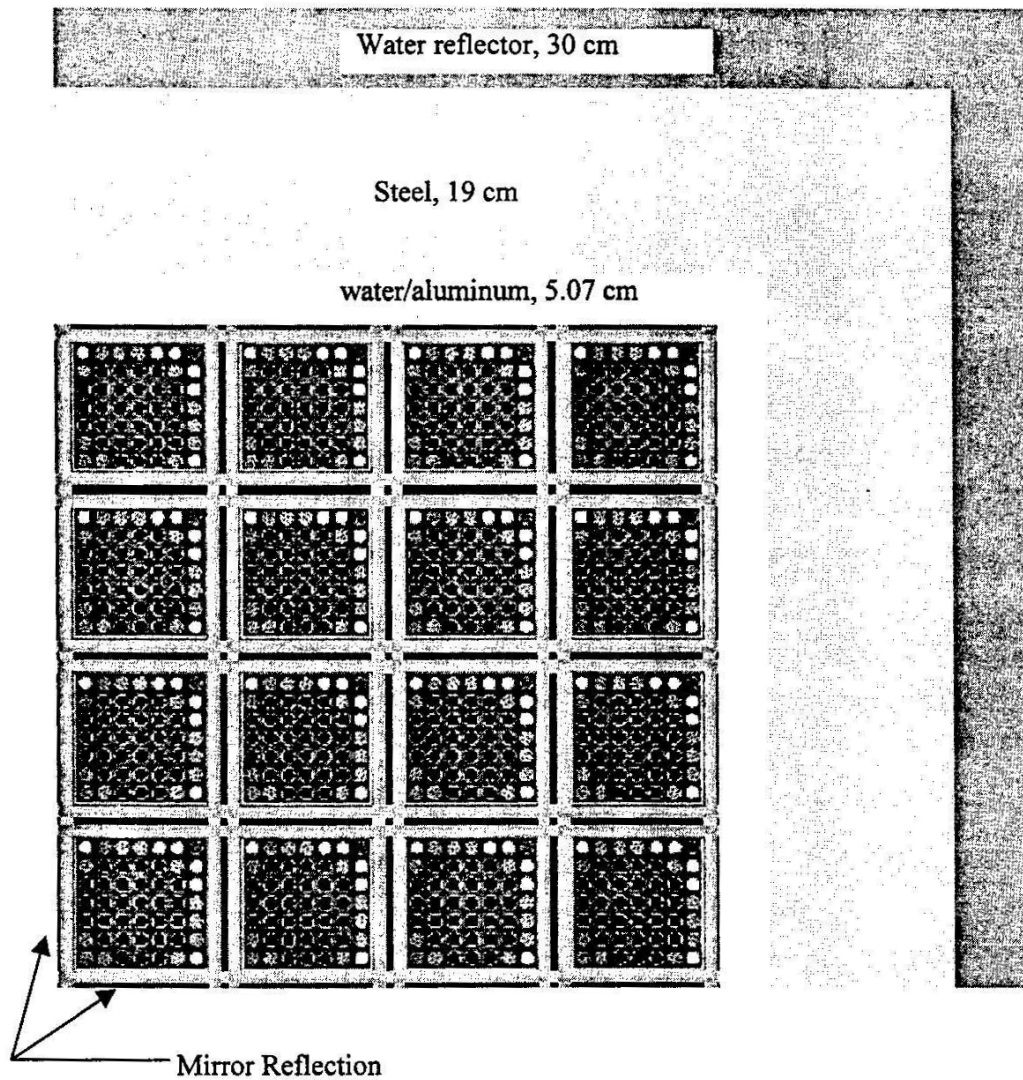


Figure 6.4-1
 TN-68 Model Cross Section, Most Reactive Lattice Evaluation



Model is 30.912 cm in the z direction, with periodic reflection top and bottom

Note: this model is not intended to be an accurate representation of the cask, but rather to provide a comparison of uniform and non-uniform pin enrichment fuel models in a configuration similar to the TN-68. All fuel assemblies are oriented with the highest enrichment corner toward the cask axis.

Figure 6.4-2
TN-68 Model Cross Section, Uniform Enrichment Validation, Case 3Var

Location of vanished partial length fuel pin

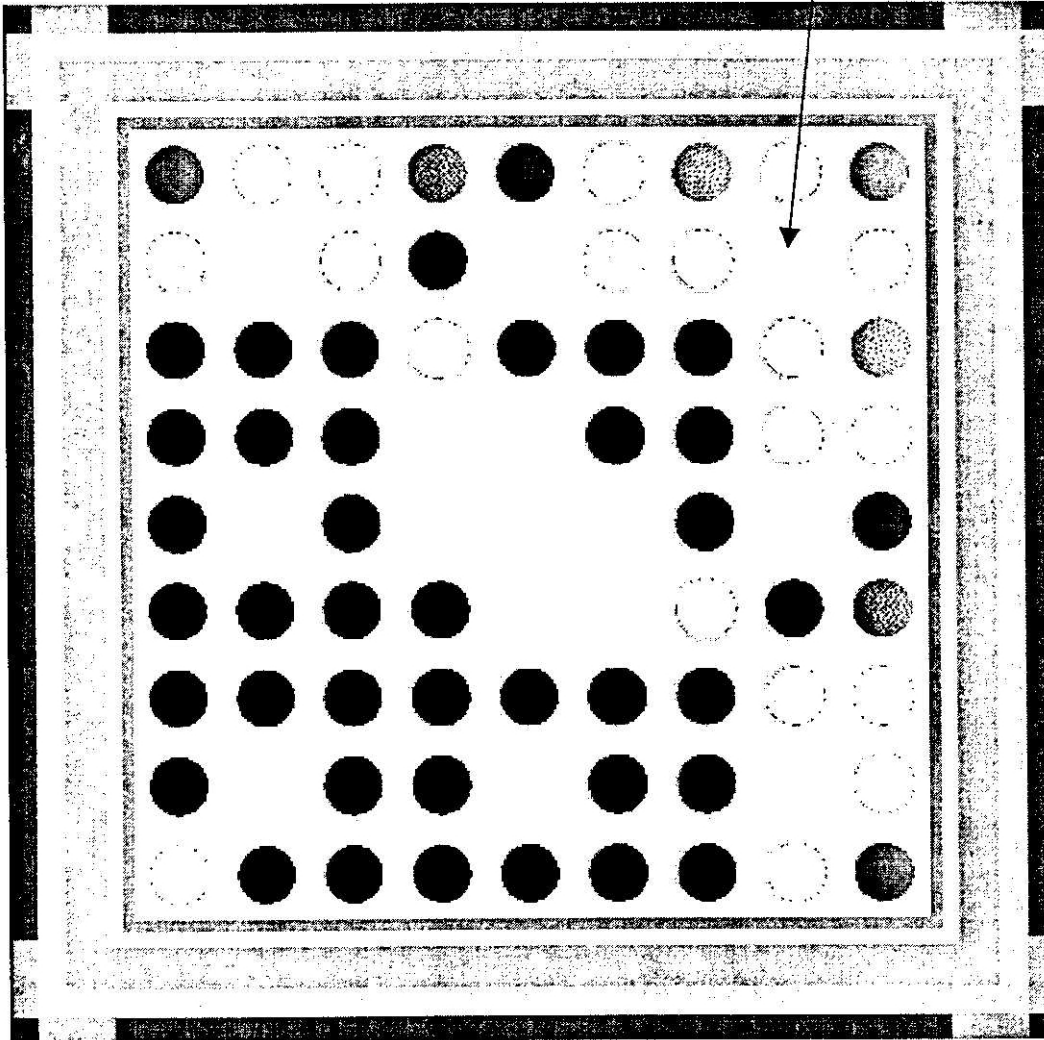


Figure 6.4-3
Vanished Lattice Model

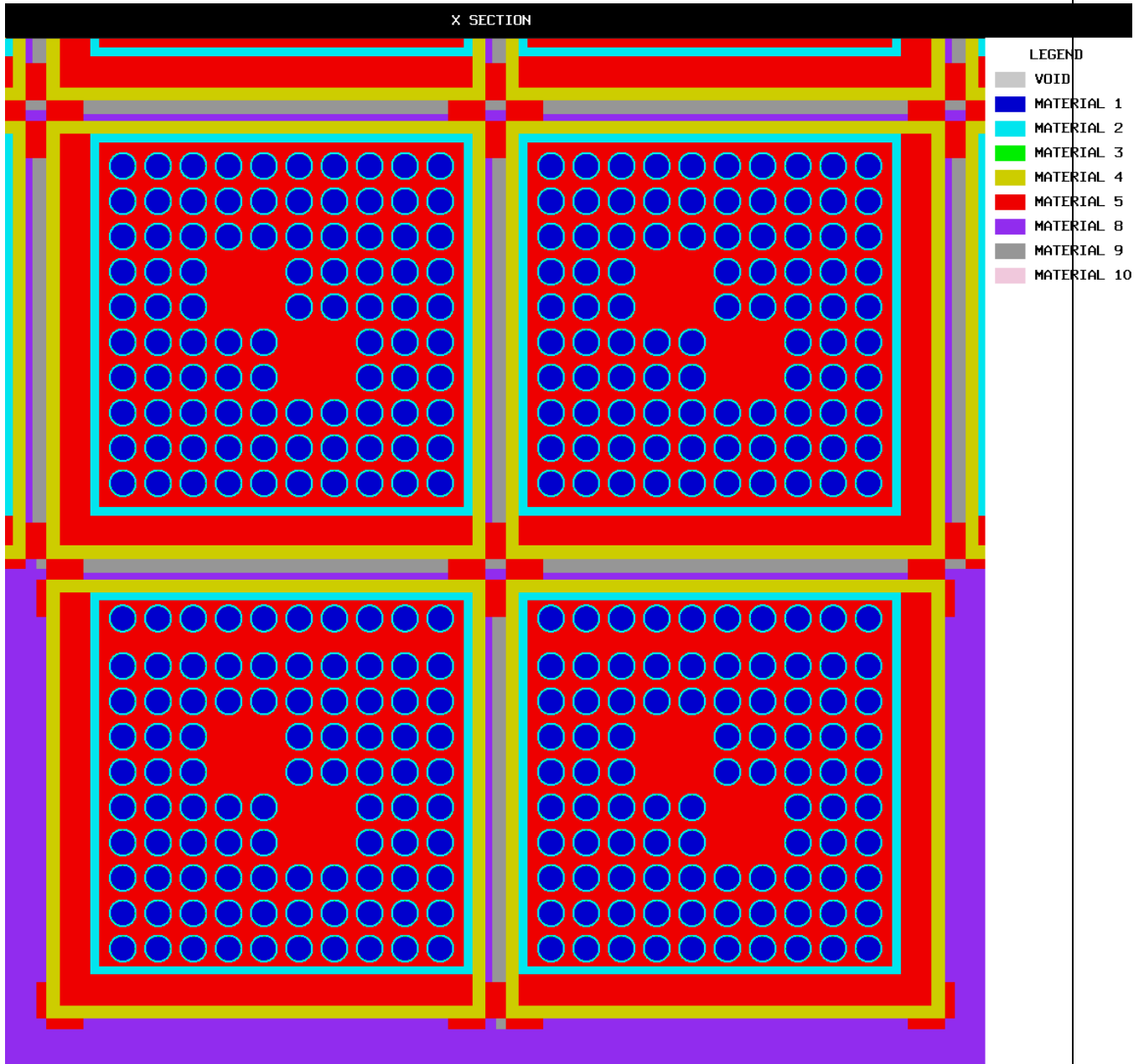


Figure 6.4-4
KENO Plot of Units 247 and 248 With Channel - Single Shear Rows

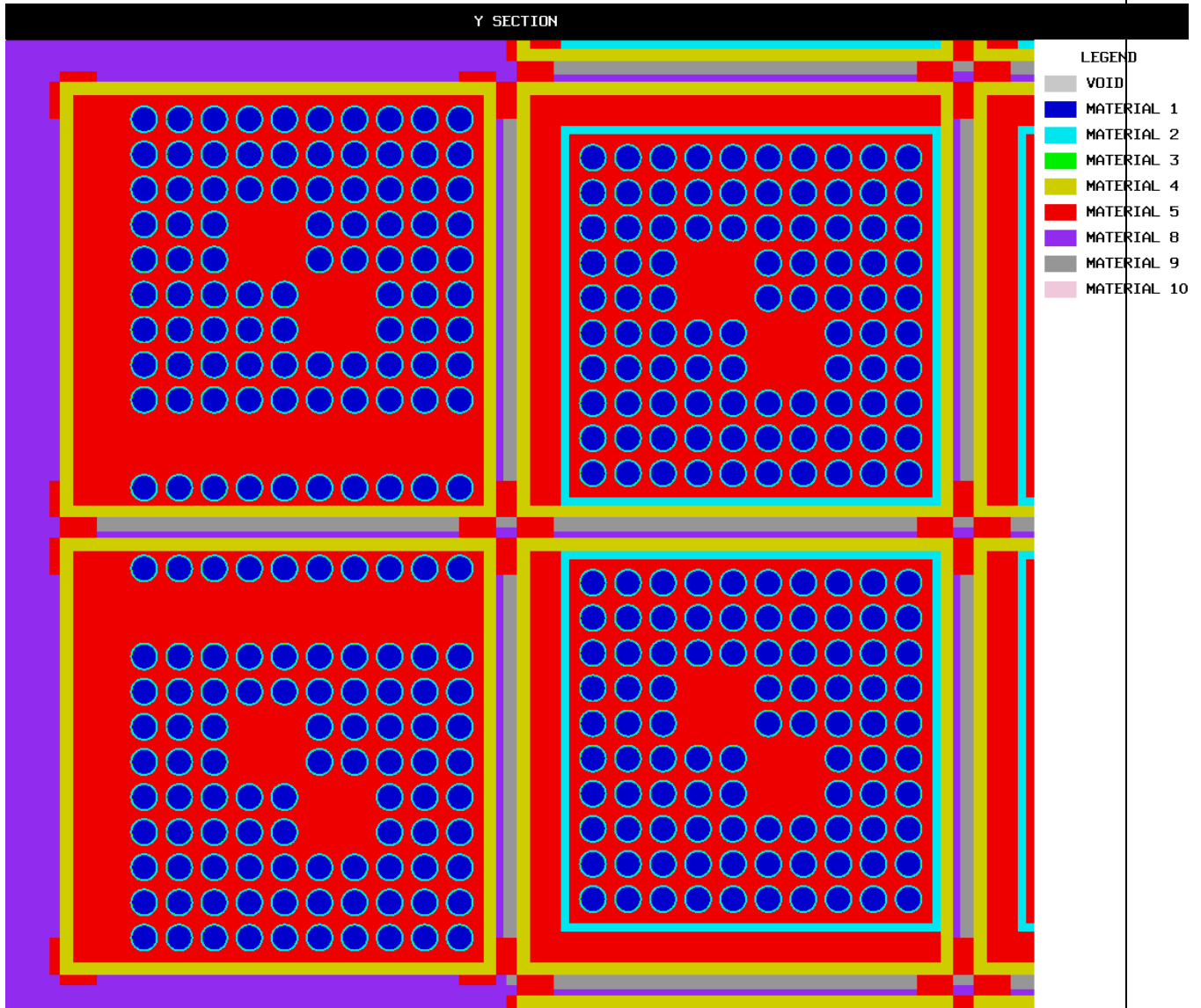


Figure 6.4-5
 KENO Plot of Units 257 and 258 Without Channel - Single Shear Rows

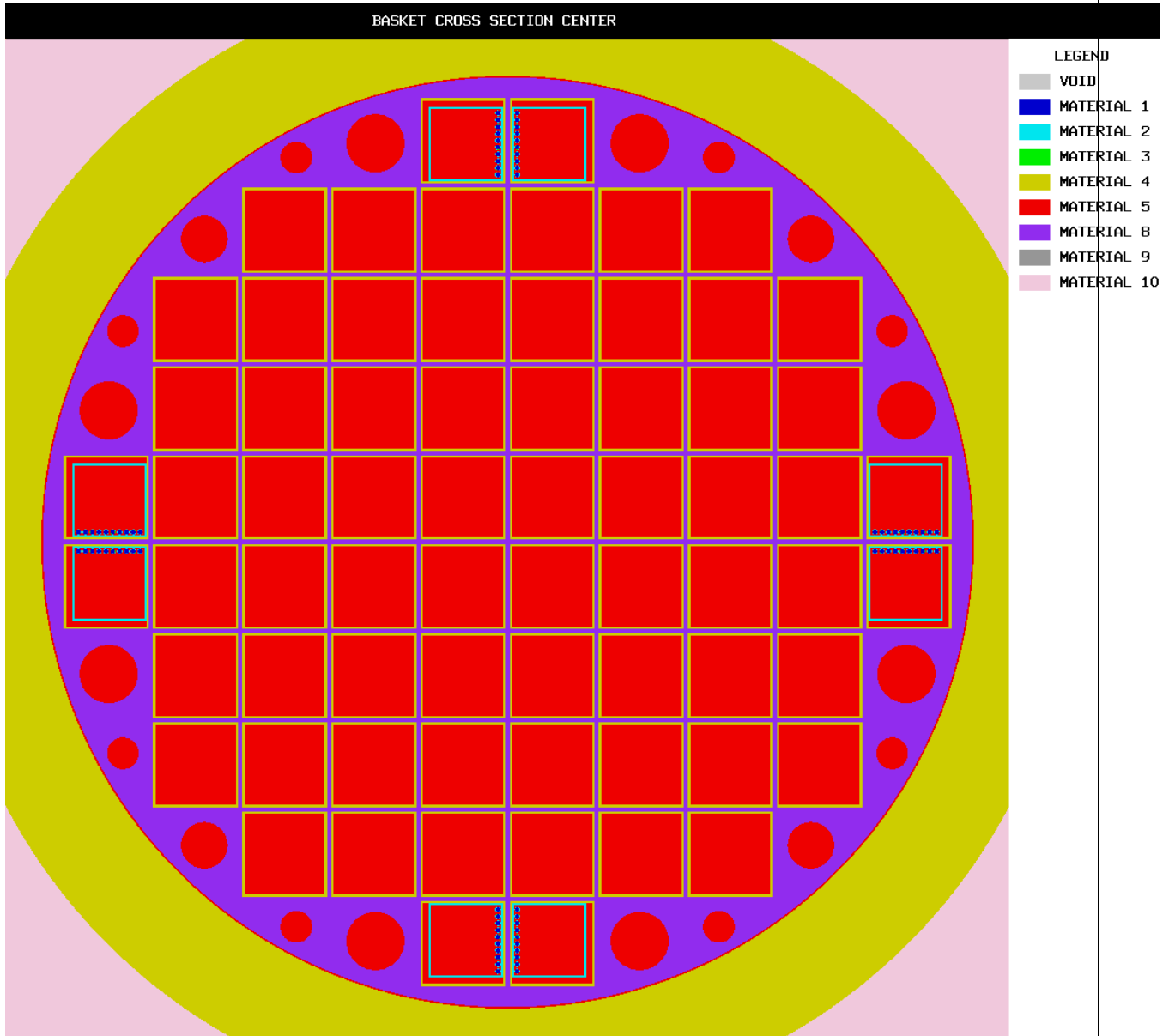


Figure 6.4-6
KENO Plot of the Single Sheared Rods with 12.18" Axial Shift

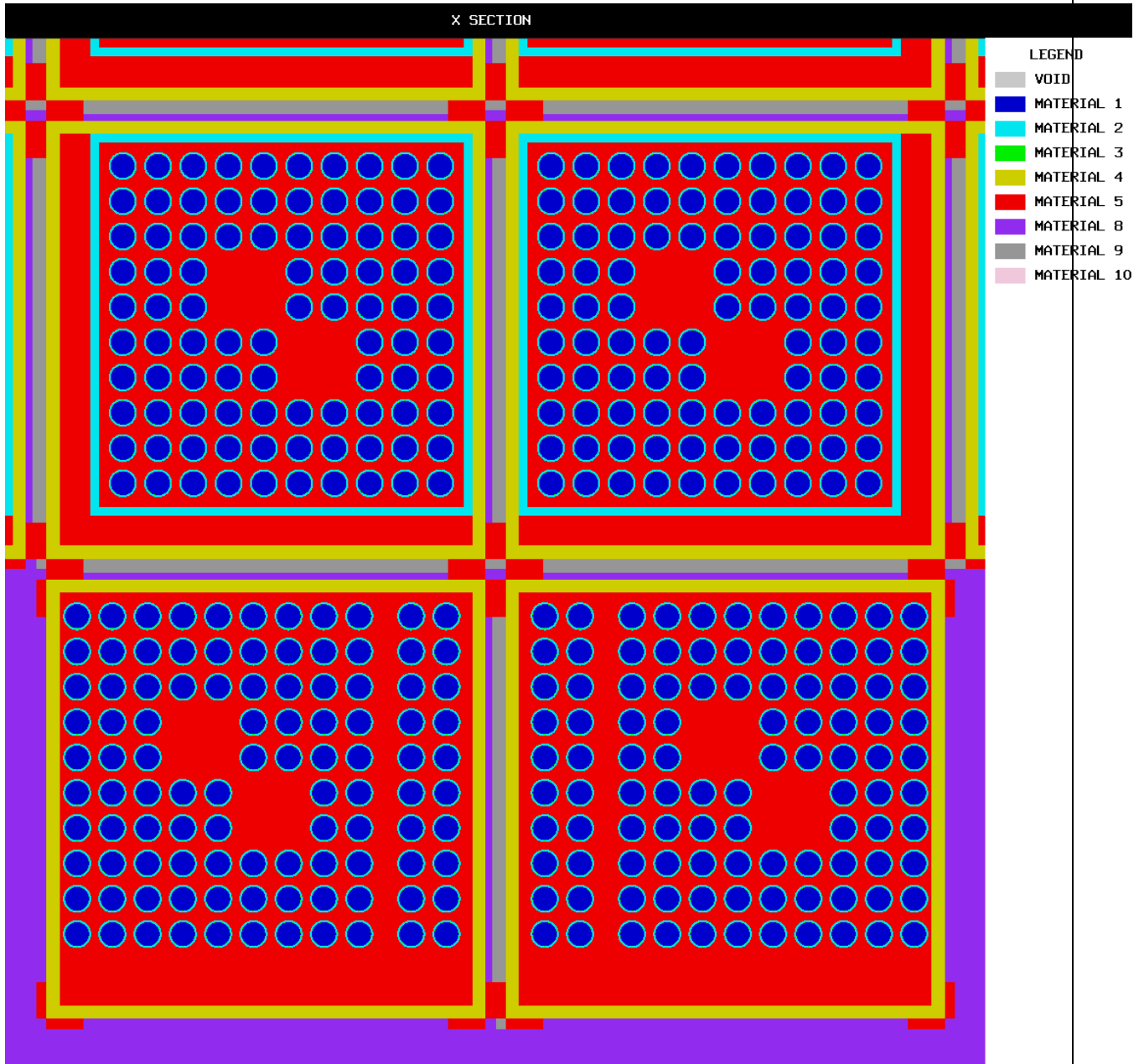


Figure 6.4-7
 KENO Plot of Units 247 and 248 With Channel - Double Shear Columns

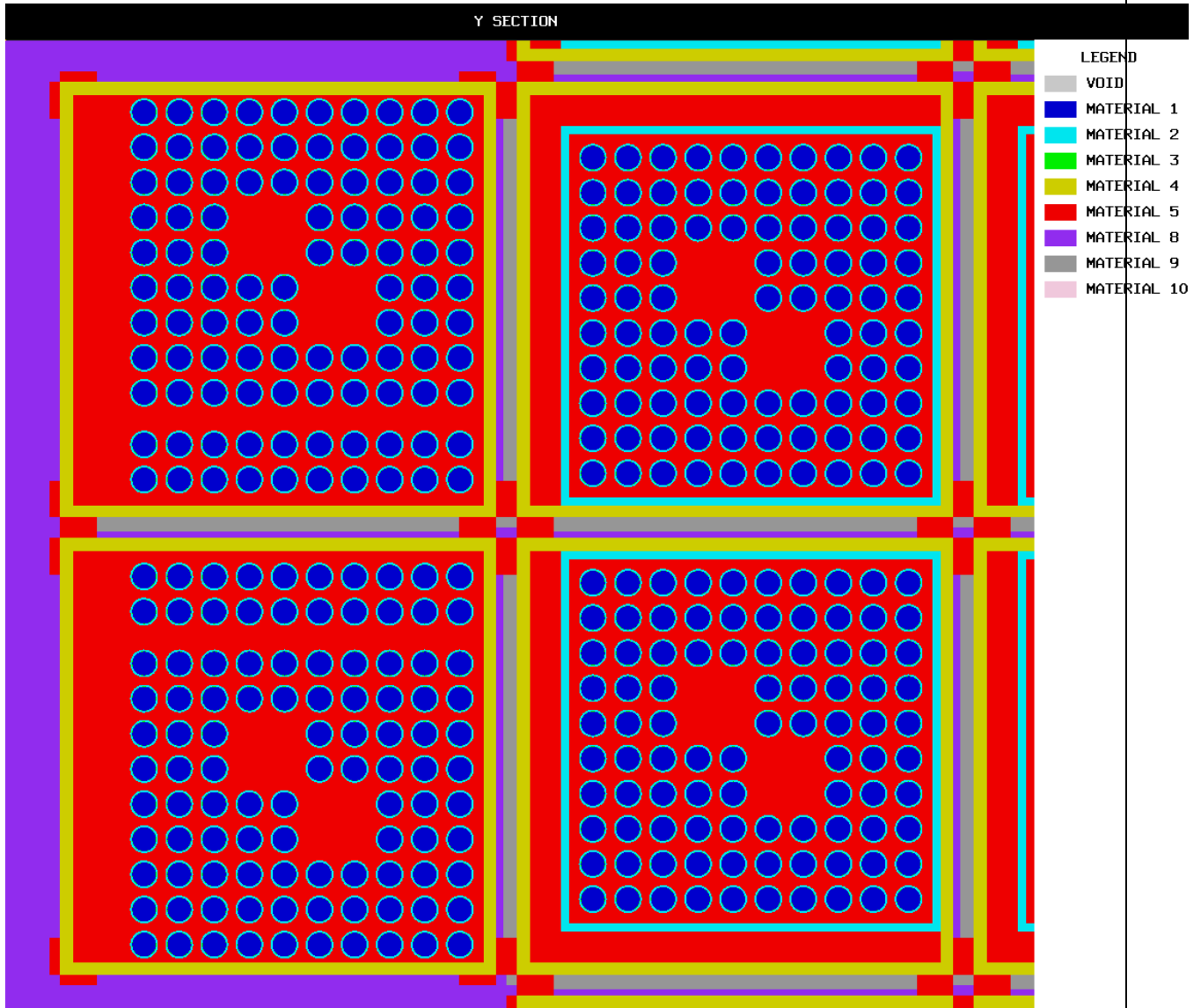


Figure 6.4-8
KENO Plot of Units 257 and 258 Without Channel - Double Shear Rows

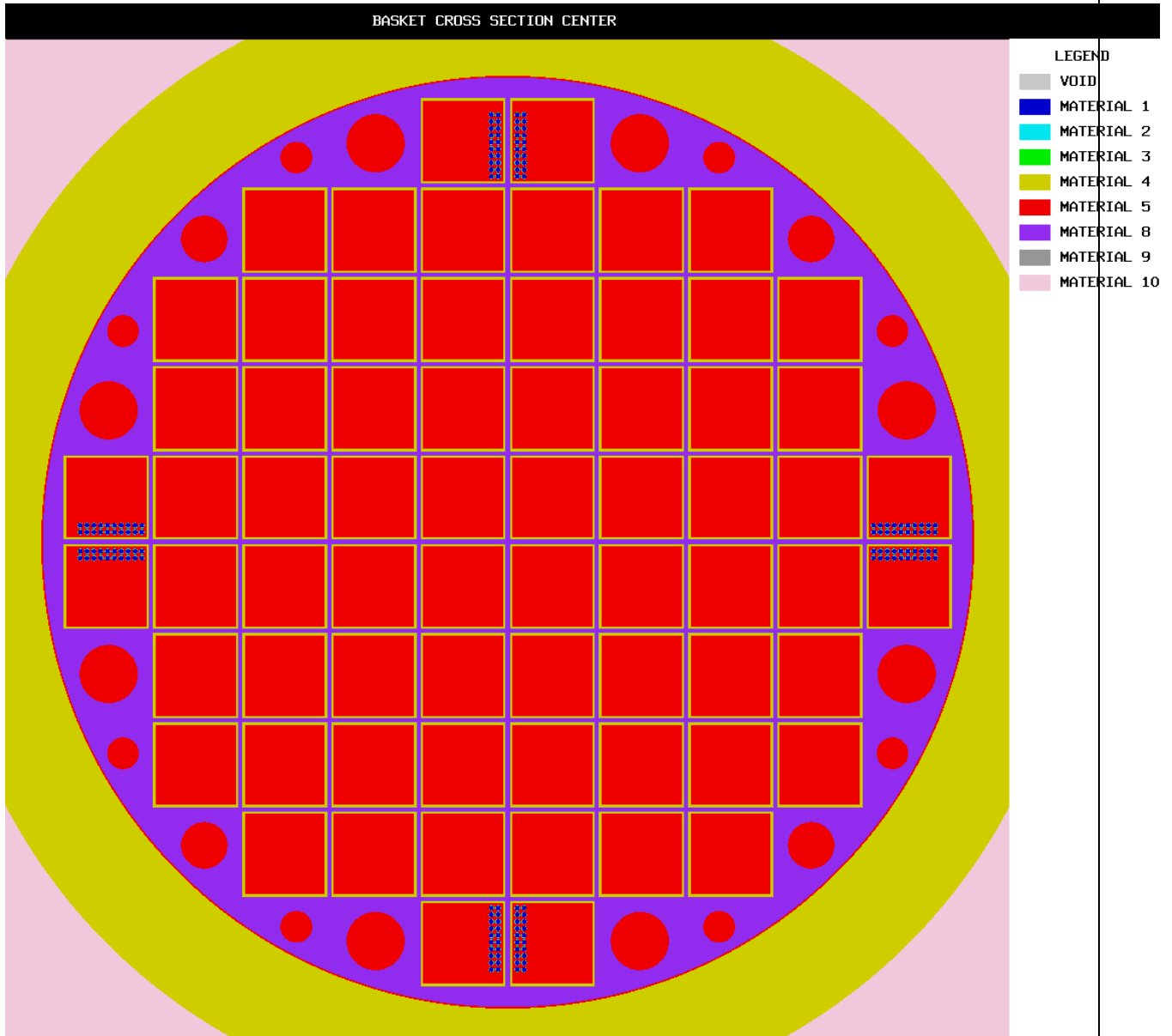


Figure 6.4-9
KENO Plot of the Double Sheared Rods with 12.18" Axial Shift

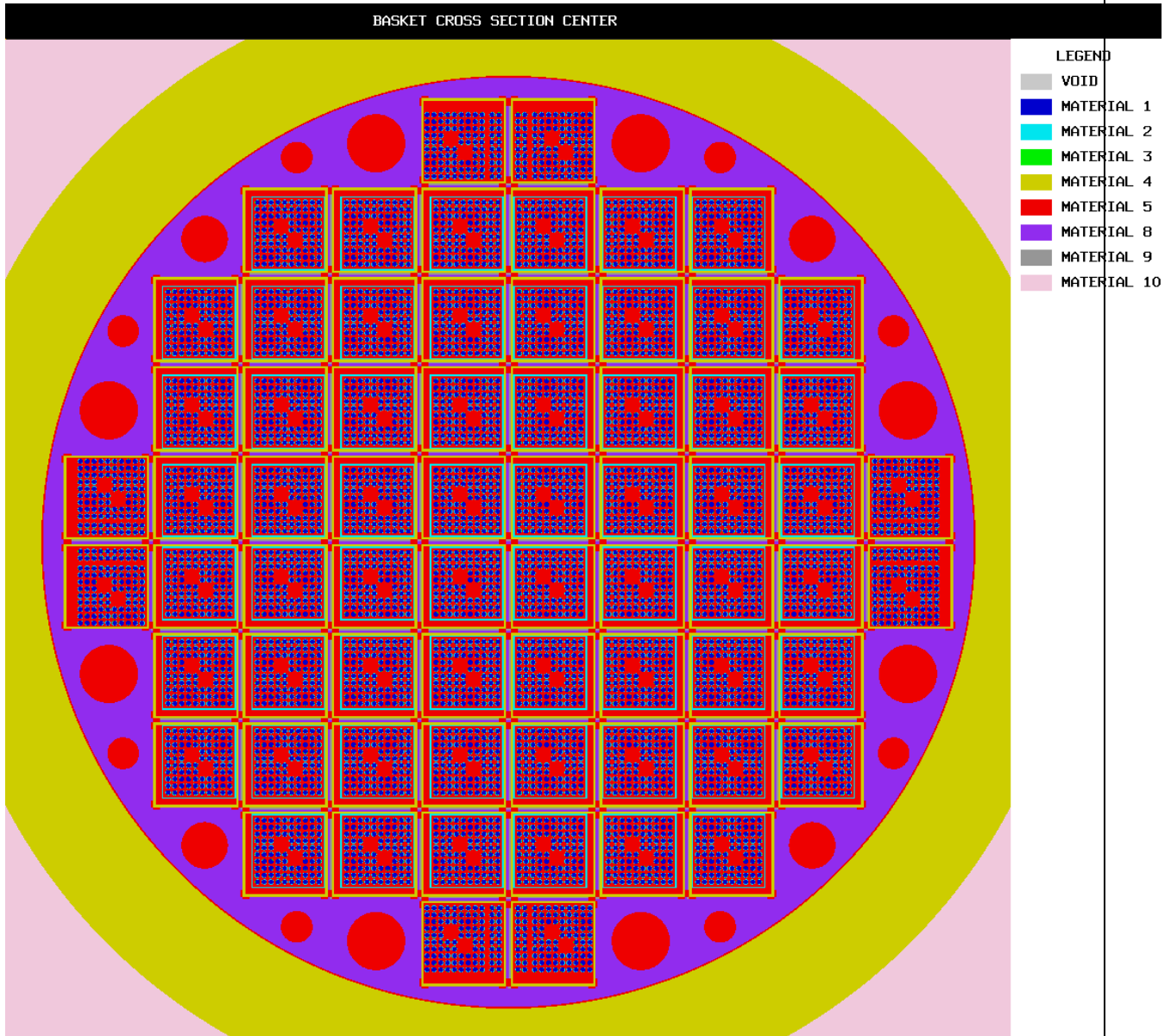


Figure 6.4-10
KENO Plot of the Design Basis Double Shear Damaged Assembly Model

